ABSTRACT

Title of Dissertation: PHYSIOLOGICAL AND MOLECULAR ASPECTS OF ORGANELLE SEQUESTRATION IN THE CILIATE *MYRIONECTA RUBRA*

Matthew David Johnson, Doctor of Philosophy, 2005

Dissertation directed by: Professor Diane K. Stoecker
Marine Estuarine Environmental Science

The phototrophic ciliate *Myrionecta rubra* was studied in order to understand the role of organelle retention from its prey, *Geminigera cryophila* (Cryptophyceae). Sequencing of SSU rRNA genes of *M. rubra,* and a close relative *Mesodinium pulex*, revealed short (<1600 bp) sequences with high substitution rates. Phylogenetic analysis yielded a basal placement within the ciliates. Application of a fluorescence *in situ* hybridization probe revealed the genes were expressed in the cytoplasm and nucleoli of the ciliates. Phylogenetic analysis of the chloroplast nucleomorph SSU rRNA gene in *M. rubra* confirmed their origin to be from *G. cryophila*. Feeding on *G. cryophila* was shown to increase growth, which remained constant for 4 weeks of starvation and then declined slowly over time. Chlorophyll *a* (chl *a*) synthesis and plastid division decreased faster than growth, resulting in declines in cell pigment over time. During starvation

photosynthetic efficiency declined slightly, while overall photosynthesis became uncoupled from growth, resulting in decreased growth efficiencies. While plastids in *M. rubra* or *G. cryophila* have equal efficiency at saturating irradiance, they are more efficient in *G. cryophila* in low light and have a greater overall quantum yield of photochemistry. Lower C-specific photosynthetic rates and chl *a*:C ratios resulted in lower growth compared to *G. cryophila*, which was reflected in increased partitioning of C to lipid fractions and lower protein production in *M. rubra*. A novel process, retention of prey nuclei (PN), was found to occur in *M. rubra*. *G. cryophila* nuclei are retained in a transcriptionally active state for >20 days, and remain in the cytoplasm for at least 30 days, apparently with no net division. Cell and plastid division are maximum during PN retention, and decline after PN loss. The PN genes *LHCC10* and GAPDH were expressed at levels greater than those observed in *G. cryophila*. Expression of a plastid (*psbA*) and nucleomorph (*cbbX*) gene was also confirmed. *M. rubra* is a unique phototroph, capable of regulating and dividing certain *G. cryophila* organelles, and reaching maximum growth potential when PN are present. Feeding on *G. cryophila* appears to be most important for obtaining PN.

PHYSIOLOGICAL AND MOLECULAR ASPECTS OF ORGANELLE SEQUESTRATION IN THE CILIATE *MYRIONECTA RUBRA*

By

Matthew David Johnson

Dissertation submitted to the Faculty of the Graduate School of the
University of Maryland, College Park, in partial fulfillment
of the requirements for the degree of
Doctor of Philosophy
2005

Advisory Committee:

Professor Diane K. Stoecker, Chair/Advisor
Professor Todd M. Kana
Professor Charles F. Delwiche, Dean's Representative
Professor David W. Oldach
Professor D. Wayne Coats

Acknowledgements

I owe much for the completion of my dissertation to my childhood fascination with the ocean, especially sharks, and my parents for fostering an appreciation and respect for animals and nature. I thank my mother and father, Charlene and Lance, for this and their continued love, encouragement, and support over the years. I thank my stepparents, Larry and Patty, for their love and support, and particularly for their encouragement with my interests in science. I am grateful for the love and support of my entire family, particularly my sisters Jen and Jess. Special thanks to Brian and Steve for your friendship and the inspiration and guidance along the way. I extend love to all my friends- I have learned much in recent years about enjoying life and I am eternally grateful for your support and company. Thanks to Canvasback for keeping a roof over my head.

I would like to thank the following people and institutions for which I am grateful for their formative educational and/or professional support and encouragement: Mr. Gehan (SHS), project oceanography (Groton, CT), David St. Aubin and Mystic Marinelife Aquarium, Karen Burnett and the Fort Johnson REU program, Carl Luer, Larry Liddle, and Lynda Shapiro. I would especially like to thank my dissertation advisor Dr. Diane Stoecker for her support, patience, and for the exciting and rewarding opportunity to work with her during the past 7 years. I thank my dissertation committee, Chuck Delwiche, Wayne Coats, David Oldach, and Todd Kana, who all opened their labs and minds for me and to whom I am grateful for helping to make my dissertation a labor of love, rather than work. Special thanks to David for providing space and support for much of my research. I thank the following people for illuminating discussions and/or

technical support: Jason Adolf, Dan Gustafson, Torstein Tengs, Holly Bowers, Chris Scholin, Tore Lindholm, Paul del Giorgio, Scott Heyward, Sean Cooney, Tsetso Bachvaroff. I thank Harri Kuosa, Riitta Autio, Outi Setälä, and Janne Rintala for funding two trips to Finland and for their hospitality and research collaborations. I thank the Horn Point Educational committee and the National Science Foundation for research support.

Table of Contents

List of Tables

List of Figures

Introduction to *Myrionecta rubra* and Organelle Sequestration

Ciliates play an important role in pelagic marine microbial food webs as one of the dominant grazers of bacterial and flagellate prey (Pomeroy 1974, Sorokin et al. 1977, Azam et al. 1982, Sherr et al. 1986, Sherr and Sherr 1994). Although ciliates occupy a similar size range as dinoflagellates, they generally have higher growth rates (Sherr and Sherr 1994). They can act as links to higher trophic levels, due to their efficient ability to repackage pico (0.2-2.0 μm) and nano (2.0-20 μm) sized biomass into a predominately micro (20-200 μm) size range (Sherr et al. 1986, Stoecker and Capuzzo 1990). Some marine ciliates have been shown to exhibit high excretion rates for nitrogen (e.g. Verity 1982) and phosphorous (Taylor and Lean 1981) and, as microzooplankton, are believed to share the dominant role of nutrient regeneration in the oceans (Caron and Goldman 1990).

Many marine ciliates are also photosynthetic, by harboring endosymbionts or sequestered plastids within their cytoplasm (Taylor et al. 1969, Blackbourn et al. 1973, Laval-Peuto et al. 1986, Stoecker et al. 1987, Dolan 1992). Photosynthetic ciliates may comprise a large proportion of total ciliates at certain times and make substantial contributions towards primary production of micro sized cells (Stoecker et al. 1987). Dolan and Pérez (2000) recently reviewed the role of mixotrophic oligotrichs in marine environments and concluded that their abundance is correlated with chlorophyll concentrations, and that they are a constant component of oligotrich communities, averaging about 30% of ciliate cell numbers. Recently Dolan et al. (1999) found that mixotrophic ciliates were more abundant and contributed to a greater proportion of oligotrich biomass in nutrient poor, low chlorophyll regions of the Mediterranean. These results support Putt's (1990) observations in the Nordic Seas, finding that one species of

plastidic oligotrich contributed up to 24% of total chlorophyll in oligotrophic regions. Stoecker et al. (1989) found that about 50% of all ciliates in the shelf and slope waters of Georges Bank, including *Myrionecta rubra*, contained chlorophyll. Despite these reports the importance of photosynthetic ciliates is often underappreciated.

M. rubra has been the subject of numerous studies to describe its 'endosymbiont' and ecology (see Taylor et al. 1971, Taylor 1982, Lindholm 1985 and Crawford 1989 for reviews), and its establishment under routine culture conditions has been sought after for certain biotechnological applications (Yih and Shim 1997). *M. rubra* is considered to have a cosmopolitan marine distribution in estuarine and coastal shelf waters, between polar and tropical regions (Taylor et al. 1971, Lindholm 1985, Crawford 1989). Red water blooms of *M. rubra* have been noted since Darwin's voyage on the *Beagle* (Darwin 1839), and are among the more spectacular and dynamic blooms of marine phototrophic organisms. These blooms are often periodic and difficult to predict in most regions, while in others they occur annually (e.g. Southampton, UK). Mostly they are found in upwelling regions or enclosed estuaries or fjords (Lindholm 1985). *M. rubra* reaches bloom densities annually in some Chesapeake tributaries (Johnson, unpub. data.), and has done so at least once within the main stem of Chesapeake Bay (Harding, per. com.).

Most primary productivity rates measured of *M. rubra* have been during red water events, and with chlorophyll concentrations of 1000 $\mu g\ l^{-1}$ and productivity rates of 2000 $\mu g\ C\ m^{-3}\ h^{-1}$, they are among the highest on record for any phytoplankton (Smith and Barber 1979). Taylor (1982) has stated that *M. rubra* has the highest primary productivity rate of any phototroph on record. This is believable when you consider that large *M. rubra* cells have as many as 100 plastids (Lindholm 1985), and it is among the fastest

swimming microorganisms of its size, at speeds in excess of 8 mm s^{-1} or roughly 200 cell lengths s^{-1} (Lindholm 1985, Crawford 1989). Measurements of *M. rubra* photosynthetic rates under non-bloom conditions may tell a different story. Stoecker et al. (1991) found considerable variation in photosynthetic rates of *M. rubra* under non-bloom conditions. Higher photosynthetic rates were measured in populations that were actively growing or peaking and were consistent with previously measured values, while much lower rates were found in declining populations (Stoecker et al. 1991).

With the knowledge that *M. rubra* is phagotrophic and requires cryptophyte prey periodically to sustain photosynthetic rates and cell growth (Gustafson et al. 2000), there is good reason to renew interest in studying the physiology and trophic role of *M. rubra*. At certain times (i.e. blooms), it is possible to envision that *M. rubra* populations could have a significant grazing impact on cryptophyte populations, but no data exist on their feeding rates in nature. Despite knowing that *M. rubra* feeds, it is unclear whether or not it gains nutrition heterotrophically. It is important to know if *M. rubra* is predominantly phototrophic or heterotrophic in its carbon physiology to properly assign a trophic placement for it. If *M. rubra* resembles other photosynthetic ciliates in its carbon metabolism than it probably has an important role in the heterotrophic cycling of ingested cryptophyte biomass, in addition to being a phototroph. If not than its classification becomes problematic. It would be a functionally phototrophic organism, that depends little upon heterotrophy, if at all, yet requires prey for sequestering organelles. The picture is actually somewhat more complicated, as it appears that *M. rubra* can synthesize chlorophyll (Gustafson et al. 2000). Preliminary data on its photosynthetic carbon metabolism suggests that fixed carbon is used primarily for production of lipid and

protein polymers (Johnson et al. 2001). In contrast, all previous studies of photosynthetic ciliates have shown that carbon fixation is mostly used for the production of carbohydrates, covering respiration and excretion costs (Putt 1991, Stoecker 1998). Furthermore chlorophyll synthesis has never been demonstrated in a plastid-sequestering organism. While *M. rubra* doesn't harbor live cells, their ability to replicate cryptophyte biomass raises the question of whether this constitutes mixotrophy or a form of symbiosis? Neither of these choices seem appropriate for the level of understanding we now have of *M. rubra*'s physiology and further investigation is necessary to clarify this problem.

Cryptomonads are a relatively small group of algae, but are ubiquitous in coastal marine systems and often very abundant. One characteristic that makes them unique is their vestigial nucleus, the nucleomorph, associated with their plastid. The cryptophyte nucleomorph is a highly reduced nucleus, and is derived from an ancestral endosymbiont of the red algal lineage (Douglass et al. 1991, Maier et al. 1991). The nucleomorph is housed within the periplastidal membrane (the vestigial symbiont plasma membrane) with one or two plastids, all of which are enclosed by rough endoplasmic reticulum (Douglas et al. 2001). In cryptomonads, the nucleomorph still encodes and expresses 18s rRNA and a number of 'house-keeping' genes, involved primarily in the expression and maintenance of the nucleomorph genetic system (Maier et al. 2000, Douglas et al. 2001). Several genes critical to plastid function, e.g. FtsZ (chloroplast division protein) and *rub* (rubredoxin, an iron containing electron carrier), have been found to be encoded by the nucleomorph (Fraunholz et al. 1998 Zauner et al. 2000, Douglas et al. 2001). The cryptophyte nucleus is known to possess genes critical to the biosynthesis of cryptophyte

plastids, such as the LHC proteins (light-harvesting complex proteins), which appear to be products of nucleomorph to nucleus gene transfers (Deane et al. 2000). A recent effort by Douglas et al. (2001) to sequence a cryptophyte nucleomorph genome, suggests that well over a thousand plastid genes must be encoded by the cryptophyte nucleus. While the nucleomorph-plastid complex is not an autonomous entity (e.g. the nucleomorph doesn't encode DNA polymerase), together the two genomes may harbor more photosynthetic genes than other algal plastids on their own.

It is possible to speculate that if cryptophyte plastids are sequestered, and the periplastidal membrane is kept intact, that some level of photosynthetic autonomy may be temporarily maintained beyond that from other algal plastids. This may explain why heterotrophic dinoflagellates appear to only sequester cryptophyte plastids (Wilcox and Wedemayer 1984, Larsen 1988, Schnepf et al. 1989, Fields and Rhodes 1991, Horiguchi and Pienaar 1992, Skovgaard 1998, Lewitus et al. 1999, Jakobsen et al. 2000). In contrast, most photosynthetic choreotrich ciliates appear to be generalists when it comes to utilizing prey for plastid retention (Stoecker et al. 1988/1989). The difference in prey selectivity between plastid-retaining dinoflagellates and oligotrich ciliates could be explained by the observations of Laval-Peuto and Febvre (1986). They found that *Tontonia appendiculariformis* (Choreotrichia) appears to digest certain chloroplast membranes of sequestered plastids, so that only the double membrane of plastids remain. If all mixotrophic choreotrichs feed in this manner, then it may not be advantageous to select for cryptophytes. In contrast, nearly all plastid-retaining dinoflagellates are myzocytotic feeders that use a feeding tube, or peduncle, to remove organelles and cytoplasm from their prey (Schnepf and Deichgräber 1984). This mechanism may be

conducive for sequestering intact organelles, and has been hypothesized to be a mechanism for evolutionary acquisition of plastids (i.e. secondary and tertiary plastids, *sensu* Delwiche 1999) within dinoflagellates and euglenoids (Schnepf and Deichgräber 1984). *M. rubra* has been described as feeding by ingesting intact cells in the reduced cytostome region (Yih et al. 2004, Stoecker & Johnson, unpub. data), and is able to sequester cryptophyte plastids with intact periplastidal membranes.

Previous studies of cryptophycean plastids in *M. rubra* reveal that they exist with cryptophyte cytoplasm and mitochondria enclosed by, presumably, a ciliate vacuole membrane. Oakley and Taylor (1978) stated that "the majority of the ciliate cells have no "dividing" CMC's [chloroplast-mitochondria-complexes] but some have well over half of them dividing." These observations support recent findings by Gustafson et al. (2000) that cultures of *M. rubra* are able to synthesize chlorophyll. Perhaps most interesting, is the possibility that cryptophyte nuclei are temporarily sequestered. Most studies of *M. rubra* cytostructure have shown 'symbiont' nuclei present, usually one per cell (e.g. Lindholm et al. 1988). Lindholm et al. (1988) described strands of algal cytoplasm extending from the nucleus in various directions. Gustafson et al. (2000) reported that cryptophyte nuclei temporarily accumulate within the cytoplasm of cultured *M. rubra* after introduction of cryptophytes, though their fate was uncertain. Perhaps if cytoplasmic connections do exist between 'symbiont' nuclei and plastids, nuclear encoded genes could be targeted to the cryptophyte plastids to support plastid biosynthesis. In the ascoglossan sea slug, *Elysia chlorotica*, proteins from sequestered plastids appear to be synthesized in the animal cytosol and subsequently translocated back into the

chloroplasts (Pierce et al. 1996). Therefore, it is possible that cryptophyte nuclear genes are also expressed and translated within the cytosol of *M. rubra*.

While the important role of ciliates within the marine microbial food web has been acknowledged (Sherr and Sherr 1994), relatively little research has been conducted on the physiology and ecology of many common ciliates. *M. rubra* is a relevant model for these studies, as we now know that it has a dynamic role in microbial communities as both a grazer and a primary producer. It is important to understand the fate of ingested cryptophyte biomass and specifically to determine if *M. rubra* is mixotrophic. Although *M. rubra* appears to be an unusual and highly specialized ciliate, its success as a species is evident in its widespread distribution and abundance. Therefore it is important to know the trophic role of *M. rubra*. By understanding the dynamics and regulation of plastid sequestration, pigment synthesis, and retention time in *M. rubra*, we will better understand its functional role, and we may have greater success in predicting the distribution and abundance of *M. rubra* in nature.

It has been hypothesized that phototrophy in protozoa is beneficial because it increases growth efficiency and allows for survival during periods of low prey abundance (Stoecker 1998). Because the evolutionary cost of maintaining a photosynthetic apparatus is high, relative to heterotrophs (Raven 1997), it may be more beneficial for photosynthetic protozoa to remain aplastidic. A recent phylogenetic analysis of glyceraldehyde-3-phosphate dehydrogenase (GAPDH) genes suggests that ciliates might be derived from a photosynthetic ancestor among the alveolates (Fast et al. 2001). If true, this may illustrate that it is also beneficial for certain protists to lose plastids. Plastid loss has occurred in other photosynthetic lineages, such as the euglenoids (Siemeister and

Hachtel 1990) and dinoflagellates (Saldarriaga et al. 2001). Therefore, plastid-retention among some protozoa could be construed as an evolutionarily stable strategy, rather than a means toward acquiring plastids.

But, while many "heterotrophic" protozoa benefit from kleptoplastidy or temporary symbiosis (Caron 2000), plastids have also been permanently acquired by diverse protist lineages via secondary and tertiary endosymbiosis (Delwiche 1999). The Alveolata in particular, seem as though they are predisposed to permanently acquiring or temporarily sequestering plastids (Delwiche 1999). Perhaps an ancestry of phototrophy, in extant aplastidic protists, may help in the acquisition of new plastids, due to the presence of nuclear encoded genes that assist in maintaining kleptoplastids (Lewitus et al. 1999, Delwiche 1999). Organelle retention has been hypothesized as a mechanism by which cells permanently acquire organelles and the genes necessary to regulate them (Schnepf and Deichgräber 1984, Delwiche 1999). *M. rubra* could be used as a model for this type of photosynthetic evolution. Due to its ability to synthesize chlorophyll and a metabolism that depends greatly (if not entirely) upon phototrophy, it appears to have adapted to a phototrophic existence. This research is important for understanding how *M. rubra* is able to successfully function as a phototroph through organelle sequestration, and to identify those unique adaptations it has made in becoming phototrophic.

CHAPTER 1: Highly Divergent SSU rRNA Genes found in the Marine Ciliates *Myrionecta rubra* and *Mesodinium pulex*

Abstract

Myrionecta rubra and *Mesodinium pulex* are among the most commonly encountered planktonic ciliates in coastal marine and estuarine regions throughout the world. Despite their widespread distribution, both ciliates have received little attention by taxonomists. In order to better understand the phylogenetic position of these ciliates, I determined the SSU rRNA gene sequence from cultures of *M. rubra* and *M. pulex*. Partial sequence data were also generated from isolated cells of *M. rubra* from Chesapeake Bay. The *M. rubra* and *M. pulex* sequences were very divergent from all other ciliates, but shared a branch with 100% bootstrap support. Both species had numerous deletions and substitutions in their SSU rRNA gene, resulting in a long branch for the clade. This made the sequences prone to spurious phylogenetic affiliations when using simple phylogenetic methods. Maximum likelihood analysis placed *M. rubra* and *M. pulex* on the basal ciliate branch, following removal of ambiguously aligned regions. Fluorescent *in situ* hybridization probes were used with confocal laser scanning microscopy to confirm that these divergent sequences were both expressed in the cytoplasm and nucleolus of *M. rubra* and *M. pulex*. I found that my sequence data matched several recently discovered unidentified eukaryotes in Genbank from diverse marine habitats, all of which had apparently been misattributed to highly divergent amoeboid organisms.

Introduction

The phototrophic ciliate *Myrionecta rubra* (=*Mesodinium rubrum*) (Lohmann 1908, Jankowski 1976) (Mesodiniidae, Litostomatea) is nearly ubiquitous in coastal marine and estuarine habitats and has long been a curiosity to evolutionary biologists, perhaps beginning with Darwin (1839). The important ecological role of this ciliate is periodically made conspicuous by massive non-toxic red tides in coastal and estuarine regions throughout the world, some of which may exceed 100 square miles (Ryther 1967, Jiménez and Intriago 1987). *M. rubra* is well documented to possess organelles of cryptophycean origin, including plastids, mitochondria (Taylor et al. 1969, 1971), and nuclei (Hibberd 1977, Oakley and Taylor 1978). While early studies debated whether these organelles represented a true symbiosis or were the result of sequestration from living prey (e.g. Taylor et al. 1969), more recent studies have provided evidence for the latter, showing that growth and photosynthesis in *M. rubra* are dependent upon ingesting free-living cryptomonads (Gustafson et al. 2000).

Mesodinium (Stein 1863) (Mesodiniidae, Litostomatea) is a commonly encountered genus of non-pigmented ciliates found in coastal marine, estuarine, and fresh water systems (Foissner et al. 1999). *M. pulex* is a heterotrophic ciliate that feeds upon bacteria, flagellates, algae, and ciliates (Dolan and Coats 1991, Foissner et al. 1999). Although there are few described species in the genus other besides *M. pulex*, it is often confused with *M. acarus* and *M. fimbriatum* (Foissner et al. 1999).

Currently no sequence data are available for the Mesodinidae, and only recently have efforts been made to determine small subunit (SSU) ribosomal RNA sequences for

other familiar pelagic marine ciliates (e.g. Snoeyenbos-West et al. 2002, Strueder-Kypke and Lynn 2003). Several recent PCR-based studies to assess microbial eukaryotic diversity in the world's oceans have led to the discovery of numerous unidentified SSU rRNA sequences, some of which constitute new branches on familiar phylogenetic lineages (e.g. López-Garcia et al. 2001). Many of these new sequences can be attributed to well described protistian groups such as alveolates (apicomplexans, ciliates, colpodellids, dinoflagellates, perkinsids), while some are sequences with uncertain phylogenetic affiliation. However, many of the rRNA genes of recognized marine protists have yet to be sequenced, suggesting that some of the new sequences may not be novel taxa. Recently Leander et al. (2003) identified some of these novel sequences as belonging to the colpodellids. In the present study I present evidence that several newly described unidentified eukaryotic sequences with uncertain taxonomic affiliation also belong to a familiar lineage of alveolates. Herein I present sequence data that show *Myrionecta* and *Mesodinium* share similar and highly divergent SSU rDNA sequences that suggest they are an early branching lineage of ciliates, and use *in situ* hybridization to verify that these sequences are present and expressed.

Methods

Culture conditions and cell isolations

Myrionecta rubra (CCMP 2563) was isolated from a nutrient enrichment of water collected in McMurdo Sound, Antarctica in 1996 as described previously (Gustafson et

al. 2000). Cultures were maintained in 33psu f/2 (-Si) culture media (Guilliard 1976) and periodically fed the cryptomonad, *Geminigera cryophila* (CCMP 2564). *Mesodinium pulex* was isolated from an estuarine portion of the Choptank River, Cambridge, MD, USA, after enriching river water with flagellate prey for several days. The culture was maintained at 15ºC in 15psu seawater, made from diluting full-strength seawater. Nutrients were not added directly to the *M. pulex* culture, except when carried over from adding its prey, *Rhodomonas* sp. *M. rubra* cells were also isolated from the Choptank River, but all efforts to culture them failed. Therefore multiple (10-50) *M. rubra* cells were isolated from water samples, washed several times with clean media, added directly to 1x TE buffer (0.1 M tris-HCl, 0.01M EDTA) and frozen (-20ºC) for later PCR. Cultures of *M. rubra* and *M. pulex* are available upon request.

DNA extraction, PCR amplification and DNA sequencing

Cultures of *M. rubra* (~3 x 10^4 cells ml^{-1}) and *M. pulex* (~1000 cells ml^{-1}) were centrifuged in 50 ml centrifuge tubes at 4ºC and 4000 g for 10 min. The Plant DNA Extraction Kit (Qiagen) was used and the manufacturers protocol was followed. PCR was conducted using 1x PCR buffer (TaqPro, Denville), 0.2μM nucleotides, 0.25mg/ml bovine serum albumin (BSA), 3mM $MgCl_2$, 0.4 μM primers, and 0.6 u Taq DNA polymerase, and were combined with 10-20 ng of genomic DNA from cultures in a volume of 25μl. To amplify the SSU rDNA gene of isolated *M. rubra* cells from Chesapeake Bay, the cells were heated at 95ºC for 2min and 10μl of the TE suspension (described above) was then added to the PCR mix. The following general eukaryotic

primers for small subunit (SSU) rRNA were used to amplify the gene from conserved regions: 4616, 4618 (Medlin et al. 1988, Oldach et al. 2000), 516 (CACATCTAAGGAAGGCAGCA), and 1416 (GAGTATGGTCGCAAGGCTGAA). PCR conditions were as follows: an initial 3 min 95ºC melting step, 40 cycles of 30 sec at 95ºC (melting), 30s at 55ºC (hybridization), and 70s at 72ºC (elongation), followed by a final 10m 72ºC elongation step. Products were then cloned using an Invitrogen TOPO TA cloning kit, following manufacturers instructions. Colonies were then isolated and gene products were reamplified with PCR using the same gene-specific primers. Cloned PCR products were sequenced directly in both directions using the above gene-specific primers and the BigDye terminator kit (Perkin Elmer). All sequencing was conducted using an ABI 377. Species-specific SSU rDNA primers (Qiagen) were designed for all novel sequences identified from sequencing the SSU rDNA clone library, and all sequences were generated at least 10 times. The species-specific primers, UNIDEUK(670R) (TATGAAGACTTGGTCTACCTTGA), UNIDEUK(880F) (ACTGAAACTATGCCAACTTGG), and UNIDEUK(1416R) GTTTCAGACTTGTGTCCATACTA), were used to verify the sequence from the cultures and to amplify the SSU rRNA gene from environmentally isolated cells.

Phylogenetic analysis

Contingent sequences were generated using Sequencher (Gene Codes Corp.) and added to sequences obtained from Genbank. All alignments were created using the Clustal X algorithm (Thompson et al. 1997) and ambiguous regions of the alignment

found in highly variable regions were removed by eye in MacClade 4.05 (Maddison and Maddison 1991). An alignment matrix was constructed of diverse alveolates and numerous other lineages of protists, and is available upon request.

The initial analysis of the data set was aimed at determining the relationship of my sequence data to a larger and more diverse group of eukaryotes, including most of the unidentified eukaryote environmental clones that shared high sequence similarity to the *M. rubra* and *M. pulex* cultures from Genbank. The analysis was performed using minimum evolution (ME) gamma (Γ)-corrected (4 category: 0.5576) distance maximum likelihood (DML) analysis, with proportion of invariable sites (pinvar: 0.1079), estimated base frequencies (A: 0.2568, C: 0.2131, G: 0.2856, T: 0.2445), and the general time-reversible (GTR) model for base substitutions (A-C: 1.2673, A-G: 2.4762, A-T: 1.4931, C-G: 0.9709, C-T: 34.2604, G-T: 1), selected using Modeltest version 3.04 (Posada and Crandall 1998). For this analysis 57 ingroup taxa and 8 outgroup taxa were used. Heuristic searches (25x) were performed using step-wise random addition and tree bisection-reconstruction (TBR) branch swapping.

For the maximum likelihood analyses I first ran a distance analysis to estimate base frequencies (A: 0.29258, C: 0.19152, G: 0.24914, T: 0.26676) and GTR substitution rates (A-C: 1.06649, A-G: 2.5439, A-T: 1.46564, C-G: 1.18343, C-T: 3.99694, G-T: 1) using stepwise addition and 25x random addition heuristic searches with TBR. These values were then used for a Γ-corrected (0.5444) maximum likelihood (ML) analysis with pinvar (0.14153), using stepwise addition and a 10x random addition heuristic search. This analysis included 26 ingroup taxa and 6 outgroup taxa. The ML tree was found 10 of 10 times with a score of 15334.84. Bootstrap analysis was performed on all

trees, with the respective initial model, on one hundred resampled datasets using stepwise addition and a 2x random addition heuristic search. All phylogenetic analyses were conducted in PAUP* version 4.0b (Swofford 1999).

Fluorescence *in situ* hybridization and confocal microscopy

A fluorescence *in situ* hybridization (FISH) oligonucleotide probe, Myr2, labeled with 5-N-N'-diethyl-tetramethylindo*di*carbocyanine (Cy5) (see Table 1 for sequence) for *M. rubra* and *M. pulex* was designed by eye from DNA alignments using MacClade. All probes were ordered from Qiagen, and tested using Primer Express 1.0 (Applied Biosystems) for possible complications due to secondary structure. A positive control probe (uniC) labeled with fluoroscein isothiocyante (FITC) was used, capable of labeling all eukaryotic SSU rRNA present in cells. Negative control probes included an anti-sense (reverse) probe of Myr2, called Myr2-neg (Cy5), as well as the anti-sense probe of the universal probe uniC, called uniR (FITC). Both uniC and uniR were designed by Scholin et al. (1996) (see also Miller and Scholin 1998). To preserve *M. rubra* and *M. pulex* cells for hybridization they were added to 4% paraformaldehyde with 5X SET (0.75 M NaCl, 5mM EDTA, 0.1M Tris-HCl, pH 7.8). Cells were fixed for 12-24 hr prior to hybridization. The FISH protocol was adopted from Miller and Scholin (1998). Preserved cells were gently filtered onto a 2.0 μm nucleopore filter, using a 5 μm backing filter, and washed twice with hybridization buffer (final concentration: 5x SET, 1% IGEPAL-CA630, 31.25 μg/ml polyadenylic acid). Cells were resuspended in 0.5 ml of hybridization buffer and 5 ng/μl of probe was added. All hybridizations were conducted

at 45ºC (determined empirically) in a water bath, for 1-2 h. After hybridization, cells were filtered onto a new membrane and washed several times with 45ºC 5x SET. Cells were then resuspended in 45ºC 5X SET and incubated for 2-3 minutes, after which the cells were filtered and resuspended in 1 ml fresh 5X SET buffer and stored at 4ºC in the dark until used for microscopy (<3h).

A Zeiss LSM 510 confocal system attached to a Zeiss inverted microscope, fitted with a C-Apochromat 63x/1.2 W lens, was used for viewing the FISH labeled cells. Cells were added to a slide chamber and at least 50 cells for each treatment were observed by optically sectioning through the cell. Single scan or Z-stack imaging analysis was preformed through several representative cells for capturing images. Images were captured using the multi-channel option at three wavelength settings: 1) blue light (for FITC) excitation (ex) 488nm, 2) far red (for Cy5) ex 633nm, and 3) green (for phycoerythrin in chloroplasts) ex 543nm. Emission filters for each channel were as follows: blue: band pass 505-560nm, far-red: long pass (LP) 650nm, and green: LP 560nm.

Genbank accession numbers

(U27500) *Alexandrium ostenfeldii*, (AF239260) *Amoebophrya* sp., (AF472555) *Amoebophrya* ex *Scrippsiella* sp., (AF274256) *Amphidinium semilunatum*, (AF283305) *Astasia longa*, (AF548006) *Babesia canis*, (AB049999) *Babesia rodhaini*, (AF029763) *Balantidium coli*, (AF317831) *Blepharisma americanum*, (33317834) *Bodo designis*, (33330170) *Cercomonas* sp., (AB062703) *Chaetomorpha moniligera*, (AB080308)

Chlorella vulgaris, (CHU97109) *Coleps hirtus*, (M97908) *Colpoda inflata*, (AB022819) *Costaria costata*, (AJ007275) *Cyanoptyche gloeocystis*, (AF111184) *Cyclospora cercopitheci*, (L19080) *Cytauxzoon felis*, (AF488386) *Dasya sinicola*, (U57771) *Didinium nasutum*, (AB073117) *Dinophysis acuminata*, (4680238) *Diplonema papillatum*, (AF339490) *Eimeria dipodomysis*, (AF339492) *Eimeria peromysci*, (M87327) *Emiliania huxleyi* , (29466123) *Euglena pisciformis*, (AJ305255) *Euplotes crassus*, (U97110) *Frontonia vernalis*, (AY187925) *Geleia fossata*, (AF274258) *Gonyaulax cochlea*, (U17354) *Ichthyophthirius multifiliis*, (AF029762) *Isotricha prostoma*, (AF272046) *Karlodinium micrum* (= *Gyrodinium galatheanum*), (L31519) *Loxodes magnus*, (L26448) *Loxophyllum utriculariae*, (U73232) *Mallomonas striata*, (AF153206) *Mastigamoeba invertens*, (33309658) *Massisteria marina*, (AJ535164) *Nitzschia frustulum* , (AF022200) *Noctiluca scintillans*, (AF123294) *Ochromonas sphaerocystis* , (Y10570) *Odontella sinensis* , (AB033717) *Oxyrrhis marina*, (AF100314) *Paramecium bursaria*, (AJ310495) *Pattersoniella vitiphila*, (AB058362) *Pavlova lutheri*, (AY033488) *Pfiesteria piscicida*, (AJ277877) *Phacodinium metchnikoffi*, (U93235) *Plasmodium vivax*, (AF099183) *Polarella glacialis*, (AF342746) *Porphyra leucosticta*, (AJ421145) *Porphyridium aerugineum*, (PVU97111) *Prorodon viridis*, (AJ246269) *Prymnesium parvum* , (U53127) *Rhodomonas abbreviata* (nucleomorph), (U53128) *Rhodomonas abbreviata*, (AF176940) *Sarcocystis hirsute*, (AJ428106) *Staurastrum lunatum*, (AF357913) *Stentor roeseli*, (AH009986) *Sarcocystis neurona*, (AF462060) *Skeletonema pseudocostatum*, (33309650) *Sponogomonas* sp., (U97112) *Strombidium purpureum*, (AJ511862) *Tetrahymena* sp., (L02366) *Theileria parva*, (L31520) *Tracheloraphis* sp., (38304358) *Trypanosoma avium*, (AF290065) uncultured marine

eukaryote DH145-EKD11, (27802617) Uncultured eukaryote clone CCW100, (27802608) Uncultured eukaryote clone CCW75, (AY331783) Uncultured marine eukaryote clone m110, (AY331778) Uncultured marine eukaryote clone m43, (AY331777) Uncultured marine eukaryote clone m112.

Results

SSU rRNA gene characteristics

The rDNA genes amplified for the Antarctic and Chesapeake Bay *M. rubra* and the Chesapeake Bay *M. pulex* were highly divergent compared to other ciliates and alveolates in general. The rDNA sequences for both *Myrionecta* and *Mesodinium* were relatively short, 1548 and 1543 bp respectively, compared to an average for alveolates of about 1750. This was primarily due to coincident deletions in the gene, for both taxa, in helices 10 (variable region [V] 2) (~20bp), 11 (~9 bp), E23-1-7 (V4) (~35bp), E23-14 (V4) (absent), and 43 (V7) (~23bp) (based on Wuyts et al. 2000 model). Furthermore both taxa have numerous substitutions in helices 8, 16, 18, 25, and 26 compared with all other alveolate taxa.

In situ hybridization analysis

Due to the highly unusual nature of the *Myrionecta* and *Mesodinium* sequences I used fluorescent *in situ* hybridization (FISH) to determine whether these sequences

originated from the ciliates in question. In addition, confocal laser scanning microscopy (CLSM) was used to localize probe binding to the nucleolus, in order to verify that the probes were hybridizing to the targeted genome. An oligonucleotide probe (Myr2) was designed from a variable region of the SSU rRNA molecule common to both *Myrionecta* and *Mesodinium*, but with numerous substitutions in other alveolates and distantly related taxa (Table 2). I found that the Myr2 probe always bound to rRNA within the ciliate cytoplasm and the nucleolus of the ciliate nuclei (Figures 1D3, 2D3), and never to RNA in other taxa (data not shown). Many *M. rubra* cells also possessed nuclei of their cryptophyte prey, *Geminigera cryophila*, to which no binding of the Myr2 probe was observed (data not shown). The macronuclei of both ciliates were found to have a single large nucleolus or sphere filled with rRNA that comprised much of the volume of each macronucleus (Figure 1B3,D3). The universal eukaryotic positive control probe uniC, labeled rRNA throughout the cell cytoplasm and within the nucleoi of all nuclei, including those of cryptophyte prey when present (Figures 1B3, 2B3). No binding of any probes to nuclear DNA within the ciliates could be detected, nor of any negative control probes to any portion of the cell. Negative control probes consisted of antisense probes for both the universal eukaryote RNA probe (uniR) (Figures 1A1-4, 2A1-4), and the *Myrionecta/Mesodinium* probe (Myr2-neg) (Figures 1C1-4, 2C1-4).

Phylogenetic analysis

The *Myrionecta/Mesodinium* SSU rDNA sequences share high sequence similarity (7% sequence difference, Table 1) in addition to the above-mentioned common

deletions, and formed a well-supported clade in all analyses (100% bootstrap support, Figures 3,4). In preliminary phylogenetic analyses of these sequences using distance and maximum parsimony methods, the *Myrionecta*/*Mesodinium* clade consistently grouped with other highly divergent sequences (e.g. *Plasmodium vivax*, *Oxyrrhis marina*), a result that can be attributed to branch-length effects (data not shown). In order to eliminate these effects, I removed ambiguously aligned regions of the data set and proceeded with maximum likelihood methods.

A matrix of 65 assorted protist taxa of 1474 characters and about 1300 nucleotides (923 were parsimony informative) was used for a Γ-corrected distance-maximum likelihood (DML) search (general time reversible model) with proportion of invariable sites. In this analysis *Myrionecta*/*Mesodinium* clade branched within the ciliates, albeit with low bootstrap support (64%) (Figure 3). Included in this analysis were several unidentified eukaryote clones with high sequence similarity to the *Myrionecta/Mesodinium* sequences, and the Chesapeake Bay *M. rubra* sequence (Table 1). These environmental taxa grouped strongly with the *Myrionecta* and *Mesodinium* cultures (100% bootstrap support), revealing the likely source of these clones (Figure 3). All previous analyses of these environmental clones, in the absence of the *Myrionecta/Mesodinium* sequences, had placed them outside of the alveolates with divergent amoeboid taxa. Of the six environmental clones that grouped with *Myrionecta* and *Mesodinium*, five appeared to be closely related to *M. rubra*, with high % sequence identity (96-98%) and alignment bit score (S'), while one (CCW75) was most similar to *M. pulex* (98%) (Table 1).

A full ML analysis was then conducted on a nearly identical matrix (1479 bp) greatly reduced in taxa (32 taxa) and composed mostly of alveolate taxa. This Γ-corrected ML (GTR model) analysis with pinvar also revealed low bootstrap support to group the *Myrionecta*/ *Mesodinium* clade within the ciliates (55%) and alveolates (68%) (Figure 4). In the ML-tree the ciliates, dinoflagellates, and apicomplexans all form monophyletic groups within the alveolates. The *Myrionecta*/*Mesodinium* clade appears with the Karyorelictids and the Heterotrichs as the sibling group to all other ciliates. The other ciliate groups formed a clade that received considerably higher bootstrap support (96%) then these basal taxa, and removal of the *Myrionecta /Mesodinium* sequences resulted in substantially higher maximum likelihood bootstrap support for the ciliates as a whole (97%; data not shown). The basal placement of *Myrionecta*/ *Mesodinium* was surprising given the traditional placement of *Myrionecta* and *Mesodinium* within the Litostomatea, raising the possibility that the model-based methods did not fully compensate for branch-length effects.

Discussion

Myrionecta and *Mesodinium* (Mesodiniidae) belong to the Litostomatea, subclass Haptorida (Lynn and Small 2000). Krainer and Foissner (1990) reclassified the order Cyclotrichida Jankowski 1980, family Mesodiniidae Jankowski 1980, as having the genera *Askenasia*, *Rhabdoaskenasia*, *Mesodinium*, and *Myrionecta*. However, Lynn (1991) remarked that the somatic ciliature of *Mesodinium* are so dramatically different

from any other litostomes that, if it is a litostome, it "has diverged significantly from the ancestral stock". Based on my SSU rDNA sequences of *Myrionecta* and *Mesodinium* it is clear that either these ciliates do not belong to the Litostomatea, or that their SSU rDNA genes have diverged so greatly as to make them a poor phylogenetic marker. Litostomes generally form a well-supported monophyletic clade within the ciliates and share the somewhat diagnostic deletions of helix E23-5 and portions of variable region 4 in the SSU rRNA gene (Wright et al. 1997). While *M. rubra* and *M. pulex* clearly have more extensive deletions and much higher substitution rates, an accurate placement of these taxa within the ciliates will require additional sequence data from other genes.

Due to the highly divergent nature of these sequences, I checked their validity using fluorescent *in situ* hybridization (FISH) and confocal laser microscopy (CLSM). FISH probes have been used successfully to differentiate closely related species of *Euplotes* ciliates that appear morphologically similar (Petroni et al. 2003). I found that the use of CLSM with FISH adds an additional level of confidence in determining that a probe is binding to a target genome, with the ability to localize binding of the probe to RNA within the nucleolus. The FISH/CLSM results clearly show that the probes designed for *Myrionecta* and *Mesodinium,* from highly variable and therefore taxon-specific regions hybridize to rRNA both within the cytoplasm of the cells and the ciliate macronucleus (Figures 1D3, 2D3).

The sequences determined in this study for *M. rubra* and *M. pulex* are highly divergent and of great phylogenetic interest. Only after removing nearly all ambiguously aligned regions of the rDNA alignment was I able to find support for these sequences within the ciliate clade. The initial affiliation of the *Myrionecta/Mesodinium* sequences

with other divergent taxa using certain distance and maximum parsimony methods in my analysis was removed by more robust phylogenetic methods. This suggests that branch length may have been an important factor in previous analyses of similar environmental sequences that resulted in an affiliation to amoeboid taxa (i.e. Lòpez-Garcia et al. 2001, Stoeck and Epstein 2003, Savin et al. 2004). Long branch attraction (LBA) has been used to explain the phenomena of seemingly unrelated but fast-evolving taxa being drawn to one another in a tree (Philippe and Laurent 1998).

These results are by no means a decisive characterization of the phylogenetic position of this group. It is possible that the rDNA gene may not be a useful one for interpreting the phylogeny of *Myrionecta* and *Mesodinium* due to their highly accelerated substitution and deletion rates. Therefore the grouping of *M. rubra* and *M. pulex* with Karyorelictids and Heterotrichs has to be treated with some caution. While rDNA genes of ciliates generally have typical eukaryotic substitution rates (e.g. Van de Peer and Wachter 1997), other ciliate genes have been shown to have high rates of sequence divergence, such as the elongation factor 1α (EF-1α) (Moreira et al. 1999), actin (Villalobo et al. 2001), and histone (H4) (Berhard and Schlegel 1998, Katz et al 2004) genes. The resulting long branch lengths of the rDNA gene for *Myrionecta* and *Mesodinium* are one of the more dramatic found thus far in the alveolates, a group already known for high genetic diversity and long branches. In other phylogenetic clades, particularly those of symbiotic or parasitic organisms, long branches have been explained by asexuality and population bottlenecks enhancing rDNA substitution rates, relaxed selection on rDNA structure, or positive selection for sequence change (Stiller and Hall 1999). In the free-living heterotrophic dinoflagellate *O. marina*, accelerated evolutionary

rates are also found in the rDNA gene, yet several protein-encoding genes (actin, α-tubulin and β-tubulin) appear to be equally as divergent as other dinoflagellate homologues (Saldarriaga et al. 2003). The protein-encoding phylogenies of *O. marina* lend support to several plesiomorphic cellular characteristics and place it at the base of the dinoflagellates near the Perkinsids, while the SSU rRNA gene groups it with *Gonyaulax* as a more recent branch in the dinoflagellate tree (Saldarriaga et al. 2003). While my data suggest that the *Myrionecta*/*Mesodinium* clade may also be an early and divergent branch of its phylum, like *O. marina*, the highly divergent rRNA gene phylogeny of these ciliates could contradict future protein phylogenies. However, additional support for an alternative taxonomic classification for *Myrionecta* and *Mesodinium* may also stem from several unusual phenotypic characteristics. These include the presence of feeding tentacles with a unique 14-microtubule structure (Lindholm et al. 1988), the complete absence of alveoli, an unusual somatic ciliature arrangement, and an unusual nuclear arrangement (two macronuclei and one micronuclei) (Taylor et al. 1971), all of which are synapomorphic within the Litostomatea. Currently I am working towards determining the sequence of several protein-encoding genes for these taxa and accumulating phenotypic data, in order to test these hypotheses.

Recent studies of amplified and sequenced rDNA from ocean samples have revealed a great deal of uncharacterized genetic diversity (e.g. López-Garcia et al. 2001, van der Staay et al. 2001, Dawson and Pace 2002). Within this recently discovered diversity, alveolates have been among the most frequently recovered sequences (Moreira and López-Garcia 2002). These studies have been valuable in identifying new branches of genetic diversity on familiar lineages of organisms. However, not all of these novel

sequences may be novel organisms. I found several sequences within Genbank purporting to represent novel eukaryotic diversity, which are closely affiliated or nearly identical to the *Myrionecta* and *Mesodinium* sequences. These environmental sequences have been determined from diverse habitats, including deep Antarctic water (López-Garcia et al. 2001), surface water from the Bay of Fundy, CAN (Savin et al. 2004), and microaerobic water samples from Cape Cod, USA, (Stoeck and Epstein 2003). I have determined nearly identical partial sequences from cells of *M. rubra* isolated from Chesapeake Bay. *Myrionecta* and *Mesodinium* have a cosmopolitan oceanic, estuarine, and fresh water (for *Mesodinium*) distribution (Taylor et al. 1971, Foissner et al. 1999). Therefore the wide geographical and ecological diversity of sites with matching environmental clones is not surprising. The presence of *M. rubra* in microaerobic water is also not unusual, as *M. rubra* has been observed to congregate near anoxic boundary layers in stratified waters (Lindholm and Mörk 1990). In all of the above studies, clones matching the *Myrionecta* sequence are described as having uncertain phylogenetic ascription, and are weakly affiliated with various amoeboid organisms such a *Mastigamoeba* (Lòpez-Garcia et al. 2001, Stoeck and Epstein 2003, Savin et al. 2004). I believe that these results were due primarily to branch length effects that were alleviated in the present study by removal of ambiguously aligned regions and using maximum likelihood methods.

In using sequence analysis alone, the artificial phylogenetic affiliation of *Myrionecta* and *Mesodinium* with other divergent taxa is perhaps unavoidable, due to the extremely divergent nature of their SSU rDNA. Only by working with cultures and employing FISH probes was it apparent that these sequences belong to the respective ciliates and not to parasites or contaminants, as I initially suspected. While it is unclear if

my analysis of the SSU rRNA genes of these ciliates has succeeded in determining their true phylogenetic position, it has revealed a striking example of divergent sequence evolution within the ciliates.

References

Altschul SF, Gish W, Miller W, Myers EW, Lipman DJ (1990) Basic local alignment search tool. J Mol Biol 215: 403-410

Bernhard D, Schlegel M (1998) Evolution of histone H4 and H3 genes I different ciliate lineages. L Mol Evol 46: 344-354

Darwin C (1839) Journal of researches into the geology and natural history of the various countries visited by the HMS Beagle under the command of Captain Fitzroy, R.N. from 1832-1836. 1st edition. Henry Colburn, London

Dawson SC, Pace NR (2002) Novel kingdom-level eukaryotic diversity in anoxic environments. PNAS 99: 8324-8329

Dolan JR, Coats DW (1991) A study of feeding in predacious ciliates using prey ciliates labeled with fluorescent microspheres. J Plank Res 13: 609-627

Foissner W, Berger H, Schaumburg J (1999) Identification of limnetic planktonic ciliates. Informationsberichte des Bayer. Landesamtes für Wasserwirtschaft, Heft 3/99, 793pp

Guillard RRL (1975) Culture of phytoplankton for feeding marine invertebrates. In Smith WL, Chanley MH (eds) Culture of marine invertebrate animals. Plenum Publishing Corp, New York, pp 29-60

Gustafson Jr DE, Stoecker DK, Johnson MD, Van Heukelem WF, Sneider K (2000) Cryptophyte algae are robbed of their organelles by the marine ciliate *Mesodinium rubrum*. Nature 405: 1049-1052

Hibberd, DJ (1977) Observations on the ultrastructure of the cryptomonad endosymbiont of the red water ciliate *Mesodinium rubrum*. J Mar Biol Assoc UK 57: 45-61

Jankowski AW (1976) Revision of the classification of the cyrtophorids. In Markevich AP, Yu I (eds) Materials of the II All-union Conference of Protozoology, Part I, general protozoology, Naukova Dumka, pp 167-168

Jiménez R, Intriago P (1987) Observations on blooms of *Mesodinium rubrum* in the upwelling area off Ecuador. Oceanol Acta Special issue No 6: 145-154

Katz LA, Bornstein JG, Lasek-Nesselquist E, Muse SV (2004) Dramatic diversity of ciliate histone H4 genes revealed by comparisons of patterns of substitutions and paralog divergences among eukaryotes. Mol Biol Evol 21: 555-562

Krainer KH, Foissner W (1990) Revision of the genus *Askenasia* Blochmann, 1895, with proposal of two new species, and description of *Rhabdoaskenasia minima* N G, N Sp (Ciliophora, Cyclotrichida). J Euk Microb 37: 414-427

Leander BS, Kuvardina ON, Aleshin VV, Mylnikov AP, Keeling PJ (2003) Molecular phylogeny and surphase morphology of *Copodella edax* (Alveolata): Insights into the phagotrophic ancestral of apicomplexans. J Euk Microbiol 50: 334-340

Lee SY (2001) Unalignable sequences and molecular evolution. TRENDS Ecol Evol 16: 681-687

Lindholm T, Lindroos P, Mörk AC (1988) Ultrastructure of the photosynthetic ciliate *Mesodinium rubrum*. BioSystems 21: 141-149

Lindholm T, Lindroos P, Mörk AC (1990) Depth maxima of *Mesodinium rubrum* (Lohmann) Hamburger and Buddenbrock- Examples from a stratified Baltic Sea inlet. Sarsia 75: 53-64

López-Garcia P, Rodríguez-Valera F, Pedrós-Alió C, Moreira D (2001) Unexpected diversity of small eukaryotes in deep-sea Antarctic plankton. Nature 409: 371-656

Lynn DH (1991) The implications of recent descriptions of kinetid structure to the systematics of the ciliated protists. Protoplasma 164: 123-142

Lynn DH, Small EB (2000) Phylum Ciliophora. In Lee JJ, Leedale GF, Bradbury P, (eds) An illustrated guide to the protozoa. Society of Protozoologists, Lawrence, pp 477-478

Maddison WP, Maddison DR (1992) MacClade- analysis of phylogeny and character evolution. Sinauer, Sunderland, MA

Medlin L, Elwood HJ, Stickel S, Sogin ML (1988) The characterization of enzymatically amplified eukaryotic 16S-like rRNA-coding regions. Gene 71: 491-499

Miller PE, Scholin CA (1998) Identification and enumeration of cultured and wild *Pseudo-nitzschia* (Bacillariophyceae) using species-specific LSU rRNA-targeted fluorescent probes and filter-based whole cell hybridization. J Phycol 34: 371-382

Moreira D, Guyader HL, Philippe H (1999) Unusually high evolutionary rate of the elongation factor 1a genes from the Ciliophora and its impact on the phylogeny of eukaryotes. Mol Biol Evol 16: 234-245

Moreira D and López-Garcia P (2002) The molecular ecology of microbial eukaryotes unveils a hidden world. TRENDS Microbiol 10: 31-38

Oakley BR and Taylor FJR (1978) Evidence for a new type of endosymbiotic organization in a population of the ciliate *Mesodinium rubrum* from British Columbia. BioSystems 10: 361-369

Oldach DW, Delwiche CF, Jakobsen KS, Tengs T, Brown, EG, Kempton JW, Schaefer EF, Bowers HA, Glasgow Jr HB, Burkholder JM, Steidinger KA, Rublee PA (2000) Heterodouplex mobility assay-guided sequence discovery: elucidation of the small subunit (18s) rDNA sequences of *Pfiesteria piscicida* and related dinoflagellates from complex algal cultures and environmental sample DNA pools. PNAS 97: 4303-4308

Petroni G, Rosati G, Vannini C, Modeo L, Dini F, Verni F (2003) *In situ* identification by fluorescently labeled oligonucleotide probes of morphologically similar, closely related ciliate species. Microb Ecol 45: 156-162

Posada D, Crandall KA (1998) MODELTEST: testing the model of DNA substitution. Bioinformatics 14: 817-818

Ryther JH (1967) Occurrence of red water off Peru. Nature 214: 1318-1319

Saldarriaga JF, McEwan ML, Fast NM, Taylor FJR, Keeling PJ (2003). Multiple protein phylogenies show that *Oxyrrhis marina* and *Perkinsus marinus* are early branches of the dinoflagellate lineage. Int J Syst Evol Microbiol 53: 355-365

Savin MC, Martin JL, LeGresley M, Giewat M, Rooney-Varga J (in press) Planktonic diversity in the Bay of Fundy as measured by morphological and molecular methods. Microb Ecol

Scholin CA, Buck KR, Britschgi T, Cangelosi, Chavez FP (1996) Identification of *Pseudo-nitzschia australis* (Bacillariophyceae) using rRNA-targeted probes in whole cell and sandwich hybridization formats. Phycologia 35: 190-197

Snoeyenbos-West OL, Salcedo T, McManus GB, Katz LA (2002) Insights into the diversity of choreotrich and oligotrich ciliates (Class: Spirotrichea) based on genealogical analyses of multiple loci. Int J Syst Evol Microbiol 52: 1901-1913

Stiller JW, Hall BD (1999) Long-branch attraction and the rDNA model of early eukaryotic evolution. Mol Biol Evol 16: 1270-1279

Stoeck T, Epstein S (2003) Novel eukaryotic lineages inferred from small-subunit rRNA analysis of oxygen-depleted marine environments. Appl Eviron Microbiol 69: 2657-2663

Struder-Kypke MC, Lynn DH (2003) Sequence analysis of the small subunit rRNA gene conform the paraphyly of oligotrich ciliates sensu lato and support the monophyly of the subclass Oligotrichia and Choreotrichia (Ciliophora, Spirotrichea). J Zool 260: 87-97

Swofford DL (1999) PAUP*: Phylogenetic analysis using parsimony. Sinauer, Sunderland, MA

Taylor FJR, Balckbourn, DJ, Blackbourn, J (1969) Ultrastructure of the chloroplasts and associated structures within the marine ciliate *Mesodinium rubrum* (Lohmann). Nature 224: 819-821

Taylor FJR, Balckbourn, DJ, Blackbourn, J (1971) The red-water ciliate *Mesodinium rubrum* and its “incomplete symbionts”: a review including new ultrastructural observations. J Fish Res Bd Canada 28: 391-407

Tengs T, Dahlberg OJ, Shalchian-Tabrizi K, Klaveness D, Rudi K, Delwiche C, Jakobsen KS (2000) Phylogenetic analyses indicate that the 19’Hexanoyloxy-fucoxanthin-containing dinoflagellates have tertiary plastids of haptophyte origin. Mol Biol Evol 17: 718-729

Thompson JD, Gibson TJ, Plewniak F, Jeanmougin F, Higgins DG (1997) The CLUSTAL_X windows interface: flexible strategies for multiple sequence alignment aided by quality analysis tools. Nuc Acids Res 25: 4876-4882

Van de Peer Y, De Wachter R (1997) Evolutionary relationships among the eukaryotic crown taxa taking into account site-to-site rate variation in 18s rRNA. J Mol Evol 45: 619-630

Villalobo E, Perez-Romero P, Sanchez-Silva R, Torres A (2001) Unusual characteristics of ciliate actins Int Microbiol 4: 167-174

Wright A-DG, Dehority BA, Lynn DH 1997. Phylogeny of the rumen ciliates *Entodinium*, *Epidinium* and *Polyplastron* (Litostomatea: Entodiniomorphida) inferred from small subunit ribosomal RNA sequences. J Euk Microbiol 44: 61-67.

Wuyts J, De Rijk P, Van de Peer Y, Pison G, Rousseeuw P, De Wachter R (2000) Comparative analysis of more than 3000 sequences reveals the existence of pseudoknots in area V4 of eukaryotic small subunit ribosomal RNA. Nuc Acid Res 28: 4698-4708.

Table 1. Environmental clones in Genbank that are closely related to cultures of *Myrionecta rubra* and *Mesodinium pulex*

Clone or culture	accession number	base pairs	S'[a]		total gaps		% identity	
			MR[b]	MP[b]	MR	MP	MR	MP
Myrionecta rubra	AY587129	1543	--	--	--	28	--	93
Mesodinium pulex	AY587130	1548	--	--	28	--	93	--
CB-MR-25[c]	AY587131	662	--	--	10	22	97	90
DH145-EKD11	AF290065[d]	1474	1398	1052	7	14	98	91
CCW100	AY180041[e]	1518	1320	1046	9	14	96	91
CCW75	AY180032[e]	1519	1146	1357	10	11	92	98
M43	AY331778[f]	1137	937	640	1	16	98	92
M112	AY331777[f]	1173	1109	803	2	17	98	92
M110	AY331783[f]	1141	1028	759	5	20	98	91

[a] bit score from BLAST search, [b] *Myrionecta rubra* and *Mesodinium pulex*, [c] Chesapeake Bay, *Myrionecta rubra* clone (partial sequences), [d] Lòpez-Garcia et al. 2001, [e] Stoeck and Epstein 2003, [f] Savin et al. 2004

Table 2. Probe and target sequence for *Myrionecta rubra* and *Mesodinium pulex* and comparisons to other taxa; target region in bold and mismatches between target taxa and other taxa highlighted in gray.

Species	sequence
	Outgroup taxa
Mastigamoeba invertens	5′..GAAATTC**TTGGATTTATTAAAGAT**GAACTA..3′
Diplonema papillatu	5′..GAAATTC**TTAGATCGTAGGAAGAC**GAACTT..3′
Echinamoeba therma	5′..GAAATTC**TAGGATTAACTGAAAAC**AAACTA..3′
	Other alveolates
Dinophysis acuminata	5′..GAAATTC**TTGGATTTGTTAAAGAC**GGACTA..3′
Plasmodium vivax	5′..GAAATTC**TTAGATTTTCTGGAGAC**AAACAA..3′
	Other ciliates
Didinium nasutum	5′..GAAATTC**TTGGATTTATTAAAGAC**TAACGT..3′
Euplotes crassus	5′..GAAATTC**TTTGAAATATTAAAGAC**TAACTT..3′
Stentor roeseli	5′..GAAATTC**TATGATTTATTAAAGAC**GAACTT..3′
Loxodes magnus	5′..GAAATTC**TTGGATTTACTGAAGAC**CAACTA..3′
	Target taxa
Myrionecta rubra	5′..GAAATTC**TTGGACCGGACGAAGAC**GACCAG..3′
Mesodinium pulex	5′..GAAATTC**TTGGACCGGACGAAGAC**GATCAG..3′
	Probe
Myr2 probe	3′..-------**TTGGACCGGACGAAGAC**------..5′

Figure 1.1. Confocal laser scanning micrographs of several typical rRNA probe hybridizations to *Myrionecta rubra* cells. Figure description: Column A: eukaryotic antisense negative control probe (uniR); column B: universal-eukaryotic rRNA positive control probe (uniC); column C: *Myrionecta/Mesodinium* antisense negative control probe (Myr2-neg); column D: *Myrionecta/Mesodinium* probe for SSU rRNA gene (Myr2); images in each column are the same cell. Row 1: differential interference contrast (DIC) images; row 2 autofluorescence of plastids (em 543nm); row 3: probe-specific fluorescence (ex 488 or 633); row 4: rows 1-3 layered. CMN = ciliate macronucleus.

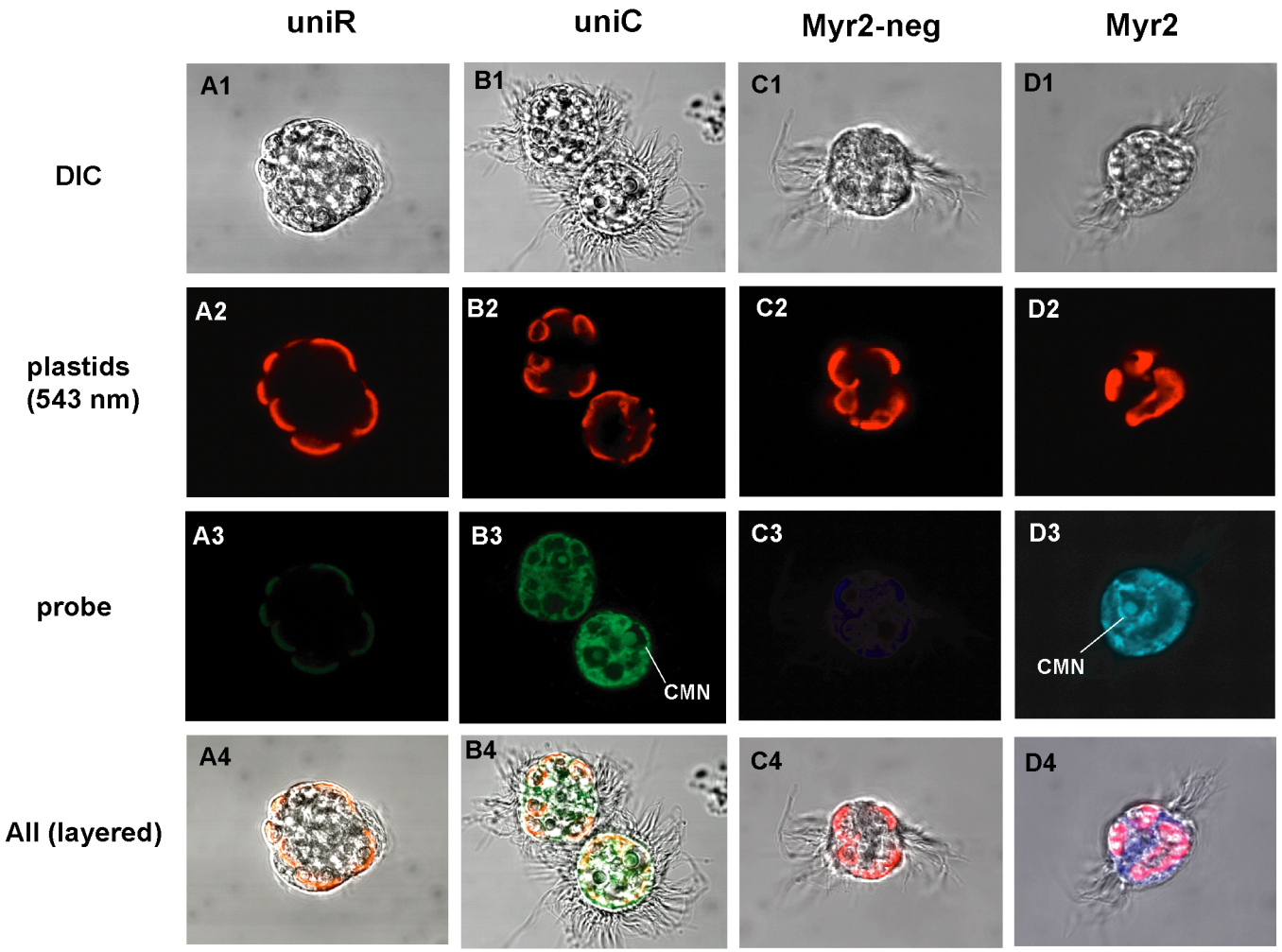
uniR
uniC
Myr2-neg
Myr2
DIC
plastids (543 nm)
probe
All (layered)
A1
B1
C1
D1
A2
B2
C2
D2
A3
B3
C3
D3
A4
B4
C4
D4
CMN
CMN

Figure 1.2. Confocal laser scanning micrographs of several typical rRNA probe hybridizations to *Mesodinium pulex* cells. Figure description: Column A: eukaryotic antisense negative control probe (uniR); column B: universal-eukaryotic rRNA positive control probe (uniC); column C: *Myrionecta/Mesodinium* antisense negative control probe (Myr2-neg); column D: *Myrionecta/Mesodinium* probe for SSU rRNA gene (Myr2); images in each column are the same cell. Row 1: differential interference contrast (DIC) images; row 2 autofluorescence of cryptophyte prey (em 543nm); row 3: probe-specific fluorescence (em 488 or 633); row 4: rows 1-3 layered. CMN = ciliate macronucleus.

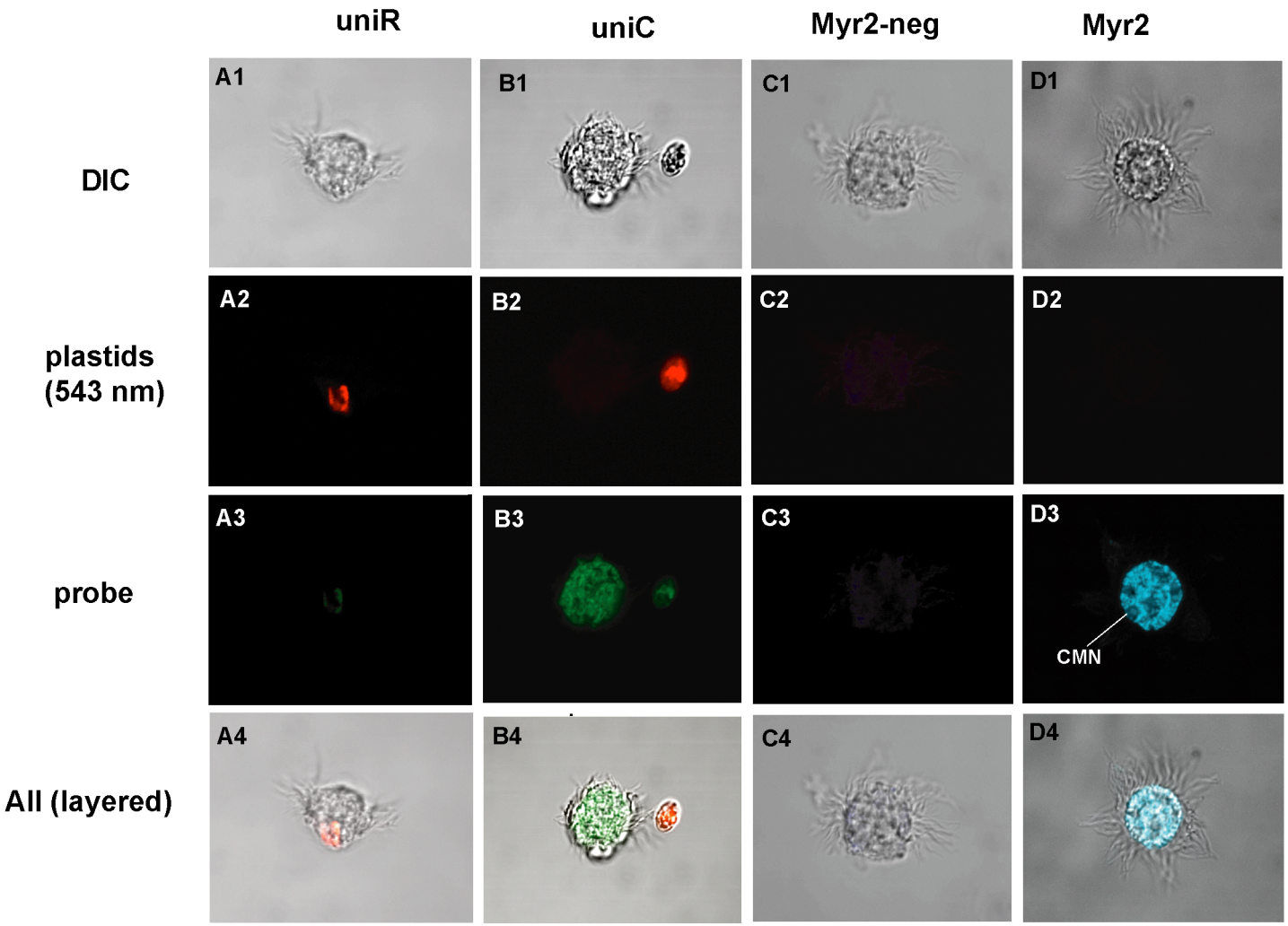
uniR
uniC
Myr2-neg
Myr2
DIC
plastids (543 nm)
probe
All (layered)
A1
B1
C1
D1
A2
B2
C2
D2
A3
B3
C3
D3
CMN
A4
B4
C4
D4

Figure 1.3. Gamma-corrected (Γ=0.5576) distance-maximum likelihood (ML) (GTR model) tree (minimum evolution) with proportion of invariable sites (0.1079), using a small subunit rDNA alignment of 1474 sites. ML parameters were estimated with Modeltest (Posada and Crandall 1998). Tree topology was found using stepwise addition and 25x heuristic searches with TBR branch swapping and random-addition sequences. Numbers on branches correspond to bootstrap values (100x with stepwise addition and heuristic searches with 2x random addition and TBR branch swapping).

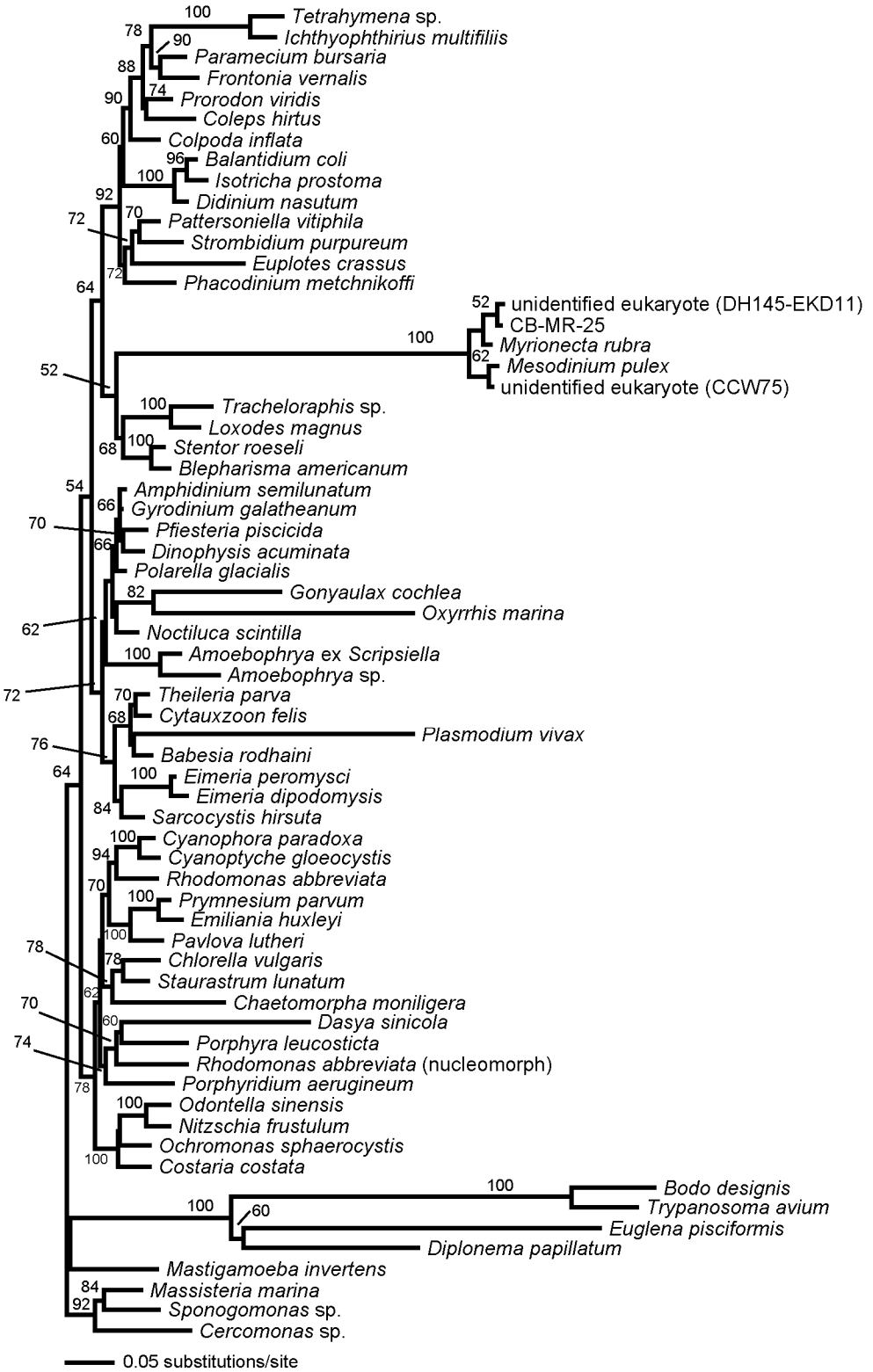
Tetrahymena sp.
Ichthyophthirius multifiliis
Paramecium bursaria
Frontonia vernalis
Prorodon viridis
Coleps hirtus
Colpoda inflata
Balantidium coli
Isotricha prostoma
Didinium nasutum
Pattersoniella vitiphila
Strombidium purpureum
Euplotes crassus
Phacodinium metchnikoffi
unidentified eukaryote (DH145-EKD11)
CB-MR-25
Myrionecta rubra
Mesodinium pulex
unidentified eukaryote (CCW75)
Tracheloraphis sp.
Loxodes magnus
Stentor roeseli
Blepharisma americanum
Amphidinium semilunatum
Gyrodinium galatheanum
Pfiesteria piscicida
Dinophysis acuminata
Polarella glacialis
Gonyaulax cochlea
Oxyrrhis marina
Noctiluca scintilla
Amoebophrya ex Scripsiella
Amoebophrya sp.
Theileria parva
Cytauxzoon felis
Plasmodium vivax
Babesia rodhaini
Eimeria peromysci
Eimeria dipodomysis
Sarcocystis hirsuta
Cyanophora paradoxa
Cyanoptyche gloeocystis
Rhodomonas abbreviata
Prymnesium parvum
Emiliania huxleyi
Pavlova lutheri
Chlorella vulgaris
Staurastrum lunatum
Chaetomorpha moniligera
Dasya sinicola
Porphyra leucosticta
Rhodomonas abbreviata (nucleomorph)
Porphyridium aerugineum
Odontella sinensis
Nitzschia frustulum
Ochromonas sphaerocystis
Costaria costata
Bodo designis
Trypanosoma avium
Euglena pisciformis
Diplonema papillatum
Mastigamoeba invertens
Massisteria marina
Sponogomonas sp.
Cercomonas sp.
0.05 substitutions/site

Figure 1.4. Gamma-corrected (Γ=0.5444) maximum likelihood (-lnL = 15334.84); GTR model) tree with proportion of invariable sites (0.14153) using a small subunit rDNA alignment of 1479 sites. Base frequencies and substitution rates were estimated with a distance-maximum likelihood search. Tree topology was found using stepwise addition and10x heuristic searches with TBR branch swapping and random-addition sequences. Numbers on branches correspond to bootstrap values (100x with stepwise addition and a heuristic search with 2x random addition and TBR branch swapping) for this ML tree.

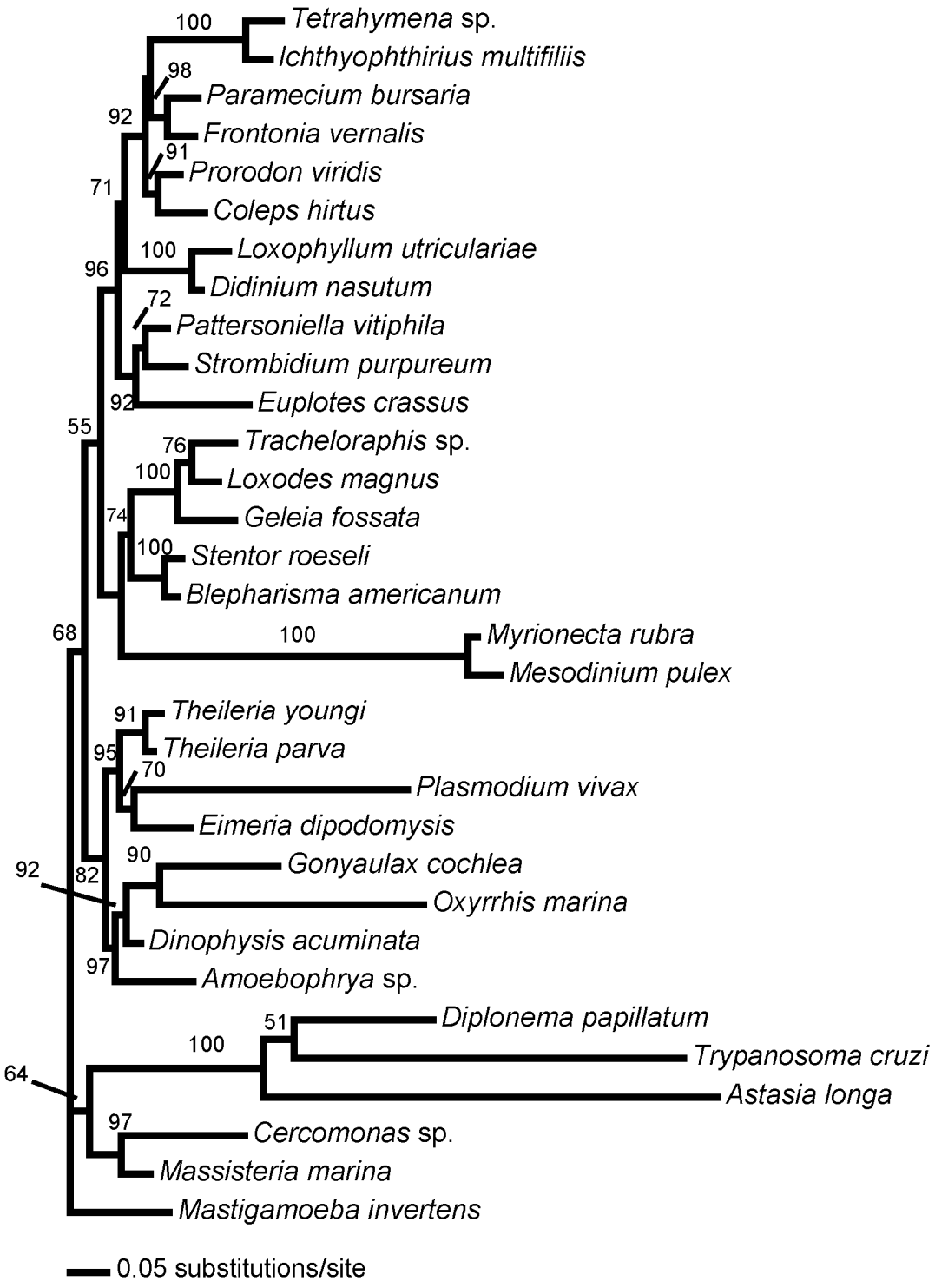
100
Tetrahymena sp.
Ichthyophthirius multifiliis
98
Paramecium bursaria
92
Frontonia vernalis
91
Prorodon viridis
71
Coleps hirtus
100
Loxophyllum utriculariae
96
Didinium nasutum
72
Pattersoniella vitiphila
Strombidium purpureum
92
Euplotes crassus
55
76
Tracheloraphis sp.
100
Loxodes magnus
74
Geleia fossata
100
Stentor roeseli
Blepharisma americanum
68
100
Myrionecta rubra
Mesodinium pulex
91
Theileria youngi
95
Theileria parva
70
Plasmodium vivax
Eimeria dipodomysis
92
82
90
Gonyaulax cochlea
Oxyrrhis marina
Dinophysis acuminata
97
Amoebophrya sp.
51
Diplonema papillatum
100
Trypanosoma cruzi
64
Astasia longa
97
Cercomonas sp.
Massisteria marina
Mastigamoeba invertens
0.05 substitutions/site

CHAPTER 2: The role of feeding in growth and the photophysiology of *Myrionecta rubra*

Abstract

Myrionecta rubra is a cosmopolitan estuarine and neritic ciliate, known to cause "red-water" blooms. The current study was conducted to better understand the relationship of photosynthetic performance and growth with feeding on cryptophyte algae in *M. rubra*. During the experiment the cryptophyte *Geminigera cryophila* was introduced for 2 consecutive growth periods (14 d each) and the cultures were then starved during 4 additional periods. In both high light (HL) and low light (LL) treatments, a significant decrease in per capita growth rates (μ) was observed over time ($p < 0.05$) in the absence of new prey. In the LL treatment chlorophyll content (chl cell^{-1}), photosynthetic capacity (P_{max}^{cell}), and photosynthetic efficiency (α^{cell}) increased after feeding and then declined during starvation. In the HL treatment, chl cell^{-1} and α^{cell} also increased and then declined after feeding, however, P_{max}^{cell} showed only a slight decrease with starvation. In both treatments *M. rubra* appeared to undergo an acclimation-like response following declines in chl cell^{-1}, with increases in P_{max}^{chl} and the light saturation parameter (I_k). While photosynthetic efficiency declined during starvation, overall photosynthetic capacity appeared to become uncoupled with growth over time. *M. rubra* demonstrated a high capacity for chl production (7-10 μg chl *a* ml^{-1} day^{-1}) after feeding, which decreased during starvation. Declines in growth and photosynthetic parameters coincided with the loss of prey nuclei from *M. rubra* cells, implicating a possible functional role for retained prey nuclei. These data show that *M. rubra* can function phototrophically for extended periods without ingesting prey, but that feeding is periodically required for optimal growth and photosynthesis, especially in high light.

Introduction

Myrionecta rubra (=*Mesodinium rubrum*) (Lohmann 1908, Jankowski 1976) (Mesodiniidae, Litostomatea) is a common phototrophic ciliate found in pelagic estuarine and neritic habitats (Taylor et al. 1971, Lindholm 1985, Crawford 1989). Blooms or "red tides" caused by *M. rubra* are recurrent events in numerous estuarine, lagoonal, and coastal upwelling zones around the world, sometimes expanding for hundreds of square kilometers (Lindholm 1985). While these blooms are nontoxic, they may induce hypoxia (Hayes et al. 1989) and on rare occasions have caused crustacean and mollusk kills during near-shore accumulations, perhaps due to irritation of gill tissue (Horstman 1981). Bloom dynamics of *M. rubra* are well studied and populations may undergo diel vertical migrations to exploit nutrient-rich water masses (Lindholm & Mörk 1990), optimal light levels (Passow 1991), and to maintain their retention within embayments (Crawford & Purdie 1992). *M. rubra* has extraordinarily high swimming speeds for a protist, capable of bursts of speeds over 8 mm s^{-1} or nearly 200 body lengths s^{-1} (Lindholm 1985, Crawford & Purdie 1992) and diurnal vertical migrations of 40 m (Smith & Barber 1979). Discrete deep layers of *M. rubra* have been shown to occur in the Baltic (Setälä & Kivi 2003) and Mediterranean Seas (Dolan & Marrasé 1996), to depths greater than 80m.

Myrionecta rubra has long been an evolutionary curiosity for possessing cryptophycean organelles, including plastids, mitochondria (Taylor et al. 1969, 1971), and sometimes nuclei (Hibberd 1977, Oakley & Taylor 1978). Gustafson et al. (2000) demonstrated that *M. rubra* feeds on cryptophyte algae to sequester organelles and to maintain enhanced photosynthetic and growth rates. Although *M. rubra* feeds to acquire

its plastids, its physiology drastically differs from that of other plastid sequestering ciliates. While plastid retaining oligotrich ciliates also require light for growth, they are unable to grow phototrophically (i.e. without prey) due to large heterotrophic requirements for growth (Stoecker et al. 1988, Putt 1990). In contrast, *M. rubra* has long been considered a functional phototroph due to its ability to form blooms, utilize dissolved inorganic nutrients (Packard et al. 1978, Wilkerson & Grunseich 1990), and the high photosynthetic rates associated with bloom events. Stoecker et al. (1991) found a large range (1.8-8.6 pg C (pg chl a)$^{-1}$ h^{-1}) of photosynthetic rates for *M. rubra* in estuaries and salt ponds in Falmouth, Massachusetts, USA. While much lower rates have been measured for cultured Antarctic *M. rubra*, 0.12-0.22 pg C (pg chl a)$^{-1}$ h^{-1} (Gustafson et al. 2000), these measurements were made at non-saturated photosynthetic irradiance levels (~30 μE m^{-2} s^{-1}) and low temperatures (≤ 5°C). Although feeding has been shown to greatly enhance growth rates of *M. rubra* (Gustafson et al. 2000, Yih et al. 2004), it remains unclear as to how long *M. rubra* is able to grow or persist without ingesting cryptophyte prey or how its photophysiology is related to feeding and starvation. Here I show that growth and photosynthetic performance are clearly linked to feeding, and that both processes diminish slowly over time and in relation to irradiance stress.

Methods

Culture and experimental conditions

Myrionecta rubra (CCMP 2563) and *Geminigera cryophila* (CCMP 2564) were isolated from McMurdo Sound, Antarctica, from a nutrient-enriched sample of sea ice and water collected in January 1996 (Gustafson et al. 2000). Cultures were grown in 1L glass flasks with 32 PSU F/2 -Si media (Guillard 1975), at 0-2° C. For normal culture maintenance, *M. rubra* is fed the cryptophyte *G. cryophila* periodically to maintain positive growth rates. In preparation for this experiment, cultures were allowed to acclimate to two 24 h light regimes, 2.5 μE m^{-2} s^{-1} (LL) and 55 μE m^{-2} s^{-1} (HL), for three months, while only receiving biweekly additions of F/2 media. Thus cell populations were starved for *G. cryophila* prey at the beginning of the experiment.

At the beginning of the experiment, *Myrionecta rubra* cultures were fed *G. cryophila* in period 1 with 3838 ±107 and 4399 ± 698 cells ml^{-1} and in period 2 with 3162 ± 21 and 3066 ± 350 cells ml^{-1}, for the HL and LL treatments, respectively (Figure 1). While no short-term sampling was conducted to measure grazing kinetics in this experiment, previous experiments with this culture have shown ingestion rates of 1.3 prey *M. rubra* $cell^{-1}$ h^{-1} and clearance rates of 128 nl $cell^{-1}$ h^{-1} (Gustafson et al. 2000). *M. rubra* concentrations at t =0 were 1266 ± 53 and 1420 ± 253 in period 1 and 718 ± 83 and 1244 ± 171 cells ml^{-1} in period 2, for HL and LL treatments, respectively. After period 2, *M. rubra* cells were only given fresh F/2 culture media every 2 weeks in order to establish starved cell populations (Figure 1). Experimental treatments each had three replicates. Growth rates were estimated during the exponential portion of the growth phase using μ (div d^{-1}) = $(\log_2(n_1/n_0))/t_1\text{-}t_0$, where n_0 and n_1 are cell concentrations at the beginning and start of the exponential growth phase, respectively.

Cellular attributes. Cell volume was determined by measuring cell length and width using a ocular micrometer on a Nikon Eclipse inverted microscope at 100x magnification, for at least 30 cells per replicate and time point. Cell volume was calculated using V (μm^3) = $(\pi/6)\cdot w^2 \cdot l$, where w is the cell width and l the length. Cell concentrations and nuclei were enumerated by staining glutaraldehyde-fixed (1% final conc.) cells with the nucleic acid stain, 4,6-diamidino-2-phenylindole (DAPI), and viewing cells at 100x magnification on a Nikon Eclipse compound microscope, equipped with a fluorescent light source, and Nikon filter sets EF-4 B-2A (exciter filter 450-490 nm, dichromatic beam splitter (DM) 500 nm, barrier filter (BA) 515 nm) and UV 2E/C (exciter filter 340-380 nm, DM 400 nm, BA 435-485 nm). Chlorophyll was extracted by filtering culture aliquots onto a GF/C filter and extracting overnight in 90% acetone at –20ºC. Chlorophyll concentrations were determined using a Turner Designs model 10-AU fluorometer.

Chlorophyll budget

Total ingested chlorophyll (chl^I) per period was calculated by measuring removal of free-living prey chl using the equation: $chl^I = [(\text{chl } a \text{ ml}^{-1})^{\text{prey}}_{t=14} - (\text{chl } a \text{ ml}^{-1})^{\text{prey}}_{t=0}] \cdot t^{-1}$, where t is the total number of days per period, and chl *a* ml^{-1} was determined by multiplying chl $cell^{-1}$ and cells ml^{-1}. The total chlorophyll budget (chl^B) for *M. rubra* was determined per period by using the equation: $chl^B = [(\text{chl } a \text{ ml}^{-1})^{MR}_{t=14} - (\text{chl } a \text{ ml}^{-1})^{MR}_{t=0}] \cdot t^{-1}$. Total chlorophyll production per period was then determined using $chl^P = chl^B - chl^I$.

Photosynthesis (^{14}C) measurements

Photosynthesis vs. irradiance (PE) measurements (Lewis & Smith 1983) were made on days 7 and 14 of each 2 week growth cycle, at 2ºC using a photosynthetron connected to a chiller. During periods 1 and 2 when *Geminigera cryophila* prey was present, PE measurements were only made when prey was at background levels (i.e. < 100 cells ml^{-1}) (Figure 1). Culture aliquots were removed and kept on ice around midday, and $NaH^{14}CO_3^-$ was added to a final activity of 1 $\mu Ci \cdot ml^{-1}$. At t = 0 controls were taken by adding 2ml of labeled culture immediately to a vial with 200µl of formalin, and used later for subtracting background levels of ^{14}C activity. Background and total activity controls were then placed in the dark at 4°C overnight. Samples for total activity were collected by adding 100 µl of sample to 200 µl of β-phenylethylamine (Sigma). ^{14}C spiked culture (2ml) was then added to 7ml scintillation vials, on ice, and immediately transferred to the chilled photosynthetron block. A total of 15 vials were used for each triplicate PE assay, and incubated for 30 min at constant irradiance between 0-800 µmol photons$\cdot m^2 \cdot s^{-1}$. At the end of the incubation, the vials were acidified with 500 µl 6N HCl to remove unincorporated ^{14}C, and placed on a shaker overnight at room temperature. In order to determine the ^{14}C activity of the vials, 4ml of Ultima Flo AP (Perkin Elmer, Boston, MA, USA) scintillation cocktail was added to the background control and light-exposed vials, while 5 ml was added to the total activity vials. All ^{14}C incorporation and control activities were determined using a Tri-Carb 2200CA liquid scintillation counter (Packard Bioscience, Meriden, CT, USA). Photosynthetic rates were determined using analytical methods described by Parsons et al. (1984), and PE data was normalized to hourly rates

and either cell or chlorophyll concentrations. Curve fitting for PE data was conducted in Sigma Plot (SPSS software, Chicago, IL, USA) using an equation based on Platt et al. (1980): photosynthesis (P) = $P_0 + P_s \cdot (1 - \exp((-E \cdot \alpha)/P_s)) \cdot \exp((-E \cdot \beta)/P_s)$, where P_0 is the y-intercept, P_s is the maximum potential rate of photosynthesis, α is the initial light-limited slope of the PE curve, E is the irradiance, and β is the slope of the photoinhibition region of the curve. From the curve-fitted data α, P_{max} (maximum rate of photosynthesis), I_k (photosynthesis-saturating light irradiance (I_k) = P_{max}/α), and β were determined. P_{max} and α rates are presented both as cellular (e.g. $P_{max}^{cell} = P_{max} \cdot ml^{-1}/cells \cdot ml^{-1}$) and chlorophyll (e.g. $P_{max}^{chl} = P_{max}^{cell}$ /chl $\cdot$ $cell^{-1}$) normalized rates in this study.

Data analysis

Statistical analysis of cell attributes and PE parameter data were conducted using the mixed model ANOVA and multiple regression options in SAS/STAT 9.0 (SAS Institute Inc., Cary, NC, USA), and $p < 0.05$ as a level of significance. Comparisons for ANOVAs between means were made between treatments (HL vs. LL) and over time using Tukey's Studentized range (HSD) test.

Results

Changes in cellular composition following feeding

More than 95% of added prey were removed in both treatments by day 14 for periods 1 and 2 (Figure 2A,B). Growth rates were highest while feeding, with the HL treatment reaching 0.19 d^{-1} and the LL treatment 0.11 d^{-1} (Figure 2C). At the end of period 2, *Myrionecta rubra* (MR) possessed 0.89 and 0.78 *Geminigera cryophila* nuclei $(MR\ cell)^{-1}$ in the HL and LL treatments, respectively (Figure 3). Cell shape and volume were highly variable in the HL treatment when exposed to *G. cryophila* prey. While the mean cell volume for HL cells over the course of the experiment was 4221 μm^3, maximum cell volume during period 1 and 2 reached 21435 and 13066 μm^3, respectively. These large cells, though rare, were sometimes irregularly shaped with multiple ciliary bands arising from different regions of the cell, and possessing numerous ciliate macronuclei (mac) and micronuclei (mic), as well as *G. cryophila* nuclei. Such cells were never observed in the LL treatment and may have been either an artifact due to higher light and/or cell division rates or perhaps due to sexual reproduction processes. LL cells averaged 3428 μm^3 during the entire experiment, and while maximum cell sizes reaching 13782 μm^3 during period 4, cell shape remained regular and such large cells were rare.

Changes in photophysiological parameters following feeding

In both treatments a dramatic rise in chl $cell^{-1}$ was observed following the introduction of prey (Figure 4). This increase was more sustained in the LL treatment, with chl $cell^{-1}$ apparently reaching a transient steady state during periods 3 and 4, averaging 45.9 ± 5.8 pg chl *a* $cell^{-1}$ during this time, without addition of new prey. Chlorophyll budgets were determined in order to assess relative contributions from

feeding vs. chl synthesis. Calculations of chlorophyll production (chl^{P}) for *Myrionecta rubra* during this study revealed that feeding is a minor source of chl, accounting for 15 and 14% in LL and 7 and 8% in HL of total chl^{P} (7000-10000 pg chl *a* ml^{-1} day^{-1}) for periods 1 and 2, respectively (Figure 5). In the LL treatment P_{max}^{cell} increased during and after the feeding periods, reaching 46 ± 4 pg C $cell^{-1}$ h^{-1}, and closely mirroring trends in chl $cell^{-1}$ during the experiment (Figure 6A). HL chl $cell^{-1}$ peaked at 28 ± 3 pg chl a $cell^{-1}$, but unlike the LL treatment these elevated concentrations were not maintained. HL P_{max}^{cell} rates showed less variation and peaked at 21 ± 3 pg C $cell^{-1}$ h^{-1} (Figure 6A). In both treatments α^{cell} increased after feeding to 0.55 ± 0.08 in the HL, and 1.74 ± 0.31 pg C $(cell)^{-1}$ $(\mu E\ m^{-2}\ s^{-1})^{-1}$ in LL (Figure 6B). P_{max}^{chl} steadily increased following feeding for both treatments, reaching a maximum of 1.18 and 1.46 pg C (pg chl a)$^{-1}$ h^{-1} for LL and HL, respectively, while α^{chl} did not reveal any obvious trend after feeding (Figure 7).

Changes in cellular composition during starvation

Following period 2, no new prey was added to either treatment and changes in cell parameters were observed during starvation for 6-8 additional weeks. The HL treatment was terminated after 6 weeks (5 periods total), due to having too few cells, while the LL treatment was continued to 8 weeks past feeding or 6 total periods. Prey nuclei $cell^{-1}$ declined in the absence of new prey, with under 10% of LL *Myrionecta rubra* cells possessing *Geminigera cryophila* nuclei by the final period (Figure 3). After 4 weeks without prey (period 4), μ for both treatments of *M. rubra* declined by nearly half of fed growth rates, to 0.072 ± 0.026 (HL) and 0.035 ± 0.009 (LL) d^{-1} (Figure 2C). By 6

weeks of starvation (period 5), no growth was observed in the HL treatment while μ remained relatively steady in the LL treatment through period 6 (~ 0.035 d^{-1}). Cell volume slightly declined in the HL treatment over time while volume increased in the LL treatment (data not shown).

Changes in photophysiological parameters during starvation

Chl $cell^{-1}$ remained at relatively constant levels in the LL treatment for about 4 weeks following period 2, despite no new additions of prey and positive growth rates for *Myrionecta rubra*. In the HL treatment chl $cell^{-1}$ continued to increase briefly in period 3 and then steadily declined during starvation to near pre-feeding levels (12.8 ± 3.4 pg chl *a* $cell^{-1}$) (Figure 4A). In the LL treatment chl $cell^{-1}$ also fell to pre-feeding levels (19.8 ± 2.6 pg chl *a* $cell^{-1}$) by period 6 (Figure 4B). Declines in chl $cell^{-1}$ were reflected in measurements of P_{max}^{cell}, however this was more pronounced in the LL treatment (Figure 6A). α^{cell} also declined during the starvation period. In the LL treatment α^{cell} was highly variable, however the pattern was similar to that observed for P_{max}^{cell} (Figure 6B). The HL treatment showed little variability in α^{cell} and, like P_{max}^{cell}, steadily declined with time. Increases in P_{max}^{chl} reached a maximum during period 5 for both treatments, at 1.86 ± 0.24 and 1.22 ± 0.14 pg C (pg chl *a*)$^{-1}$ (μE m^{-2} s^{-1})$^{-1}$ for the HL and LL, respectively, before leveling off in both treatments (Figure 7A). α^{chl} showed no clear pattern for either treatment during the experiment (Figure 7B). Data for the β parameter (slope of light saturated portion of PE curve) revealed low levels of photoinhibition for the LL treatment (mean β: 6.5 x 10^{-5} pg C (pg chl *a*) h^{-1}), while the HL treatment (mean β: -1.07 x 10^{-4} pg C

(pg chl *a*) h^{-1}) never reached photoinhibited levels (data not shown). Within both treatments β was highly variable, with no significant trend over time. However, overall β between treatments was significantly higher in LL vs. HL through periods 1-5 (paired T-test; $p = 0.0004$). The I_k parameter continued to increase throughout the starvation period, nearly doubling values from period 1 and reaching 60 and 40 μE m^{-2} s^{-1} for HL and LL treatments, respectively (Figure 6C).

Discussion

The physiology and survival strategy of *Myrionecta rubra* is unique. While other ciliated protists have been shown to sequester plastids and mitochondria from their prey (Johnson et al. 1995), none appear to retain prey nuclei or function completely as a phototroph. Plastidic ciliates are important members of marine and freshwater planktonic communities (Stoecker et al. 1987). In coastal marine and estuarine systems, *M. rubra* is frequently the dominant plastidic ciliate (e.g. Sanders 1995, Witek 1998, Sorokin et al. 1999) and the only species known to cause recurrent red water events. Other plastidic ciliates may also have high photosynthetic rates, but are predominantly mixotrophic (Stoecker et al. 1988). Putt (1990) found that most carbon acquired via photosynthesis in the oligotrich *Laboea strobila* was used for respiration, while ingested carbon was used primarily for growth. While many plastidic oligotrichs are obligate phototrophs, their plastids have short residence times (hours) and thus are highly dependent on phagotrophy not only for heterotrophic growth, but also to replace aging chloroplasts (Stoecker & Silver 1990). Clearly *M. rubra* is unique in this regard, in that it can grow

phototrophically for long periods without prey, and has capacity for substantial, albeit transient, pigment synthesis.

The effects of ingesting cryptophyte prey upon the photophysiological capacity of *Myrionecta rubra* in this study were immediate and dramatic. Chl cell^{-1} quickly increased for both HL and LL treatments when fed and resulted in maximum observed μ for this experiment. The dramatic rise in chl cell^{-1} and maintenance of elevated chl concentrations without further addition of prey, suggests a capacity for chl synthesis in *M. rubra* as shown previously by Gustafson et al (2000). While elevated chl cell^{-1} was maintained longer in LL, actual chl production for both treatments was nearly identical (Figure 5). The faster decline of chl cell^{-1} in HL (Figure 3) is most likely due to higher growth rates, and a lower acclimation state chl quotient (i.e. for acclimation to high light). While it is possible that the more precipitous decline in chl cell^{-1} and μ in HL treated cells were due to greater photooxidative stress than LL cells, I have no evidence to support such a conclusion. Despite dramatic changes in chl cell^{-1} over time, α^{chl} was relatively steady throughout the experiment for both treatments, suggesting no real loss in photosynthetic efficiency per unit chlorophyll over time (Figure 7B). That *Myrionecta rubra* is able to grow phototrophically (i.e. in the absence of prey) while synthesizing chl, suggests at least some transient capacity for maintaining and repairing sequestered plastids. Interestingly, *Geminigera cryophila* nuclei were retained by *M. rubra* and remained within the cell population for up to 6 weeks into the starvation period. These nuclei apparently do not undergo division in *M. rubra* and while > 90% of cells may have them after feeding the proportion of cells with prey nuclei is diluted through cell division. The absence of new prey and the eventual loss of prey nuclei from the population may

have resulted in loss of certain functions associated with plastid biosynthetic pathways, pigment synthesis and regulation.

As expected, highest rates for P_{max}^{cell} and α^{cell} closely followed maximum chl cell^{-1} levels, especially in the LL treatment. The photosynthetic rates measured here are somewhat modest for *Myrionecta rubra*, as previous measurements during blooms have shown extremely high chlorophyll-specific, light-saturated carbon assimilation rates of >10 pg C (pg chl a)$^{-1}$ h^{-1} (Smith & Barber 1979). The reason for this discrepancy may be that the Antarctic strain is grown at 4°C (PE curves at 2°C) and in constant light, both of which may decrease light saturated rates of photosynthesis (Cota et al. 1994). Indeed, light-saturated photosynthetic measurements of Antarctic *M. rubra* field populations are also relatively low at 1.04 pg C (pg Chl a)$^{-1}$ h^{-1}, falling within the range of those presented here (Satoh & Watanabe 1991). The increase in I_k with time is also attributable to chl cell^{-1} loss, and indicates a loss of steady state acclimation to experiment growth irradiance (Figure 6C). During the experiment I_k remained at or below growth irradiance for the HL treatment, while I_k was always higher than growth irradiance in LL. Overall I_k values were low, perhaps due not only to the relatively low growth irradiance used in this experiment, but also to adaptation to low temperature as seen with polar algae (e.g. Cota et al. 1994).

Myrionecta rubra cells in this experiment appeared to be acclimated to their respective irradiance regimes and regulate chl cell^{-1} levels to apparently optimize growth. While declines in P_{max}^{cell} over time can simply be explained by decreasing chl cell^{-1} during starvation, reasons for variation in P_{max}^{chl} are less obvious. However, increases in P_{max}^{chl}

for both treatments represented an increase in photosynthetic efficiency with time and the leveling off of P_{max}^{chl} coincided with a new, lower chl cell^{-1} steady state.

In this experiment maximum chl cell^{-1} and P_{max}^{cell} levels occurred after period 2 and were out of sync with maximum observed μ, perhaps indicating that growth for *Myrionecta rubra* is greatest after sequestering new organelles from cryptophyte algae. Alternatively, this imbalance with photosynthesis and growth may suggest that mixotrophy enhanced growth rates while feeding. To evaluate the importance of ingesting prey carbon I used C cell^{-1} measurements of the *Geminigera cryophila* culture (unpublished data) and observed prey removal (per day) during the first two periods. Maximum potential C contributions from ingestion were calculated as being 10.0 and 10.6% for HL and 10.8 and 8.8% for LL, of total growth requirements in periods 1 and 2, respectively. However, these calculations are probably gross overestimates as they assume total C assimilation and do not account for organelle retention. Therefore mixotrophic C gain from ingestion of cryptophyte prey does not account for the substantially higher growth rates observed when *M. rubra* is feeding. To further evaluate the C budget of *M. rubra*, I calculated carbon contributions from observed photosynthetic rates (C^P), prey removal rates (C^U), and estimated C cell^{-1} values (C^{cell}) (Menden-Deuer & Lessard 2000), to calculate mixotrophic gross growth efficiencies (GGE^M) during each period. Here I define GGE^M as G/C*·100, where G = C^{cell} · yield, and yield is the maximum population size during period (assuming no mortality) and C* = C^P + C^U. This estimate of GGE^M is therefore based on mixotrophic growth, as it includes parameters for both phototrophy (C^P) and heterotrophy (C^U). During the feeding period GGE^M were greatest, suggesting some enhancement of μ associated with feeding, while during late

starvation, GGE^M declined, indicating an imbalance between C assimilation and growth (i.e. a C sink) (Figure 8). Maximum GGE^M values were 52 and 74% for the HL and LL treatments, respectively. During starvation, the decline in GGE^M was dramatic in the HL treatment, approaching zero in period 5, while the LL treatment was near 30% (Figure 8). The total collapse of μ in the HL treatment, despite ongoing C fixation, suggests that *M. rubra* loses anabolic functions related to photosynthesis when starved from cryptophyte prey for long periods, and that fixed C is either stored or excreted. The difference in rates of GGE^M decline between treatments was perhaps due to greater photooxidative stress in the HL.

GGE for heterotrophic protists is generally between 40-60% (Caron and Goldman 1990). Skovgaard (1998) compared GGE of a heterotrophic dinoflagellate, *Gyrodinium* sp., to that of the similar sized plastid retaining dinoflagellate, *G. gracilentum*, finding 23-27% higher GGE in *G. gracilentum*. While optimal net growth efficiency (i.e. for fixed C) for some phototrophs can exceed 80% (Herzig and Falkowski 1989), plastid maintenance has been estimated to be a major energetic sink in phototrophs, requiring up to 50% of cell energy costs and resulting in lower growth rates compared to heterotrophs (Raven 1997). Thus in kleptoplastidic protists photosynthesis may be viewed as a luxury carbon source, resulting in higher GGE (e.g. Skovgaard 1998), and perhaps allowing cells to endure periods of limited prey availability (e.g. Blackbourn et al. 1973). When feeding and sequestering new plastids, *M. rubra* may benefit from reduced costs associated with plastid maintenance, and thus have higher growth rates. However, because *M. rubra* is capable of plastid division and long-term phototrophic growth, it does not gain a free photosynthetic "ride" as do other kleptoplastidic protists. Using data from Skovgaard

(1998) I calculated GGE^M for *G. gracilentum* to be ~48% in high irradiance (90 μmol photons m^{-2} s^{-1}). While this value is comparable to those obtained here for *M. rubra*, plastids in *G. gracilentum* were determined to be useful for only ~2 d (Skovgaard 1998). These comparisons underscore the paradoxical nature of *M. rubra*. While it functions as a phototroph and has the capacity to synthesize chlorophyll, it occasionally requires ingestion of prey to sequester new organelles. Thus, *M. rubra* defies comparison with most other functional classifications for protists.

I have shown that while *Myrionecta rubra* attains higher growth rates under HL conditions, cell populations have longer sustained growth under LL conditions. Under low temperature conditions as used in this study, respiration rates would be relatively low (Caron et al. 1990) and therefore survival under prolonged starvation may be longer than that expected for cells grown at higher temperatures. Low respiration rates under polar conditions and the ability, shown here, of *M. rubra* to survive and even grow at low photosynthetically active radiation levels (PAR), may explain how populations of *M. rubra* can remain active during winter in certain regions of Antarctica. During winter in Ace Lake, a brackish lake in Antarctica, PAR at 2 m under ice is <1μE m^{-2} s^{-1} and active populations of *M. rubra* have been shown to occur at up to 80 cells ml^{-1}. Studies in temperate regions have shown *M. rubra* cells to form discrete layers at great depths (Setälä & Kivi 2003). Furthermore, recurrent blooms of this ciliate have been shown to occur at dynamic boundaries in various upwelling regions (i.e. Ryther 1967), or following stratification in partially mixed estuaries (i.e. Crawford et al. 1997), or in fjords (i.e. Fenchel 1968, Lindholm 1978) around the world. These observations and photophysiological measurements shown here suggest that *M. rubra* may be adapted for

survival under low light conditions, while thriving for shorter periods in high light. In conclusion, while feeding on cryptophyte algae ultimately limits growth and photosynthetic performance in *M. rubra*, the ciliate is able to function for long periods as a phototroph before feeding again.

References

Blackbourn DJ, Taylor FJR, Blackbourn J (1973) Foreign organelle retention by ciliates. J Protozool 20: 286-288

Caron DA, Goldman JC (1990) Protozoan nutrient regeneration. In: Capriulo GM (ed) Ecology of marine protozoa. Oxford Univ Press, New York

Caron DA, Goldman JC, Fenchel T (1990) Protozoan respiration and metabolism. In: Capriulo GM (ed) Ecology of marine protozoa. Oxford Univ Press, New York

Cota GF, Smith WO Jr, Mitchell BG (1994) Photosynthesis of *Phaeocystis* in the Greenland Sea. Limnol Oceanogr 39: 948-953

Crawford DW (1989) *Mesodinium rubrum*: the phytoplankter that wasn't. Mar Ecol Prog Ser 58: 161-174

Crawford DW, Purdie DA (1992) Evidence for avoidance of flushing from an estuary by a planktonic, phototrophic ciliate. Mar Ecol Prog Ser 79: 259-265

Crawford DW, Purdie DA, Lockwood APM, Weissman P (1997) Recurrent red-tides in the Southampton Water Estuary by the phototrophic ciliate *Mesodinium rubrum*. Estuar Coast Shelf Sci 45: 799-812

Dolan JR, Marrasé C (1995) Planktonic ciliate distribution relative to a deep chlorophyll maximum: Catalan Sea, NM Mediterranean, June 1993. Deep-Sea Res I 42: 1985-1987

Fenchel T (1968) On "red water" in the Isefjord (inner Danish waters) caused by the ciliate *Mesodinium rubrum*. Ophelia 5: 245-253

Gibson, JAE, Swalding KM, Pitman TM, Burton HR (1997) Overwintering populations of *Mesodinium rubrum* (Ciliophora: Haptorida) in lakes of the Vestfold Hills, East Antarctica. Polar Biol 17: 175-179.

Gustafson DE, Stoecker DK, Johnson MD, Van Heukelem WF, Sneider K (2000) Cryptophyte algae are robbed of their organelles by the marine ciliate *Mesodinium rubrum*. Nature 405: 1049-1052

Hayes GC, Purdie DA, Williams JA (1989) The distribution of ichthyoplankton in Southampton Water in response to low oxygen levels produced by a *Mesodinium rubrum* bloom. 1989. J Fish Biol 34: 811-813

Herzig R, Falkowski PG (1989) Nitrogen limitation in *Isochrysis galbana* (Haptophyceae). I. Photosynthetic energy conversion and growth efficiencies. J Phycol 25: 462-471

Hibberd, DJ (1977) Observations on the ultrastructure of the cryptomonad endosymbiont of the red water ciliate *Mesodinium rubrum*. J Mar Biol Assoc UK 57:
45-61

Horstman DA (1981) Reported red-water outbreaks and their effects on fauna of the west and south coasts of South Africa, 1959-1980. Fish Bull S Afr 15: 71-88

Jankowski AW (1976) Revision of the classification of the cyrtophorids. In Markevich AP, Yu I (eds) Materials of the II All-union Conference of Protozoology, Part I, general protozoology, Naukova Dumka, pp 167-168

Johnson PW, Donaghay PL, Small EB, Sieburth JMcN (1995) Ultrastructure and ecology of *Perispira ovum* (Ciliophora: Litostomatea): an anaerobic, planktonic ciliate that sequesters the chloroplasts, mitochondria and paramylon of *Euglena proxima* in a micro-ocix habitat. J Euk Microbiol 42: 323-335

Lewis MR, Smith JC (1983) A small volume, short-incubation-time method for measurement of photosynthesis as a function of incident irradiance. Mar Ecol Prog Ser 13: 99-102

Lindholm T (1978) Autumnal mass development of the "red water" ciliate *Mesodinium rubrum* in the Åland archipelago. Mem Soc Fauna Flora Fennica 54: 1-5

Lindholm T (1985) *Mesodinium rubrum*- a unique photosynthetic ciliate. Adv Aquat Microbiol 3: 1-48

Lindholm T, Lindroos P, Mörk AC (1990) Depth maxima of *Mesodinium rubrum* (Lohmann) Hamburger and Buddenbrock- Examples from a stratified Baltic Sea inlet. Sarsia 75: 53-64

Menden-Deuer S, Lessard EJ (2000) Carbon to volume relationships for dinoflagellates, diatoms, and other protist plankton. Limnol Oceanogr 45: 569-579

Oakley BR and Taylor FJR (1978) Evidence for a new type of endosymbiotic organization in a population of the ciliate *Mesodinium rubrum* from British Columbia. BioSystems 10: 361-369

Packard TT, Blasco D, Barber RT (1978) *Mesodinium rubrum* in the Baja California upwelling system. In upwelling ecosystems, Eds. Boje, Tomczak M, Springer-Verlag, Berlin

Parsons TR, Maita Y, Lalli CM (1984) A manual of chemical and biological methods for seawater analysis. Pergamon Press, Oxford

Passow U (1991) Vertical migration of *Gonyaulax catenata* and *Mesodinium rubrum*. Mar Biol. 110: 455-463

Platt T, Gallegos CL, Harrison WG (1980) Photoinhibition of photosynthesis in natural assemblages of marine phytoplankton. J Mar Res 38: 687-701

Putt M (1990) Metabolism of photosynthate in the chloroplast-retaining ciliate *Loboea strobila*. Mar Ecol Prog Ser 60: 271-282

Ryther JH (1967) Occurrence of red water off Peru. Nature 214: 1318-1319

Sanders RW (1995) Seasonal distributions of the photosynthesizing ciliates *Laboea strobila* and *Myrionecta rubra* (=*Mesodinium rubrum*) in an estuary of the Gulf of Maine. Aquat Microb Ecol 9: 237-242

Satoh H, Watanabe K (1991) A red-water bloom caused by the autotrophic ciliate, *Mesodinium rubrum*, in the austral summer in the fast ice area near Syowa station, Antarctica, with note on their photosynthetic rate. J Tokyo Univer Fish 78: 11-17

Setälä O, Kivi K (2003) Planktonic ciliates in the Baltic Sea in summer: distribution, species association, and estimated grazing impact. Aquat Microb Ecol 32: 287-297

Smith WO Jr, Barber RT (1979) A carbon budget for the autotrophic ciliate *Mesodinium rubrum*. J Phycol 15: 27-33

Skovgaard A (1998) Role of chloroplast retention in a marine dinoflagellate. Aqu Microb Ecol 15: 293-301

Sorokin YI, Sorokin PY, Ravagnan G (1999) Analysis of lagoonal ecosystems in the Po River Delta associated with intensive aquaculture. Estuar Coast Shelf Sci 48: 325-341

Stoecker DK, Michaels AE, Davis LH (1987) Large proportion of marine planktonic ciliates found to contain functional chloroplasts. Nature 326: 790-792

Stoecker DK, Silver MW, Michaels AE, Davis LH (1988) Obligate mixotrophy in *Loboea strobila*, a ciliate which retains chloroplasts. Mar Biol 99: 415-423

Stoecker DK, Silver MW (1990) Replacement and aging of chloroplasts in *Stombidium capitatum* (Ciliophora: Oligotrichida). Mar Biol 107: 491-502

Stoecker DK, Putt M, Davis LH, Michaels AE (1991) Photosynthesis in *Mesodinium rubrum*: species-specific measurements and comparison to community rates. Mar Ecol Prog Ser 73: 245-252

Taylor FJR, Balckbourn, DJ, Blackbourn, J (1969) Ultrastructure of the chloroplasts and associated structures within the marine ciliate *Mesodinium rubrum* (Lohmann). Nature 224: 819-821

Taylor FJR, Blackbourn DJ, Blackbourn J (1971) The red-water ciliate *Mesodinium rubrum* and its "incomplete symbionts": a review including new ultrastructural observations. J Fish Res Bd Canada 28: 391-407

Wilkerson FP, Grunseich G (1990) Formation of blooms by the symbiotic ciliate *Mesodinium rubrum*: the significance of nitrogen uptake. J Plank Res 12: 973-989

Witek M (1998) Annual changes of abundance and biomass of planktonic ciliates in the Gdansk Basin, Southern Baltic. Internat Rev Hydrobiol 83: 163-182

Yih W, Kim HS, Jeong HJ, Myung G, Kim YG (2004) Ingestion of cryptophyte cells by the marine photosynthetic ciliate *Mesodinium rubrum*. Aquat Microb Ecol 36: 165-170

Figure 2.1. Schedule showing addition of *Geminigera cryophila* prey, new F/2 media, and execution of photosynthesis vs. irradiance (PE) curves during experiment. The x-axes illustrate relationship between periods and days during experiment.

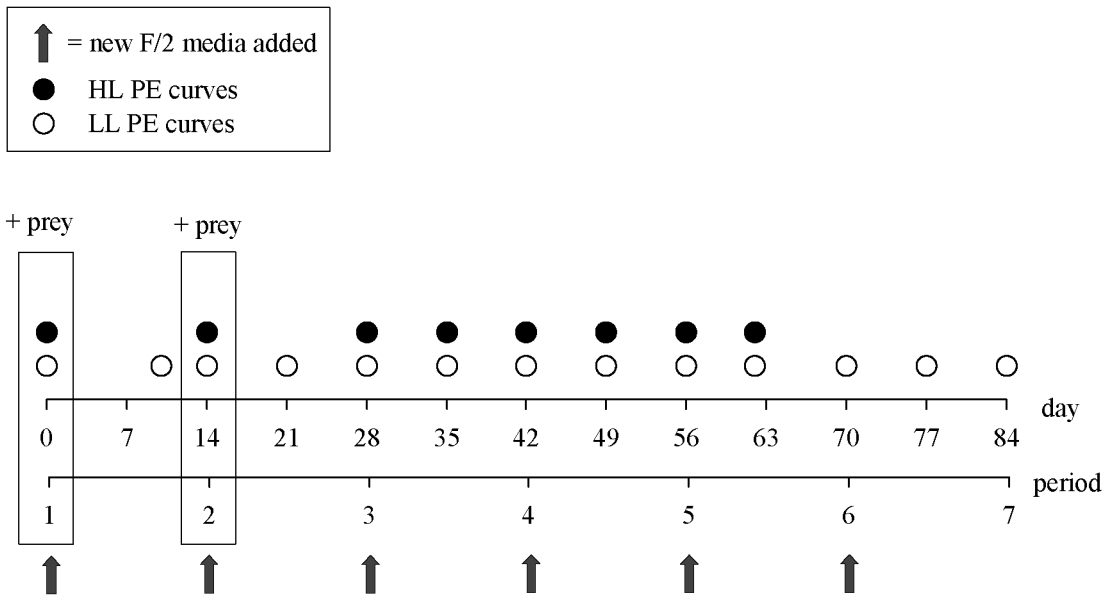
= new F/2 media added
HL PE curves
LL PE curves
+ prey
+ prey
day
0
7
14
21
28
35
42
49
56
63
70
77
84
period
1
2
3
4
5
6
7

Figure 2.2. Cellular concentration and growth rates of *Myrionecta rubra* during experiment in which *M. rubra* is initially fed (until day 28) and then starved in high (HL) and low (LL) light conditions with replete nutrients. (a) Concentration of *M. rubra* and *Geminigera cryophila* cells over time in high light and (b) low light. (c) Observed growth rates (μ) of *M. rubra* over time in HL and LL conditions. Data points for (a) and (b) represent individual samples (n=3); while data points for (c) are mean ± standard deviation.

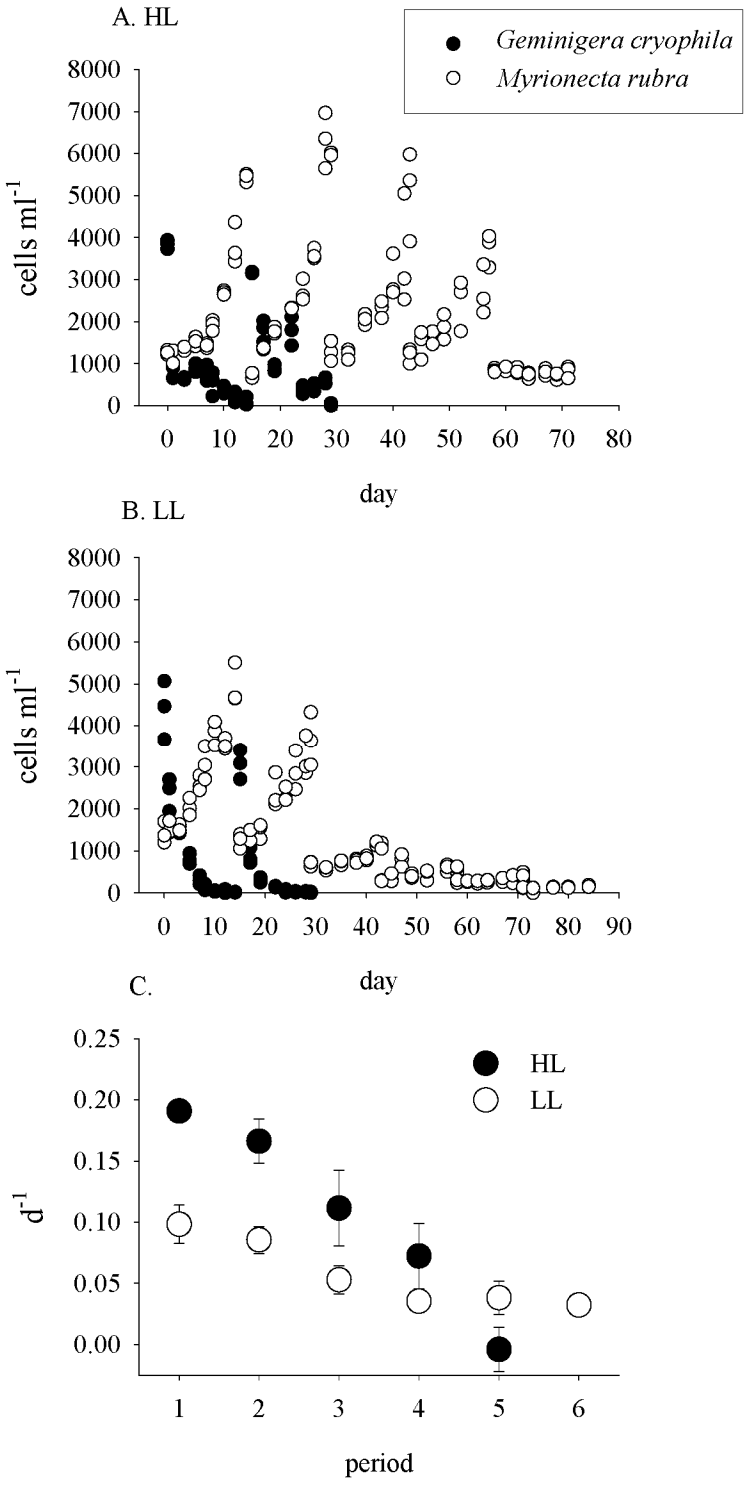
A. HL
Geminigera cryophila
Myrionecta rubra
cells ml-1
8000
7000
6000
5000
4000
3000
2000
1000
0
0 10 20 30 40 50 60 70 80
day
B. LL
cells ml-1
8000
7000
6000
5000
4000
3000
2000
1000
0
0 10 20 30 40 50 60 70 80 90
day
C.
HL
LL
d-1
0.25
0.20
0.15
0.10
0.05
0.00
1 2 3 4 5 6
period

Figure 2.3. Number of *Geminigera cryophila* (prey) nuclei per *Myrionecta rubra* cell at the end of each growth period (= 2 weeks) for high and low light treatments during the experiment. *M. rubra* cultures were fed *G. cryophila* only during first 28 days, and then starved in high (HL) and low (LL) light conditions with replete nutrients. Data points are mean ± standard deviation.

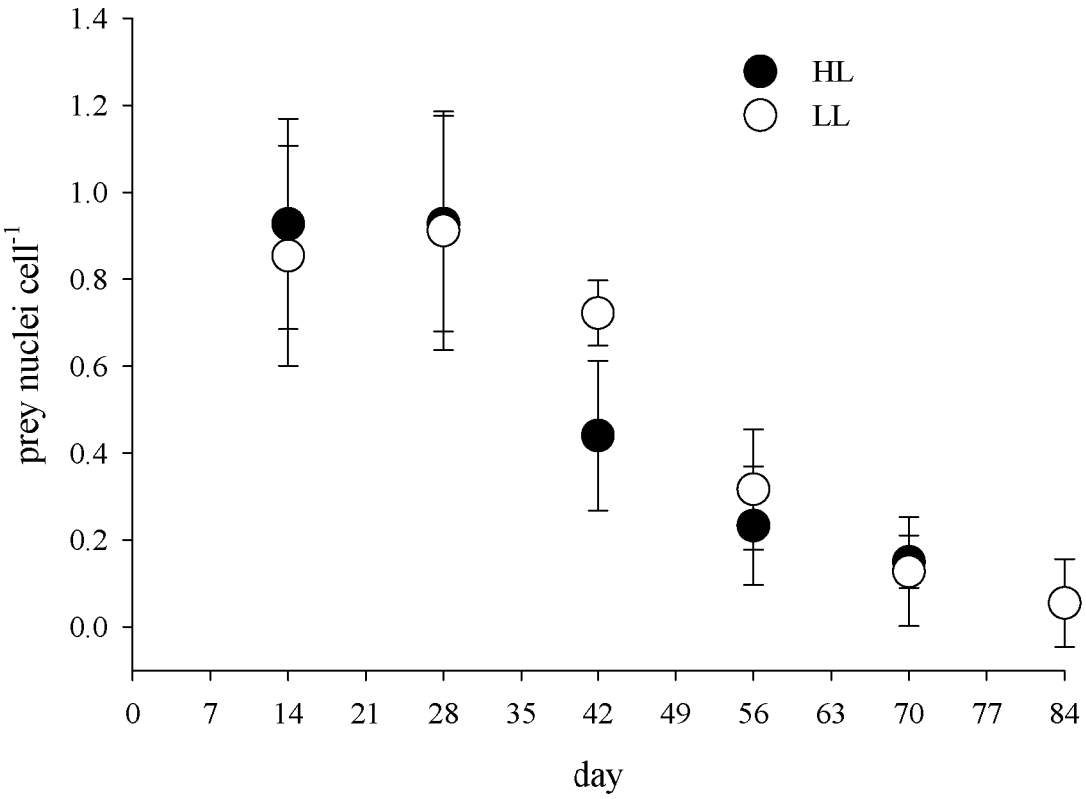
1.4
1.2
1.0
0.8
0.6
0.4
0.2
0.0
prey nuclei cell-1
HL
LL
0
7
14
21
28
35
42
49
56
63
70
77
84
day

Figure 2.4. Cellular concentrations of chlorophyll *a* cell^{-1} in *Myrionecta rubra* during experiment in which *M. rubra* is initially fed (until day 28) and then starved in high (HL) and low (LL) light conditions. (a) Chl cell^{-1} in HL acclimated *M. rubra* and (b) chl cell^{-1} in LL acclimated *M. rubra*. Data points represent individual sample replicates.

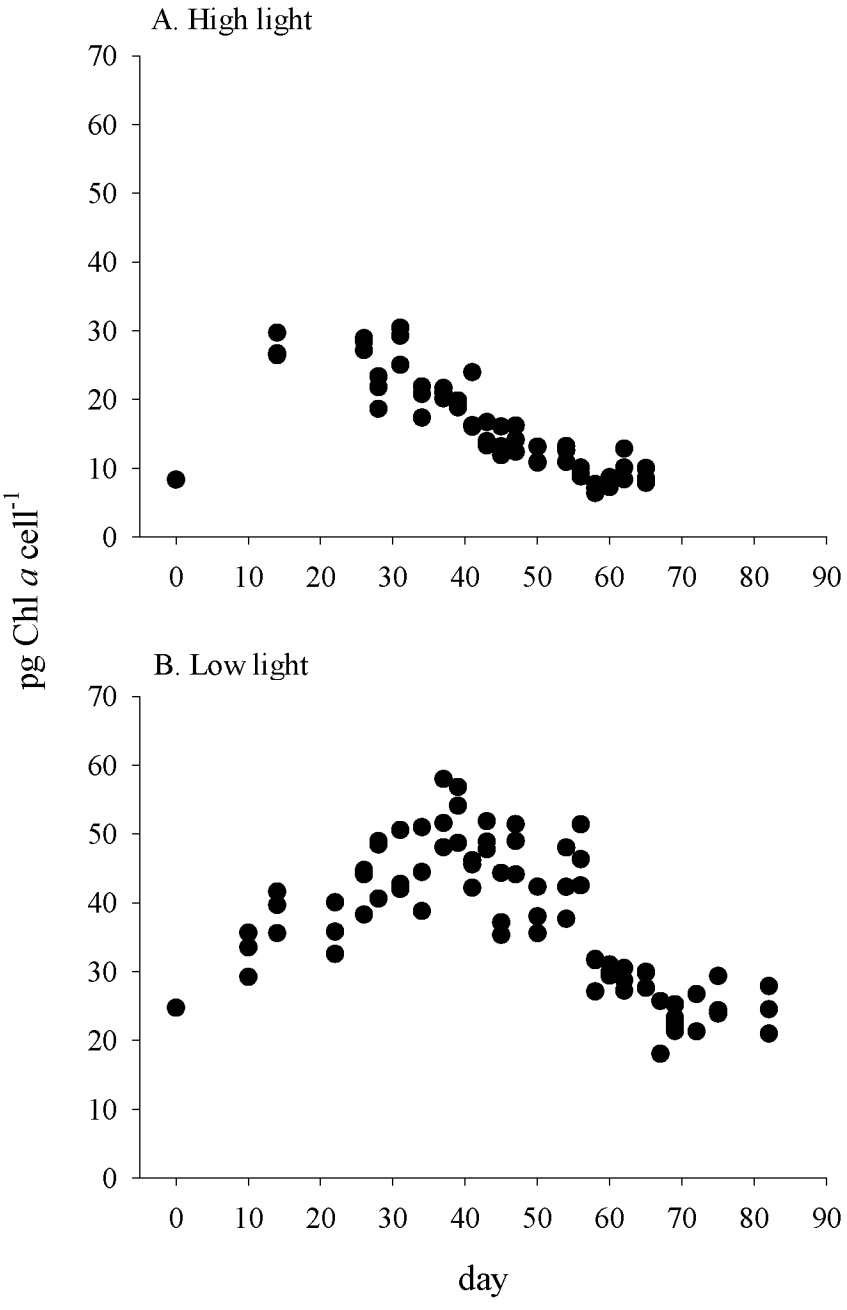
A. High light
B. Low light
pg Chl a cell-1
day
0
10
20
30
40
50
60
70
80
90

Figure 2.5. Estimates of chlorophyll production and chlorophyll gained by ingestion of cryptophyte prey by *Myrionecta rubra* per each 2 week period during experiment where *M. rubra* is initially fed cryptophyte prey (until end of period 2) and then starved in high (HL) and low (LL) light conditions with replete nutrients. Stacked bars represent sample means.

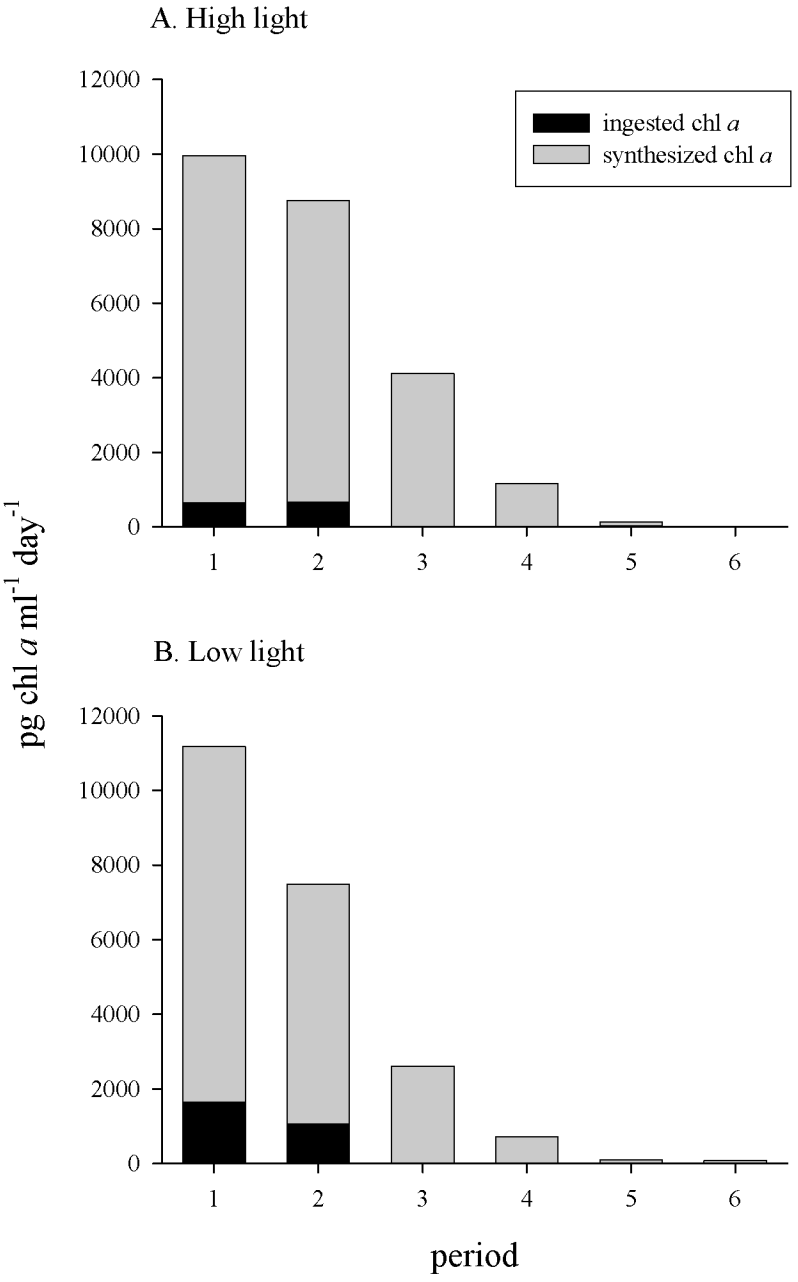
A. High light
ingested chl a
synthesized chl a
12000
10000
8000
6000
4000
2000
0
1
2
3
4
5
6
B. Low light
pg chl a ml-1 day-1
period

Figure 2.6. Cell-specific photosynthesis vs. irradiance (PE) parameters for *Myrionecta rubra* during experiment in which *M. rubra* is initially fed cryptophyte prey (until day 28) and then starved in high (HL) and low (LL) light conditions with replete nutrients. (a) Maximum rate of photosynthesis (P_{max}^{cell}), (b) the initial slope of the PE curve (α^{cell}) and (c) the light saturation parameter (I_k) in HL and LL conditions. Data points represent individual sample replicates.

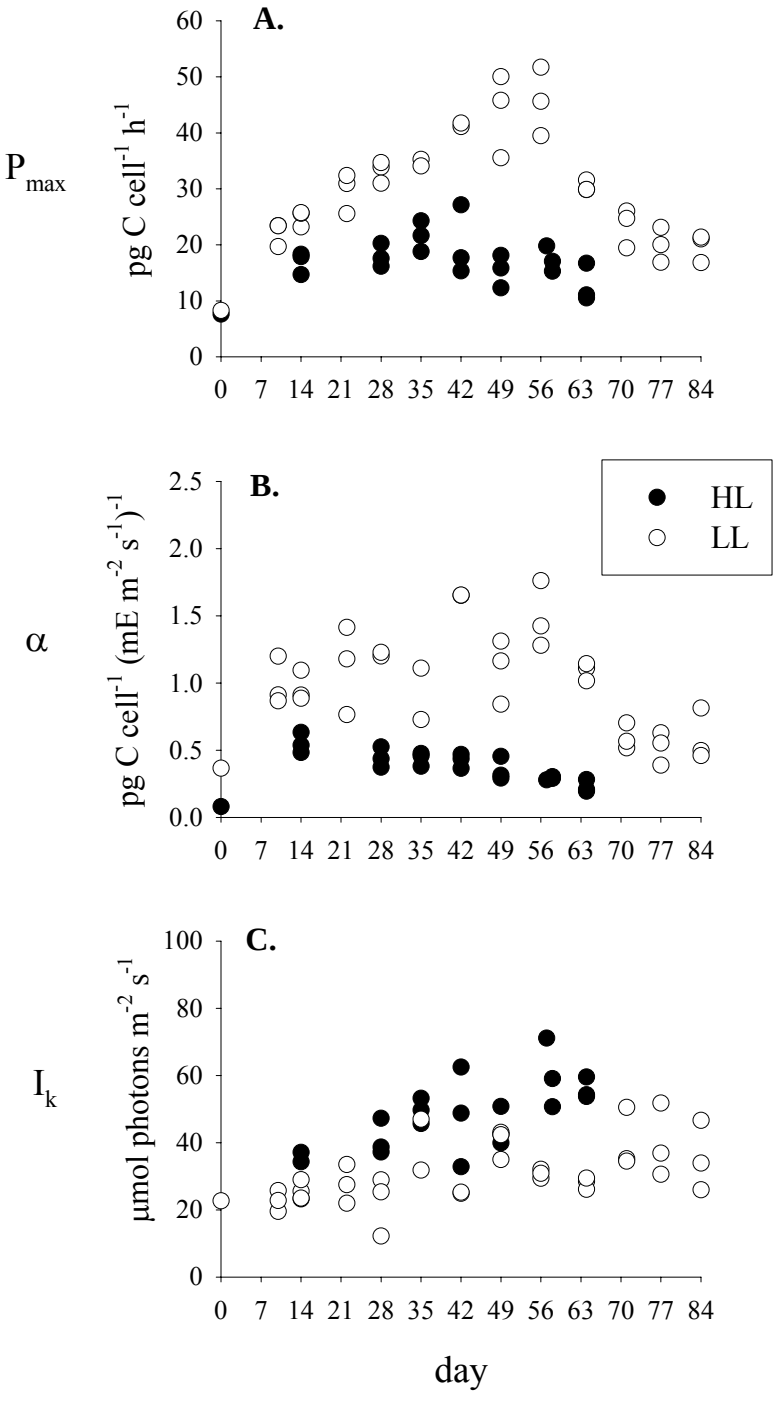
A.
B.
C.
HL
LL
P_{max}
α
I_k
pg C cell^{-1} h^{-1}
pg C cell^{-1} (mE m^{-2} s^{-1})$^{-1}$
µmol photons m^{-2} s^{-1}
day
0 7 14 21 28 35 42 49 56 63 70 77 84
0 10 20 30 40 50 60
0.0 0.5 1.0 1.5 2.0 2.5
0 20 40 60 80 100

Figure 2.7. Chlorophyll-specific photosynthesis vs. irradiance (PE) parameters for *Myrionecta rubra* during experiment in which *M. rubra* is initially fed cryptophyte prey (until day 28) and then starved in high and low light conditions with replete nutrients. (a) Maximum rate of photosynthesis (P_{max}^{chl}) and (b) the initial slope of the PE curve (α^{chl}). Data points represent individual sample replicates.

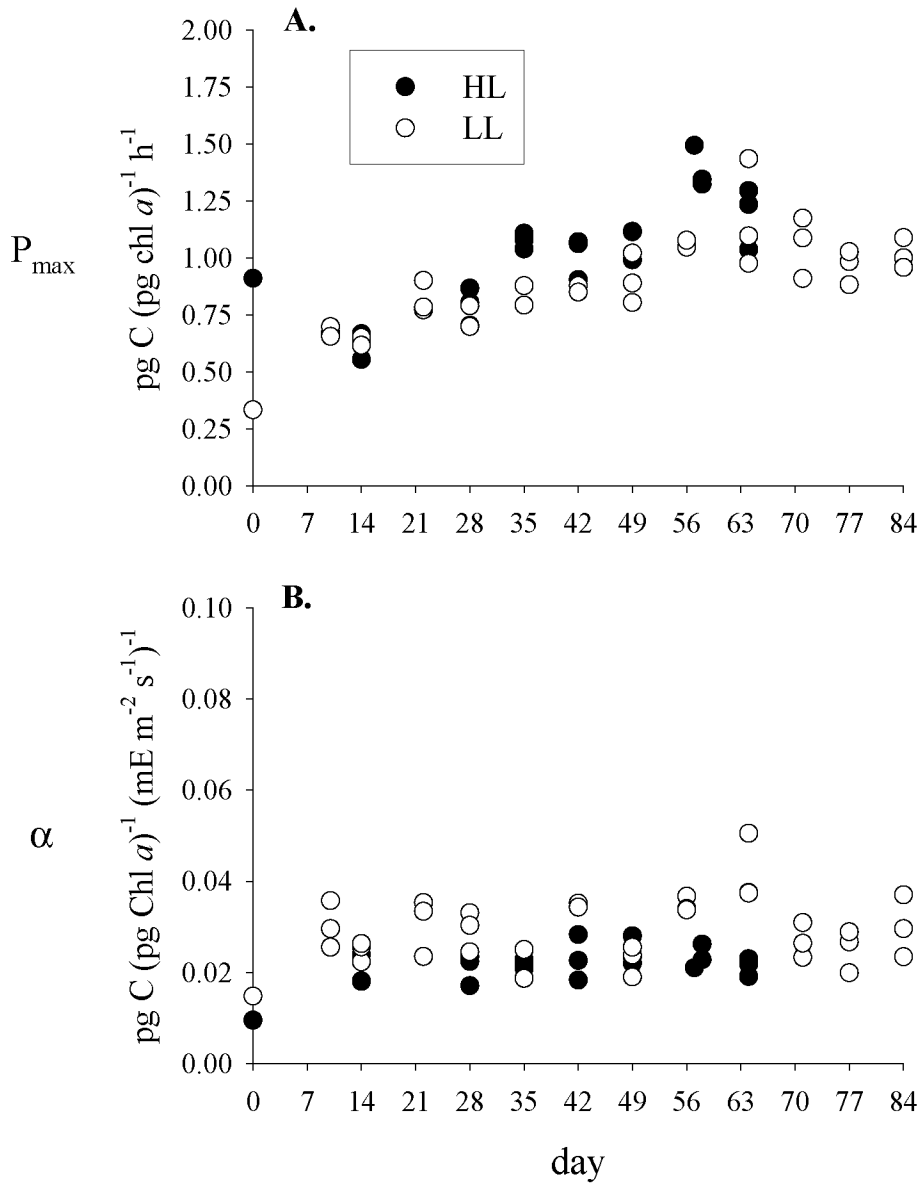
A.
HL
LL
P_{max}
pg C (pg chl *a*)$^{-1}$ h^{-1}
2.00
1.75
1.50
1.25
1.00
0.75
0.50
0.25
0.00
B.
α
pg C (pg Chl *a*)$^{-1}$ (mE m^{-2} s^{-1})$^{-1}$
0.10
0.08
0.06
0.04
0.02
0.00
0 7 14 21 28 35 42 49 56 63 70 77 84
day

Figure 2.8. Estimated gross growth efficiencies (GGE^M) for combined autotrophic and heterotrophic growth of *Myrionecta rubra* during experiment where *M. rubra* was initially fed cryptophyte prey (until day 28) and then starved in high (HL) and low (LL) light conditions with replete nutrients. GGE^M estimated per each 2-week period. *M. rubra* was not fed after day 28 (period 2). Data points are mean ± standard deviation.

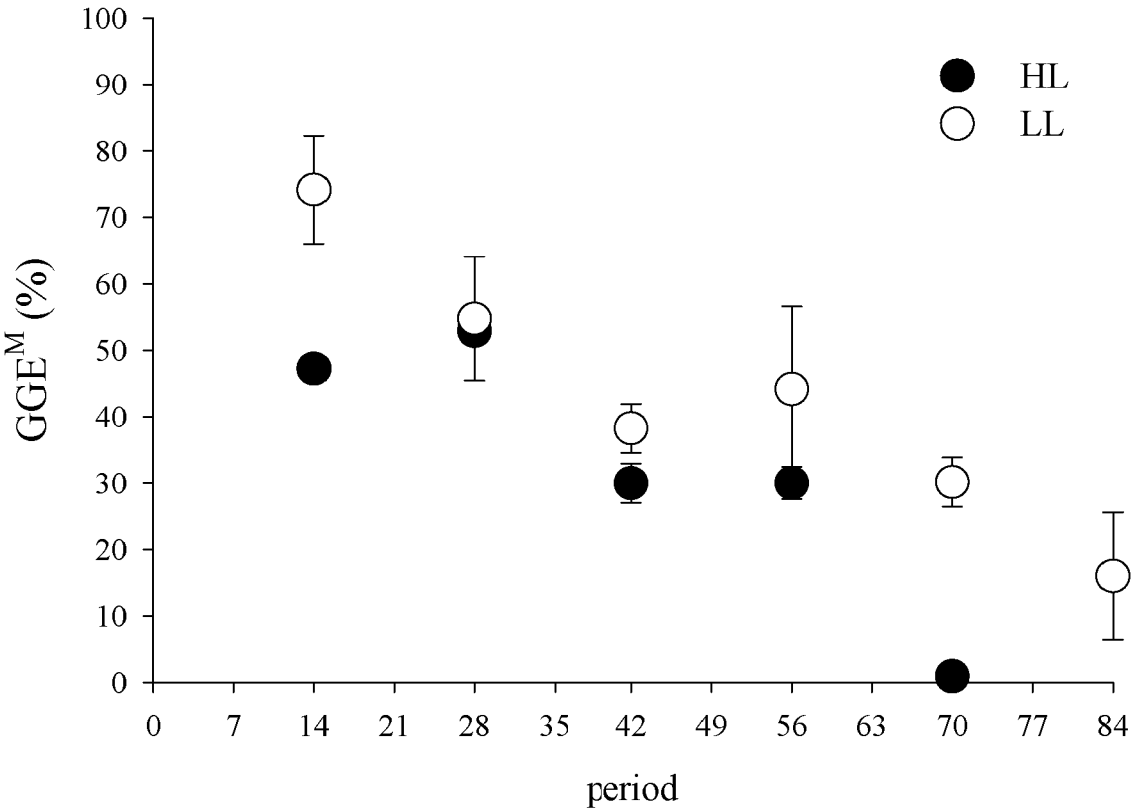
100
90
80
70
60
50
40
30
20
10
0
GGE^M (%)
0
7
14
21
28
35
42
49
56
63
70
77
84
period
HL
LL

CHAPTER 3: Sequestration and Performance of Plastids from the Cryptophyte *Geminigera cryophila* in the Ciliate *Myrionecta rubra*

Abstract

Myrionecta rubra is a photosynthetic ciliate with a global distribution in neritic and estuarine habitats, and has long been recognized to possess organelles of cryptophycean origin. Here I have shown, using nucleomorph SSU rRNA gene sequence data, quantitative PCR, and pigment absorption scans, that a *M. rubra* culture has identical plastids to its cryptophyte prey, '*Geminigera cryophila'*, and thus appears to rely on ingesting cryptophytes to acquire them. Using qPCR I demonstrated that '*G. cryophila'* plastids undergo division in growing *M. rubra*. *M. rubra* maintained chl cell^{-1} and maximum cellular photosynthetic rates (P_{max}^{cell}) that were 6-8x that of '*G. cryophila'*. While maximum chl-specific photosynthetic rates (P_{max}^{chl}) are identical between the two, *M. rubra* is less efficient at light harvesting in low light (LL) (lower α^{chl}) and has lower overall quantum efficiency (Fv/Fm). The photosynthetic saturation parameter (E_k) was not different between taxa in high light (HL) and was significantly higher in *M. rubra* in LL. Lower Chl:C ratios (θ), and hence P_{max}^{C} rates, in *M. rubra* resulted in lower growth rates compared to '*G. cryophila'*. '*G. cryophila'* possessed a greater capacity for synthesizing protein from photosynthate, while *M. rubra* used 3.2 times more of fixed C for synthesizing lipids. While cryptophyte plastids in *M. rubra* may not be permanently genetically integrated, they undergo replication, and are apparently temporarily regulated by *M. rubra*, allowing the ciliate to function as a phototroph.

Introduction

Myrionecta rubra (= *Mesodinium rubrum*) (Lohmann 1908, Jankowski 1976) (Mesodiniidae, Litostomatea) is a photosynthetic ciliate with a widespread global distribution and is known to cause recurrent red-water blooms in numerous regions (Taylor et al. 1971, Lindholm 1985). Photosynthetic measurements during *M. rubra* blooms have been among the highest primary production rates ever measured (Smith and Barber 1979). Blooms of *M. rubra* can be massive in scale and highly dynamic in their water column position (Ryther 1967, Crawford et al. 1997). *M. rubra* feeds on cryptophyte algae (Gustafson et al. 2000), retaining plastids, mitochondria (Taylor et al. 1969, 1971), and nuclei from their prey (Hibberd 1977, Oakley and Taylor 1978). Unlike most plastid-retaining ciliates, *M. rubra* is able to grow phototrophically for long periods, without feeding on new prey and has the ability to synthesize chlorophyll (Gustafson et al. 2000, Johnson and Stoecker 2005). *M. rubra* is considered a phototroph, despite the fact that it ingests cryptophyte algae. Evidence for mixotrophy, i.e. photosynthesis and heterotrophic digestion of prey carbon, is lacking and most of the ingested cryptophyte organelles and cytoplasm appear to be retained in membrane-delineated compartments (Taylor et al. 1969, 1971). Recent estimated C budgets for *M. rubra* suggest that ingested prey C accounts for negligible C growth requirements compared with photosynthesis (Yih et al. 2004, Johnson and Stoecker 2005). In contrast, most kleptoplastidic protists form recognizable food vacuoles and have been shown to be capable of heterotrophy, and generally do not sequester other prey organelles (e.g.

Stoecker et al. 1988/1989). Because *M. rubra* is capable of phototrophic growth and pigment synthesis, it falls into a special functional category (Gustafson et al. 2000).

While many protists are thought to sequester chloroplasts from algal prey, relatively few studies have been conducted to evaluate plastid performance and function in "host" cells. Most studies that have evaluated carbon metabolism in kleptoplastidic protists have focused on oligotrich ciliates. Plastid-retaining oligotrich ciliates have been shown to possess high cellular photosynthetic rates (Stoecker et al. 1988), high plastid turnover rates (Stoecker and Silver 1990), and appear to use photosynthate predominantly for respiration (Putt 1990). Kleptoplastidic dinoflagellates, while widely documented, are less well understood in regards to their physiology. *Gymnodinium 'gracilentum'* and *Pfiesteria piscicida* can acquire photosynthate from kleptochloroplasts for up to a week, however the amount is insufficient to cover their entire C budget (Skovgaard 1998, Lewitus et al. 1999). Recent research with *M. rubra* has shown that plastids remain functional for up to 8 weeks in low light, while growth and pigment synthesis become negligible (Johnson & Stoecker 2005). Herein I contrast plastid function and performance in the cryptophyte *'G. cryophila'* with plastid function and performance in its organelle-sequestering predator, *M. rubra*.

Methods

Culture and experimental conditions

Myrionecta rubra (CCMP 2563) and *'Geminigera cryophila'* (CCMP 2564) were isolated from McMurdo Sound, Antarctica, from a nutrient-enriched sample of sea ice and water collected in January 1996 (Gustafson et al. 2000). Cultures were grown in 1L glass flasks with 32 PSU F/2 -Si media (Guillard 1975), at 4° C. In preparation for this experiment, cultures were allowed to acclimate to four 24 h light regimes at 90, 75, 25 and 10 μmol photons m^{-2} s^{-1} for greater than three months, while receiving biweekly additions of F/2 media and prey. I was unable to grow *M. rubra* at 10 μmol photons m^{-2} s^{-1}, due to accumulation of free-living prey. This was probably due to lower ingestion and growth rates by *M. rubra,* and as a result, no data were available from this light intensity for the ciliate. All cell attribute and photosynthesis measurements were made on cells in mid to late log phase. Prey concentrations were checked in *M. rubra* cultures prior to experimental measurements to verify they were at "background" levels (i.e. <50 cells ml^{-1}). Experimental treatments each had three replicates unless otherwise noted. Growth rates were estimated during the exponential portion of the growth phase using μ (div d^{-1}) = $(\log_2(n_1/n_0))/t_1\text{-}t_0$, where n are cell concentrations at the beginning and start of the exponential growth phase. All cultures were fed about 2 weeks prior to experimental measurements, using prey acclimated to the same growth conditions.

DNA extraction, PCR amplification and DNA sequencing

Cultures of *M. rubra* (~3 x 10^4 cells ml^{-1}) and '*G. cryophila'* (~1 x10^5 cells ml^{-1}) were centrifuged in 50 ml centrifuge tubes at 4ºC and 4000 g for 10 min. The Plant DNA Extraction Kit (Qiagen) was used and the manufacturers protocol was followed. PCR was

conducted using 1x PCR buffer (TaqPro, Denville), 0.2 mM nucleotides, 0.25 mg/ml bovine serum albumin (BSA), 3 mM $MgCl_2$, 0.4 mM primers, and 0.6 u Taq DNA polymerase, and were combined with 10-20 ng of genomic DNA from cultures in a volume of 25 ml. The following general eukaryotic primers for small subunit (SSU) rRNA were used to amplify the gene from conserved regions: 4616, 4618 (Medlin et al. 1988, Oldach et al. 2000), 516, and 1416 (Johnson et al. 2004). PCR conditions were as follows: an initial 3 min 95ºC melting step, 40 cycles of 30 sec at 95ºC (melting), 30s at 55ºC (hybridization), and 70s at 72ºC (elongation), followed by a final 10m 72ºC elongation step. Products were then cloned using an Invitrogen TOPO TA cloning kit, following manufacturers instructions. Colonies were then isolated and gene products were reamplified with PCR using manufacturer supplied vector primers. Cloned PCR products were sequenced directly in both directions using the above gene-specific primers and the BigDye terminator kit (Perkin Elmer). All sequencing was conducted using an ABI 377. Species-specific SSU rDNA primers (Qiagen) were designed for all novel sequences identified from sequencing the SSU rDNA clone library, and all sequences were generated at least 10 times.

Phylogenetic analysis

Contingent sequences were generated using Sequencher (Gene Codes Corp.) and added to sequences obtained from Genbank. All alignments were created using the Clustal X algorithm (Thompson et al. 1997) and ambiguous regions of the nucleomorph alignment, found in highly variable regions, were excluded by eye in MacClade 4.05 (Maddison and

Maddison 1991). An alignment matrix was constructed of diverse cryptophytes and red algae for the nucleomorph analysis (1842 characters), while the nuclear SSU rRNA analysis (1829 characters) included cryptophyte and Glaucocystophyte taxa. Both are available upon request.

A maximum likelihood analyses analysis was used to infer phylogenetic relationships using stepwise addition with1x random addition heuristic searches and TBR, Γ-corrected (Nucleomorph [Nm] = 0.4317; nucleus [Nu] = 0.6326), and pinvar (Nm = 0.5179; Nu = 0.4364). Base frequencies (Nm = A: 0.2653, C: 0.1993, G: 0.2488, T: 0.2866; Nu = A: 0.2573, C: 0.2030, G: 0.2664, T: 0.2733) and GTR substitution rates (Nm = A-C: 1.665, A-G: 6.018, A-T: 2.219, C-G: 2.188, C-T: 8.514, G-T: 1; Nu = A-C: 0.9447, A-G: 1.755, A-T: 0.8768, C-G: 1.184, C-T: 3.434) were estimated. The analyses included 15 (Nm) and 16 (Nu) ingroup taxa and 2 outgroup taxa for both analyses. ML tree scores of 7686.45 and 7339.95 were found for the Nm and Nu analyses, respectively. Bootstrap analysis was performed on all trees, with the respective initial model, on one hundred resampled datasets using stepwise addition and a 1x random addition heuristic search. All phylogenetic analyses were conducted in PAUP* version 4.0b (Swofford 1999).

Quantitative (q) PCR

Primers and probes for conducting (q) PCR were designed by eye in MacClade and ordered from Operon (Alameda, CA). Primers and probes were added at a final concentration of 0.2 and 0.3 μM, respectively. Taq polymerase was used at final

concentration of 0.1 U μl^{-1} (TaqPro, Denville); $MgCl_2$ at a final concentration of 4 mM (Life Technologies, Rockville, MD); a deoxynucleoside triphosphate (dNTP) mixture with each dNTP at a final concentration of 0.2 mM; PCR buffer was at a final concentration of 1x (Denville). For the *G. cryophila* assay, the forward primer (FP) TMTA_Nm-F (CCGAGGCTCTTTGGTTAGACT), reverse primer (RP) TMTA_Nm-R (GCCATGCGATTCGGTTAGT), and probe (P) TMTA_Nm-P (6-FAM-TCGCCATTCATCACCTGATGGAAG-TAMRA) were used, while for the *M. rubra* assay, FP MR-F (ACGTCCGTAGTCTGTAC), RP MR-R (ATGATCCTAAGACGAGAAACTTA), and P MR-P (FAM-GAATGCGGTAGTTTCTGCAGTCACTC-BHQ1) were used. All real-time PCR was conducted in a Smart Cycler (Cepheid, Sunnyvale, CA), using 25 μl reaction tubes. A standard curve for the Nm SSU rRNA gene was created using a dilution series of cells from the '*G. cryophila*' culture. The resulting cycle numbers were then plotted against cell number and an equation was obtained using a best-fit linear regression ($y = -1.3854Ln(x) + 36.316$; $r^2 = 0.987$). Nm ssu rRNA gene content was then normalized to that of *M. rubra* nuclear ssu rRNA gene content, determined using the same approach ($y = -1.5863Ln(x) + 28.576$; $r^2 = 0.999$), and expressed as a ratio that should be roughly equivalent to Nm genomes $cell^{-1}$ (NGC). Assuming one Nm genome $plastid^{-1}$, NGC should approximate plastid number $cell^{-1}$. In order to use qPCR for enumerating '*G. cryophila*' plastid number in *M. rubra* over time, replicate recently fed *M. rubra* cultures were grown at 45 μmols m^{-2} s^{-1} in the absence of prey for ~2 weeks and DNA was extracted on days 2, 5, 9, 12, and 15 for qPCR.

TEM

Cells were fixed with 4% paraformaldehyde, 2% gluteraldehyde, 0.05 M cacodylic acid, and 0.1 M sucrose for 2h at 4°C, spun (4000 rpm 10 min), washed with 0.05 M cacodylic acid and 0.1 M sucrose buffer, and washed again with 0.05 cacodylic buffer. Cells were then postfixed with 1% osmium for 3 h. Dehydration was in ethanol and embedding in Spurr's resin. Embedded cells were thin sectioned, placed on a copper grid, and stained with urinal acetate and lead for TEM viewing on a JEOL 1200-EX.

Cellular attributes

Cell volume was determined by measuring cell length and width using a ocular micrometer on a Nikon Eclipse inverted microscope at 100x magnification, for at least 30 cells per replicate and time point. Cell volume was calculated using $V\ (\mu m^3) = (\pi/6)\cdot w^2\cdot l$, where w is the cell width and l the length. Cell concentrations were enumerated by counting gluteraldehyde-fixed (1% final conc.) cells at 100x magnification on a Nikon Eclipse standard microscope, equipped with a fluorescent light source, and Nikon filter sets EF-4 B-2A (exciter filter 450-490 nm, dichromatic beam splitter (DM) 500 nm, barrier filter (BA) 515 nm). Chlorophyll was extracted by filtering culture aliquots onto a GF/C filter and incubating overnight in 90% acetone at –20ºC. Chlorophyll concentrations were determined using a Turner Designs model 10-AU fluorometer.

Light absorption measurements

Cell cultures were filtered onto Whatman GF/F filters in order to measure total particulate absorption (a_{tot}) spectra (Kishino et al. 1985) using a Shimadzu UV-VIS 2401 dual beam spectrophotometer (Shimadzu, Columbia, MD, USA), equipped with a Shimadzu IRS-2100 integrating sphere. Detrital absorption (a_d) was determined by scanning the same filter following pigment extraction with methanol and 10% bleach (to remove phycobilins). Pigment absorption (a_p) was then determined as $a_{tot} - a_d$. Due to incomplete removal of cryptophyte phycobilins, a portion of the detrital scan was removed and remaining data used to fill in the gap by interpolating a power function curve. A β-correction factor $a^{(suspension)} = 0.59 \cdot a^{(filter)}$, $r^2 = 0.94$) determined for the Shimadzu IRS-2100 (Adolf et al. 2003).

Photosynthesis (^{14}C) measurements

Photosynthesis vs. irradiance (PE) measurements (Lewis & Smith 1983) were made during exponential cell growth phase, at 4ºC using a photosynthetron connected to a chiller. Culture aliquots were removed and kept on ice around midday, and $NaH^{14}CO_3^-$ was added to a final activity of 1 $\mu Ci \cdot ml^{-1}$. At t = 0 controls were taken by adding 2ml of labeled culture immediately to a vial with 200µl of formalin, and used later for subtracting background levels of ^{14}C activity. Background and total activity controls were then placed in the dark at 4°C overnight. Samples for total activity were collected by adding 100 µl of sample to 200 µl of β-phenylethylamine (Sigma). ^{14}C spiked culture

(2ml) was then added to 7ml scintillation vials, on ice, and immediately transferred to the chilled photosynthetron block. A total of 15 vials were used for each replicate PE assay, and incubated for 30 min at constant irradiance between 0-800 μmol photons·m^2·s^{-1}. At the end of the incubation, the vials were acidified with 500 μl 6N HCl to remove unincorporated ^{14}C, and placed on a shaker overnight at room temperature. In order to determine the ^{14}C activity of the vials, 4 ml of Ultima Flo AP (Perkin Elmer, Boston, MA, USA) scintillation cocktail was added to the background control and light-exposed vials, while 5 ml was added to the total activity vials. All ^{14}C incorporation and control activities were determined using a Tri-Carb 2200CA liquid scintillation counter (Packard Bioscience, Meriden, CT, USA). Photosynthetic rates were determined using analytical methods described by Parsons et al. (1984), and PE data was normalized to hourly rates and either cell or chlorophyll concentrations. Curve fitting for PE data was conducted in Sigma Plot (SPSS software, Chicago, IL, USA) using an equation based on Platt et al. (1980): photosynthesis (P) = $P_0 + P_s \cdot (1 - \exp((-E \cdot \alpha)/P_s)) \cdot \exp((-E \cdot \beta)/P_s)$, where P_0 is the y-intercept, P_s is the maximum potential rate of photosynthesis, α is the initial light-limited slope of the PE curve, E is the irradiance, and β is the slope of the photoinhibition region of the curve. From the curve-fitted data α, P_{max} (maximum rate of photosynthesis), I_k (photosynthesis-saturating light irradiance (I_k) = P_{max}/α), and β were determined. P_{max} and α rates are presented both as cellular (e.g. $P_{max}^{cell} = P_{max} \cdot ml^{-1}/cells \cdot ml^{-1}$) and chlorophyll (e.g. $P_{max}^{chl} = P_{max}^{cell}/chl \cdot cell^{-1}$) normalized rates in this study.

Variable fluorescence measurements

A pulse amplitude modulated (PAM) fluorometer (Walz PAM-101 fluorometer) was used with a high sensitivity detector. 10-20 ml of culture was place in a glass test tube, and the tube was illuminated using irradiance from a 150-W xenon lamp (company) and filtered with Schott long-pass filters. Steady-state *in vivo* chl fluorescence (F_s) of cells was measured during illumination with actinic irradiance. At 1-min intervals a saturating pulse (400-ms duration) was applied to obtain a maximum yield (F'_m). The relative efficiency of excitation energy capture by photosystem II was calculated as $(F'_m-F_s)/F'_m$.

Carbon partitioning measurements

M. rubra or '*G. cryophila*' cells were labeled with 0.1 $\mu Ci \cdot ml^{-1}$ $NaH^{14}CO_3^-$ for 24 hr at culture growth conditions. For analysis of *M. rubra* cultures, care was taken not to use cultures with free-living cryptophyte prey present. After incubations, cells were gently filtered onto GF/C filters and placed in a glass 20 ml scintillation vial and acidified with 0.1 ml of 10% HCl and heated at 55°C until dry, then stored at –20°C until extraction. Filters were processed for biochemical partitioning of carbon fixation, using the serial extraction method adapted from Morris et al. (1974). Filters were folded in half and placed in a microtube with 1 ml of chloroform, vortexed, and placed on ice for 10 min. Tubes were spun at 10000 rpm for 5 min (for all steps) and the supernatant was decanted. This extraction was repeated with an additional 0.5 ml of chloroform. Filters were then extracted with methanol, vortexed, and placed on ice for 10 min, centrifuged, and the supernatant was decanted. A second methanol wash step was repeated with 0.5 ml. Filters were then extracted with 1ml of 5% trichloric acetic acid (TCA) at 90°C for 1 h. Tubes

were then vortexed, centrifuged, and the supernatant was decanted. Filters were then washed with 0.5 ml of cold TCA. Various cell fractions were processed for carbon fixation partitioning by adding scintillation fluid and processing the samples as described above for PE curves.

Data analysis. Statistical analysis of cell attributes and PE parameter data were conducted using the mixed model ANOVA and multiple regression options in SAS/STAT 9.0 (SAS Institute Inc., Cary, NC, USA), and $p < 0.05$ as a level of significance. Comparisons for ANOVAs between means were made between treatments (HL vs. LL) and over time using Tukey's Studentized range (HSD) test.

Results

Nucleomorph and Nuclear SSU RNA cryptophyte gene analysis

In order to identify the phylogenetic origin of plastids in *Myrionecta rubra*, DNA sequences were determined for the small subunit (SSU) rRNA gene of the plastid nucleomorph in both *M. rubra* and the prey cryptophyte. Highly variable regions and insertions within the gene were removed from the analysis, totaling 656 bp, as they were impossible to align among all taxa. Identical sequences were found from both the *M. rubra* culture and the cryptophyte-only culture. Maximum likelihood (ML) analysis (Figure 1A) revealed that this sequence is most closely related to *Geminigera cryophila*

(3 substitutions, 6 indels per 1783 bp), with 98% bootstrap (BS) support. The culture has been referred to in the past as *Teleaulax acuta*, based on microscopic examination (i.e. Gustafson et al. 2000, Johnson et al. 2004, Johnson & Stoecker 2005). While no *T. acuta* nucleomorph sequence was available in Genbank for comparison, a nuclear SSU rRNA *T. acuta* sequence was used to help clarify the identity of the cryptophyte culture. ML analysis revealed that the cultured cryptophyte was more closely related to *G. cryophila* (3 substitutions, 2 indels per 1777 bp) then *T. acuta* (18 substitution, 5 indels per 1777 bp), with 100% BS support (Figure 1B). Herein the *G. cryophila* culture is referred to with in quotes until a more detailed description of its identity is conducted.

In order to rule out the possibility that the major plastid type in the *M. rubra* culture was not detected, quantitative PCR (qPCR) was conducted for the '*G. cryophila*' Nm sequence. The *M. rubra* culture used for this experiment had not been fed for three weeks and no free-living prey were detected using microscopy during the entire time. Nm genomes cell^{-1} (NGC) (~ plastid number cell^{-1}) during the first 10 days was between 9.3-10, during which time cell number nearly doubled (Figure 2). At the end of 15d the cell population had undergone 1.32 divisions and NGC was 8.2 ± 0.1 (Figure 2). While these NGC (~ plastids cell^{-1}) numbers are slightly greater than measured MR: GC chl cell^{-1} ratios for this experiment (varying between 6.8-7.9 over 15d), it is likely that chl content of sequestered plastids in *M. rubra* change due to varying physiological and light conditions.

Growth and cellular characteristics

Cultures of '*Geminigera cryophila'* had significantly higher growth rates than *Myrionecta rubra* at all irradiance levels (Table 2, 3). Growth rates for '*G. cryophila'* decreased with decreasing irradiance, while *M. rubra* growth rates were not different between high and low light (Table 2). Observations of thin sections of *M. rubra* using TEM revealed the presence of membrane-delineated chloroplast-mitochondrial complexes, as described previously (e.g. Taylor et al. 1969, 1971, Hibberd 1977, Oakley and Taylor 1978) (Figure 3a,b). The chloroplasts possess a stalked pyrenoid, often with two starch grains, and a nucleomorph, surrounded by the periplastidal double membrane (Figure 3b). A single membrane then surrounds the periplastidal unit, along with cryptophyte mitochondria (with flattened christae), cytoplasm, endoplasmic reticulum, and sometimes lipid droplets (Figure 3a,b). Chl cell^{-1} was about 6 times greater in *M. rubra* than '*G. cryophila*' on average, across all irradiance levels (Table 3). For both cultures chl cell^{-1} did not differ at the two highest irradiance levels, and increased at lower irradiance levels (Table 2). C cell^{-1} was estimated based on cell volume (Menden-Deuer and Lessard 2000) yielding HL values of 564 ± 173 and 62.2 ± 8.5, and LL values of 561 ± 194 and 44.5 ± 7.4, for *M. rubra* and "*G. cryophila*", respectively. Chlorophyll specific absorption spectra (a^{chl}) were essentially identical for both cultures within the visible spectral range, with a phycoerythrin peak at 550 nm (Figure 4). However, in the UV portion of a^{chl} spectra, high and unexpected absorption at 335 nm (UVB) was found in *M. rubra*, absent in '*G. cryophila'*, suggesting the production of mycosporine-like amino acids in the ciliate (Figure 4, Table 3).

Photophysiology

Maximum cellular photosynthetic rates (P_{max}^{cell}) for *M. rubra* were 5.26-7.45 times greater than those for '*G. cryophila'* (Table 3). For both *M. rubra* and '*G. cryophila'*, P_{max}^{cell} increased with decreasing irradiance and chlorophyll concentration (Table 2). Maximum chlorophyll-specific photosynthetic rates (P_{max}^{chl}) were identical between cultures in both LL and HL (Table 2). Carbon-specific maximum photosynthetic rates were greater in '*G. cryophila'*, and increased for both cultures in LL (Table 2). Cell-specific carbon fixation efficiency (α^{cell}) increased with decreasing light for both taxa, and were 3-4 times greater in *M. rubra* (Table 3). Chlorophyll-specific carbon fixation efficiency (α^{chl}) was greater at all growth irradiances in '*G. cryophila*', as were measurements of photochemical efficiency (Fv/Fm) in high light (Table 2). Significant increases were seen in α^{chl} in the cryptophyte at lower irradiance levels ($p = 0.033$, paired Ttest), while no change was observed in *M. rubra* (Table 2). The saturation irradiance parameter (E_k) was greater in *M. rubra* in LL, suggesting greater light-harvesting potential but poorer photochemical acclimation at low irradiance (Table 2, 3).

Carbon partitioning

Lipid production in *M. rubra* comprised a proportionately greater (3.2 fold) fraction of photosynthetically fixed C, and about 20% of total C production (Figure 5A). Photosynthate-mediated protein synthesis was 31% greater in '*G. cryophila'*, while low molecular weight compound (LMWC) and polysaccharide production were similar. The

majority of fixed C in both cultures was found in the protein fraction, 64 and 44% for '*G. cryophila*' and *M. rubra*, respectively. Comparisons of C partitioning were also made at three light levels for *M. rubra* only. In high light, *M. rubra* produced greater amounts of lipids and less protein, while more C remained in the polysaccharide pool in low light (Figure 5B). No difference was observed in the LMWC fraction.

Discussion

Plastid origin

I have shown that plastids in cultured *M. rubra* are phylogenetically identical to those of its prey, '*Geminigera cryophila'*, as all sequences amplified from the *M. rubra* and prey-only cultures were identical. In light of this finding, and proof that *M. rubra* actively ingests cryptophytes (Gustafson et al. 2000, Yih et al 2004, Johnson et al. 2005), it is doubtful that these plastids are permanent symbiotic fixtures of the cell. While non-pigmented cells can be observed in extremely low numbers within the *M. rubra* culture, their role and physiological status remain undescribed.

M. rubra maintained 8-10 '*G. cryophila*' plastids per cell and these plastids undergo division in growing *M. rubra*, as evidenced by measurements of nucleomorph genomic copies of the SSU rRNA gene. However, plastid content in *M. rubra* also undoubtedly varies with feeding history (Gustafson et al. 2000, Johnson et al. 2005). While this is perhaps the first documentation of division of a sequestered organelle in a

protist, the results are not surprising considering previously evidence for chlorophyll synthesis and phototrophic growth in this ciliate (Gustafson et al. 2000, Johnson and Stoecker 2005). These qPCR estimates of plastids cell^{-1} agree well with ratios of chl cell^{-1} in *M. rubra* and free-living '*G. cryophila*', which can average between 5-12 cell^{-1} for a population depending on feeding history (estimated from Johnson & Stoecker 2005). Individual cell variability for plastid content in *M. rubra* is certainly much greater then the numbers presented above, as both unusually large and small cells are frequently observed within the culture. My plastid cell^{-1} data are similar to those of Hibberd (1979), who estimated 12 chloroplast-mitochondria complexes (CMC's) cell^{-1}, while other estimates far outnumber those presented here. Oakley and Taylor (1978) estimated 50-100 CMC's cell^{-1} in populations of large *M. rubra* in British Columbia, while Fenchel (1968) estimated 10-20 in cells collected in the Isefjord of Denmark. In the Baltic Sea, distinct size classes of co-occurring large and small *M. rubra* are well known (e.g. Lindholm 1978, Rychert 2004), yet it is unclear if this is due to differences in division rate, life history stages, or undescribed species variation. The ultrastructure of CMC's in the *M. rubra* culture is consistent with those described elsewhere, with the plastid and nucleomorph intact within the periplastidal membrane complex (PMC), together with cryptophyte mitochondria, cytoplasm, and endoplasmic reticulum enclosed within a single membrane (e.g. Taylor et al. 1969, 1971, Hibberd 1977, Oakley and Taylor 1978). Clearly the degree of phenotypic variability described for *M. rubra* and its "symbionts" warrants comparative ultrastructural and molecular analyses to determine if it is truly a single species or a complex of closely related species.

Photosynthetic physiology

Myrionecta rubra plastids are used in an independent fashion, with optimal performance and sustained maintenance dependent upon recurrent feeding (Johnson and Stoecker 2005). Comparison of photosynthetic physiology between *M. rubra* and its prey '*G. cryophila*' revealed several important differences in performance between cultures. In high light, plastids in *'G. cryophila'* have greater photosynthetic efficiency (i.e. α^{chl}) and optimal quantum efficiency (Fv/Fm), suggesting differences in plastid packaging, repair mechanisms, and/or energy dissipation. However, P_{max}^{chl} rates were about the same between cultures, indicating similar capacity for photosynthesis under saturating irradiance. Lower Fv/Fm in *M. rubra* indicates a slight loss of absorbed energy from entering photochemistry. Differences in quantum efficiency between the two cultures could be explained by differential abundance of important electron transport chain (ETC) proteins, differences in N assimilatory pathways, or other factors that may affect the flow of electrons through plastoquinone (e.g. Falkowski and Raven 1997).

While higher measurements of P_{max}^{chl} have been observed previously for this *M. rubra* culture (up to 1.5 pg C pg chl*a*$^{-1}$ h^{-1}), photosynthetic performance of *M. rubra* depends greatly on recent feeding history, increasing as cells become starved and chl cell^{-1} declines (Johnson and Stoecker 2005). Satoh and Watanabe (1991) measured similar P_{max}^{chl} rates for *M. rubra* in Antarctic waters of 1.04 pg C (pg chl *a*)$^{-1}$ h^{-1}. While my measurements for P_{max}^{chl} in *'G. cryophila'* and *M. rubra* are low for phytoplankton, they fall well within the range of measured polar microalgae, which generally varies between 0.3-2.0 pg C (pg chl *a*)$^{-1}$ h^{-1} (Sakshaug and Slagstad 1991, Robinson et al. 1997). It is

generally thought that low temperature limits the activity of carbon fixation enzymes (e.g. RUBISCO), thus limiting photosynthesis (Berry and Bjorkman 1980). One major difference found between cultures, was the absorbance of compounds in *M. rubra* that resemble mycosporine-like amino acids (MAA), absent in the *'G. cryophila'* culture (Figure 4). MAAs have been shown to protect against UV inhibition of photosynthesis in *Akashiwo sanguinea* (=*Gymnodinium sanguineum*) (Neale et al. 1998), and have been reported in diverse phytoplankton lineages (Jeffrey et al. 1999) including ciliates (Tartarotti et al. 2004). In *M. rubra*, MAA production increased with increasing E_g, suggesting that irradiance levels induce MAA production, as is found in *A. sanguinea* (Neale et al. 1998).

In phytoplankton, α^{chl} generally does not vary phenotypically (e.g. with acclimation state) and variation among taxa can be attributed to differences in pigment composition and packaging (MacIntyre et al. 2002). α^{chl} rates for *M. rubra* did not change between HL and LL in this study and were significantly lower than *'G. cryophila'* at all light levels. Lower α^{chl} in *M. rubra* is likely because of a "packaging effect", where absorption of light per unit chl *a* is less efficient due to high chl *a* $cell^{-1}$ concentrations. Surprisingly, α^{chl} did change for *'G. cryophila'* by increasing in LL, suggesting that changes in α^{chl} may be due to something other than chl *a* concentration. In cyanobacteria α^{chl} increases with decreasing E_g due to increases in phycobillin concentration, as phycobilins are the major light harvesting pigment in cyanobacteria (Kana & Glibert 1987). In cryptophytes, however, this is generally thought not to be the case (e.g. Adolf et al. 2003) and thus changes in α^{chl} reported here for *'G. cryophila'* might be due to changes in pigment packaging or optical qualities of the cell. Based on measurements of

saturation irradiance (E_k), neither *M. rubra* nor *'G. cryophila'* were exposed to saturating growth irradiance in low light. Previous research with *M. rubra* suggest that in HL, E/E_k is greater than 1 following feeding, and declines during starvation as cells lose the ability to make chl *a*, and essentially become light limited (Johnson and Stoecker 2005). While *M. rubra* functions like a phototroph and is capable of temporary chl *a* synthesis (Gustafson et al. 2000, Johnson and Stoecker 2005), it may not be able to photoacclimate to E_g as efficiently as other phototrophs.

Growth and Carbon metabolism

Myrionecta rubra is well known for its ability to generate red tides and its high photosynthetic rates (Smith and Barber 1979). Thus measurements for P and μ presented here and elsewhere (Gustafson et al. 2000, Johnson and Stoecker 2005) for this Antarctic strain of *M. rubra* appear quite modest. Recently, Yih et al. (2004) found maximum growth for a strain of *M. rubra* growing at 15ºC to be 0.521 d^{-1}. Using maximum growth rates observed for the Antarctic strain (~0.2 d^{-1}) at 5ºC, this would suggest a Q_{10} of about 2.6, which is similar to median Q_{10} values for respiration rates in protists (Caron et al. 1990). Q_{10} for photosynthesis in microalgae for temperatures within the 2-8ºC range is generally around 3 (Palmisano et al. 1987). Thus using data presented here and elsewhere (Johnson and Stoecker 2005) one may expect *M. rubra* growing at 15ºC would have a P_{max}^{chl} between 3-5 pg C (pg chl*a*)$^{-1}$ h^{-1}, which is more consistent with measurements of Stoecker et al. (1991) who measured 1.8-8.6 (pg chl*a*)$^{-1}$ h^{-1} at temperatures between 15-22ºC.

As expected, differences in P_{max}^{cell} rates for *M. rubra* and *'G. cryophila'* scaled with observed differences in chl *a* $cell^{-1}$ with values for *M. rubra* being ~6x greater. Averaged μ for *M. rubra* was 62.6 ± 6.6 % of *'G. cryophila'*, which agreed well with observed P_{max}^{C} rates (64.8 ± 4.2% of *'G. cryophila'*) and θ ratios (57.9 ± 11% of *'G. cryophila'*) across all irradiance levels (E_g). θ is a key physiological parameter, as chl *a* and C are widely used to normalize light-limited (e.g. α^{chl}) and saturated (e.g. P_{max}^{C}) photosynthetic rates, respectively (MacIntyre et al. 2002). Lower θ quotas in *M. rubra* are probably the major cause of lower μ for *M. rubra*, as both P_{max}^{chl} and P_{max}^{C} rates were greater in *'G. cryophila'*. Johnson and Stoecker (2005) demonstrated that μ in *M. rubra* is ultimately limited by availability of *'G. cryophila'* prey, but declines slowly during periods of prolonged starvation, despite the presence of inorganic nutrients and somewhat sustained photosynthetic rates. Therefore in *M. rubra* θ, μ, and to a lesser extent P, are sensitive to prior feeding history. The effects of variable prey concentration were not controlled for in this study and thus their affect on cellular and C-specific photosynthetic rates and μ in *M. rubra* cannot be evaluated here. Growth rates presented here for *M. rubra* are similar to previous observations for this culture (~0.19 d^{-1}) (Johnson and Stoecker 2005), as well as to values reported for *M. rubra* in brackish Antarctic lakes (~0.18 d^{-1}; Laybourn-Parry et al. 2000). Growth for HL *'G. cryophila'* (~0.26 d^{-1}) was substantially higher than *M. rubra*, as well as reported μ for cryptophytes in brackish Antarctic lakes (~0.08-0.14 d^{-1}; Laybourn-Parry et al. 2000). However, comparisons of *'G. cryophila'* μ at E_g close to *in situ* irradiance levels for Antarctic Lakes (3.5-13 μmol photons m^{-2} s^{-1}) reveal similar rates (Marshall and Laybourn-Parry 2002). Likewise, P_{max}^{cell} measurements for *'G. cryophila'* acclimated to E_g of 10 μmol photons m^{-2} s^{-1},

reveal values similar to those reported for Lake Fryxell (~1.3 pg C $cell^{-1}$ h^{-1}; Marshall and Laybourn-Parry 2002).

Calculations of the % growth day^{-1} (as C) attributable to photosynthesis indicates that in HL *M. rubra* and *'G. cryophila'* both fix similar proportions of new C per day (~147% cell C d^{-1}), while in LL *'G. cryophila'* fixes proportionately 35% more C (256 and 189 % cell C d^{-1}, for '*G. cryophila*' and *M. rubra*, respectively). In order to compare *M. rubra* to other plastid-sequestering protists, I calculated phototrophic C production for the plastidic oligotrich, *Laboea strobila* (Stoecker et al. 1988), and the kleptoplastidic dinoflagellate *Gyrodinium gracilentum* (Skovgaard 1998). While *L. strobila* has high P_{max}^{chl} rates, photosynthetically fixed C only accounts for 19.7% of new cell C d^{-1}. *G. gracilentum* was found to fix a greater proportion of cell C (83.3%), but still requires substantial heterotrophic C assimilation to cover growth and respiration requirements. Calculations for % new C fixed d^{-1} for *M. rubra* in this study and previous observations (Johnson and Stoecker 2005), varied between 148-263% d^{-1}, and are similar to other phototrophs.

Comparisons of the fate of C partitioning to major biochemical fractions in microalgal cultures and phytoplankton assemblages has been used to infer mechanisms of C storage, major differences in C metabolism between taxa, and to evaluate effects of nutrient limitation (Morris 1981). My results suggest that *M. rubra* stores high quantities of fixed C as lipids, which increases in HL. While both *M. rubra* and *'G. cryophila'* produced large quantities of protein, greater protein production in *'G. cryophila'* may simply reflect higher growth rates. Putt (1990) compared C partitioning of retained plastids in the photosynthetic oligotrich ciliate, *Laboea strobila*, to those of prey, and

found that proportionately less C from photosynthesis in *L. strobila* was used for production of protein and lipids, while more remained within the polysaccharide fraction. Thus photosynthesis in *L. strobila* is primarily used to cover respiratory costs (Putt 1990). My calculation of C production d^{-1} for *L. strobila* (above) also supports the notion that plastidic oligotrichs have high heterotrophic C requirements. *M. rubra* appears to have little need for heterotrophic C gain, and while growth is optimal following feeding on cryptophytes, it appears to be a result of enhanced growth efficiency and phototrophy (Johnson and Stoecker 2005). Estimates of heterotrophic C contribution to the C budget of *M. rubra* indicate that feeding accounts for an insignificant amount of growth, suggesting that the need for periodic ingestion of prey is simply to replenish cryptophyte organelles (Yih et al. 2004, Johnson et al. 2005). Differences in lipid production between *M. rubra* and *'G. cryophila'* may reflect differences in membrane structures or variation in the extent and form of storage products. High production of lipids in algal cells has also been attributed to N limitation and adaptation to living in polar ice (Kirst and Wiencke 1995).

References

Adolf JE, Stoecker DK, Harding Jr LW (2003) Autotrophic growth and photoacclimation in *Karlodinium micrum* (Dinophyceae) and *Storeatula major* (Cryptophyceae). J Phycol 39: 1101-1108

Berry J, Bjorkman O (1980) Photosynthetic response and adaptation to temperature in higher plants. Annul Rev Plant Physiol 31: 491-543

Caron DA, Goldman JC, Fenchel T (1990) Protozoan respiration and metabolism. In: Capriulo GM (ed) Ecology of marine protozoa. Oxford Univ Press, New York

Crawford DW, Purdie DA, Lockwood APM, Weissman P (1997) Recurrent red-tides in the Southampton Water Estuary by the phototrophic ciliate *Mesodinium rubrum*. Estuar Coast Shelf Sci 45: 799-812

Gustafson DE, Stoecker DK, Johnson MD, Van Heukelem WF, Sneider K (2000) Cryptophyte algae are robbed of their organelles by the marine ciliate *Mesodinium rubrum*. Nature 405: 1049-1052

Falkowski PG, Raven JA (1997) Aquatic photosynthesis. Malden: Blackwell, pp

Hibberd, DJ (1977) Observations on the ultrastructure of the cryptomonad endosymbiont of the red water ciliate *Mesodinium rubrum*. J Mar Biol Assoc UK 57:
45-61

Jankowski AW (1976) Revision of the classification of the cyrtophorids. In Markevich AP, Yu I (eds) Materials of the II All-union Conference of Protozoology, Part I, general protozoology, Naukova Dumka, pp 167-168

Jeffrey SW, MacTavish HS, Dunlap WC, Vesk M, Groenewoud K (1999) Occurrence of UVA- and UVB-absorbing compounds in 152 species (206 strains) of marine microalgae. Mar Ecol Prog Ser 189: 35-51

Johnson MD, Tengs T, Oldach DW, Delwiche CF, Stoecker DK (2004) Highly divergent SSU rRNA genes found in the marine ciliates *Myrionecta rubra* and *Mesodinium pulex*. Protist 155: 347-359

Johnson MD, Stoecker DK (2005) The role of feeding in growth and the photophysiology of *Myrionecta rubra*. Aquat Microb Ecol 39: 303-312

Kana TM, Glibert PM (1987) Effect of irradiances up to 2000 μE m^{-2} s^{-1} on marine *Synechococcus* WH7803: I. Growth, pigmentation, and cell composition. Deep Sea Res 34: 479-495

Kirst GO, Wiencke C (1995) Ecophysiology of polar algae. J Phycol 31: 181-199

Kishino M, Takahashi M, Okami N, Ichimura S (1985) Estimation of the spectral absorption coefficients of phytoplankton in the sea. Bull Mar Sci 37: 634-642

Laybourn-Parry J, Bell EM, Roberts EC (2000) Protozoan growth rates in Antarctic Lakes. Pol Biol 23: 445-451

Lewis MR, Smith JC (1983) A small volume, short-incubation-time method for measurement of photosynthesis as a function of incident irradiance. Mar Ecol Prog Ser 13: 99-102

Lewitus AJ, Glasgow HB, Burkholder JM (1999) Kleptoplastidy in the toxic dinoflagellate *Pfiesteria piscicida* (Dinophyceae). J Phycol 35: 303-312

Lindholm T (1978) Autumnal mass development of the "red water" ciliate *Mesodinium rubrum* in the Åland archipelago. Mem Soc Fauna Flora Fenn 54: 1-5

Lindholm T (1985) *Mesodinium rubrum*- a unique photosynthetic ciliate. Adv Aquat Microbiol 3: 1-48

MacIntyre HL, Kana TM, Anning T, Geider R (2002) Photoacclimation of photosynthesis irradiance response curves and photosynthetic pigments in microalgae and cynaobacteria. J Phycol 38: 17-38

Marshall W, Laybourn-Parry J (2002) The balance between photosynthesis and grazing in Antarctic mixotrophic cryptophytes during summer. Fresh Biol 47: 2060-2070

Menden-Deuer S, Lessard EJ (2000) Carbon to volume relationships for dinoflagellates, diatoms, and other protist plankton. Limnol Oceanogr 45: 569-579

Morris I, Glover HE, Yentsch CS (1974) Products of photosynthesis by marine phytoplankton: the effect of environmental factors on the relative rates of protein synthesis. Mar Biol 27: 1-9

Morris I (1981) Photosynthesis products, physiological state, and phytoplankton growth. In: Platt T (Ed) Physiological basis of phytoplankton ecology. Can Bull Fish Aquat Sci 210: 83-102

Neale PJ, Banaszak AT, Jarriel CR (1998) Ultraviolet sunscreens in *Gymnodinium saunguineum* (Dinophyceae): mycosporine-like amino acids protect against inhibition of photosynthesis. J Phycol 34: 928-938

Oakley BR and Taylor FJR (1978) Evidence for a new type of endosymbiotic organization in a population of the ciliate *Mesodinium rubrum* from British Columbia. BioSystems 10: 361-369

Palmisano AC, Smith GA, White DC, Nichols PD, Lizotte MP, Cota G, Sullivan CW (1987) Changes in photosynthetic metabolism in sea-ice microalgae during a spring bloom in McMurdo Sound. Antarc J 22: 176-7.

Parsons TR, Maita Y, Lalli CM (1984) A manual of chemical and biological methods for seawater analysis. Pergamon Press, Oxford

Platt T, Gallegos CL, Harrison WG (1980) Photoinhibition of photosynthesis in natural assemblages of marine phytoplankton. J Mar Res 38: 687-701

Putt M (1990) Metabolism of photosynthate in the chloroplast-retaining ciliate *Loboea strobila*. Mar Ecol Prog Ser 60: 271-282

Robinson DH, Kolber Z, Sullivan CW (1997) Photophysiology and photoacclimation in surface sea ice algae from McMurdo Sound, Antarctica. Mar Ecol Prog Ser 147: 243-256

Rychert K (2004) The size structure of the *Mesodinium rubrum* population in the Gdansk Basin. Oceanologia 46(3): 439-444

Ryther JH (1967) Occurrence of red water off Peru. Nature 214: 1318-1319

Sakshaug E, Slagstad D (1991) Light and productivity of phytoplankton in polar marine ecosystems: a physiological view. In: Sakshaug E, Hopkins CCE, Oritsland NA (Eds) Proceedings of the Pro Mare Symposium on polar marine ecology. Pol Res 10: 69-85

Satoh H, Watanabe K (1991) A red-water bloom caused by the autotrophic ciliate, *Mesodinium rubrum*, in the austral summer in the fast ice area near Syowa station, Antarctica, with note on their photosynthetic rate. J Tokyo Univer Fish 78: 11-17

Skovgaard A (1998) Role of chloroplast retention in a marine dinoflagellate. Aqu Microb Ecol 15: 293-301

Stoecker DK, Michaels AE, Davis LH (1987) Large proportion of marine planktonic ciliates found to contain functional chloroplasts. Nature 326: 790-792

Stoecker DK, Silver MW, Michaels AE, Davis LH (1988) Obligate mixotrophy in *Loboea strobila*, a ciliate which retains chloroplasts. Mar Biol 99: 415-423

Stoecker DK, Silver MW (1990) Replacement and aging of chloroplasts in *Stombidium capitatum* (Ciliophora: Oligotrichida). Mar Biol 107: 491-502

Stoecker DK, Putt M, Davis LH, Michaels AE (1991) Photosynthesis in *Mesodinium rubrum*: species-specific measurements and comparison to community rates. Mar Ecol Prog Ser 73: 245-252

Taylor FJR, Balckbourn, DJ, Blackbourn, J (1969) Ultrastructure of the chloroplasts and associated structures within the marine ciliate *Mesodinium rubrum* (Lohmann). Nature 224: 819-821

Taylor FJR, Blackbourn DJ, Blackbourn J (1971) The red-water ciliate *Mesodinium rubrum* and its "incomplete symbionts": a review including new ultrastructural observations. J Fish Res Bd Canada 28: 391-407

Tartarotti B, Baffico G, Temporetti P, Zagarese HE (2004) Mycosporine-like amino acids in planktonic organisms living under different UV exposure conditions in Patagonian lakes. J Plank Res 26: 753-762

Yih W, Kim HS, Jeong HJ, Myung G, Kim YG (2004) Ingestion of cryptophyte cells by the marine photosynthetic ciliate *Mesodinium rubrum*. Aquat Microb Ecol 36: 165-170

Table 3.1. Abbreviations used throughout the text.

Symbol	Definition
μ	Growth rate, d^{-1}
a^{chl}	Chl a specific spectral absorbance
$a(p)^{chl\ 335}$	Chl *a* specific spectral absorbance at 335 nm
Fv/Fm	Variable fluorescence (dimensionless)
$P_{max}{}^{cell}$	Cellular photosynthetic capacity, pg C $cell^{-1}$ h^{-1}
$P_{max}{}^{chl}$	Chl *a*-specific photosynthetic capacity, pg C pg chl a^{-1} h^{-1}
$P_{max}{}^{c}$	C-specific photosynthetic capacity, pg C $(pg\ C)^{-1}$ h^{-1}
α^{cell}	Cellular photosynthetic efficiency, pg C $cell^{-1}$ h^{-1} (μmol photons m^{-2} s^{-1})$^{-1}$
α^{chl}	Chl *a*-specific photosynthetic efficiency, pg C pg chl a^{-1} h^{-1} (μmol photons m^{-2} s^{-1})$^{-1}$
E_k	Light saturation parameter from PE curve, μmol photons m^{-2} s^{-1}
θ	Chl *a*: C ratio

Table 2. Physiological parameters for *Myrionecta rubra* and *Geminigera cryophila* in high light (HL: 75 and 90 μmol photons m^{-2} s^{-1}) and low light (LL: 10 and 25 μmol photons m^{-2} s^{-1}) at 5°C.

	Myrionecta rubra		*Geminigera cryophila*		HL	LL
	HL	LL[a]	HL	LL	*P*	*P*
μ	0.179 (0.027)	0.125 (0.034)	0.260 (0.022)	0.195 (0.029)	***	*
chl *a* $cell^{-1}$	15.4 (2.8)	27.8 (5.9)	2.6 (0.14)	4.5 (0.6)	***	***
Fv/Fm	0.54 (0.04)	0.66 (0.01)	0.64 (0.02)	0.73 (0.05)	**	*
P_{max}^{cell}	10.1 (1.9)	21.9 (1.8)	1.7 (0.23)	2.87 (0.24)	***	**
P_{max}^{chl}	0.64 (0.16)	0.68 (0.04)	0.65 (0.07)	0.65 (0.13)	n.s.	n.s.
P_{max}^{c}	0.019 (0.005)	0.040 (0.003)	0.028 (0.006)	0.065 (0.004)	**	***
α^{cell}	0.158 (0.014)	0.394 (0.031)	0.039 (0.009)	0.116 (0.039)	***	***
α^{chl}	0.010 (0.001)	0.012 (0.001)	0.015 (0.004)	0.025 (0.006)	**	**
E_k	60.2 (9.9)	56.9 (3.5)	49.4 (2.7)	23.7 (7.8)	n.s.	***

[a]25 μmol photons m^{-2} s^{-1} only. Values in parentheses are standard deviations. Values in *P* columns indicate results of a paired T-test analysis ($p < 0.05$) between *M. rubra* and *G. cryophila*, *p < 0.05, **p < 0.005, ***p<0.001, n.s.: not significant

Table 3. *Myrionecta rubra*: *Geminigera cryophila* ratios of various physiological parameters in high light (HL: 75 and 90 μmol photons m^{-2} s^{-1}) and low light (LL: 10 and 25 μmol photons m^{-2} s^{-1}) at 5°C.

Irradiance:	HL ratio	LL ratio
C	8.903	12.38
μ	0.689	0.6418
chl $cell^{-1}$	5.891	6.140
chl*a*:C	0.662	0.496
$a(p)^{chl\ 335}$	9.376	3.457
Fv/Fm	0.849	0.900
P_{max}^{cell}	5.953	7.607
P_{max}^{chl}	0.980	1.043
P_{max}^{c}	0.672	0.612
α^{cell}	4.018	3.396
α^{chl}	0.637	0.485
E_k	1.218	2.405

Figure 3.1. Phylogenetic analysis of cryptophyte (A) nucleomorph (Nm) and (B) nuclear (Nu) SSU rRNA genes for *Geminigera cryophila* and *Myrionecta rubra* using gamma-corrected (Nm: Γ = 0.4317; Nu: Γ = 0.6326) maximum likelihood (Nm: -lnL = 7686.45; Nu = 7339.95); GTR model) model with proportion of invariable sites (Nm = 0.5179; Nu = 0.4364) on DNA alignments of 1842 (Nm) and 1829 (Nu) sites. Base frequencies and substitution rates were estimated with a maximum likelihood search. Tree topology was found using stepwise addition and1x heuristic searches with TBR branch swapping and random-addition sequences. Numbers on branches correspond to bootstrap values (100x with stepwise addition and a heuristic search with 2x random addition and TBR branch swapping) for each ML tree.

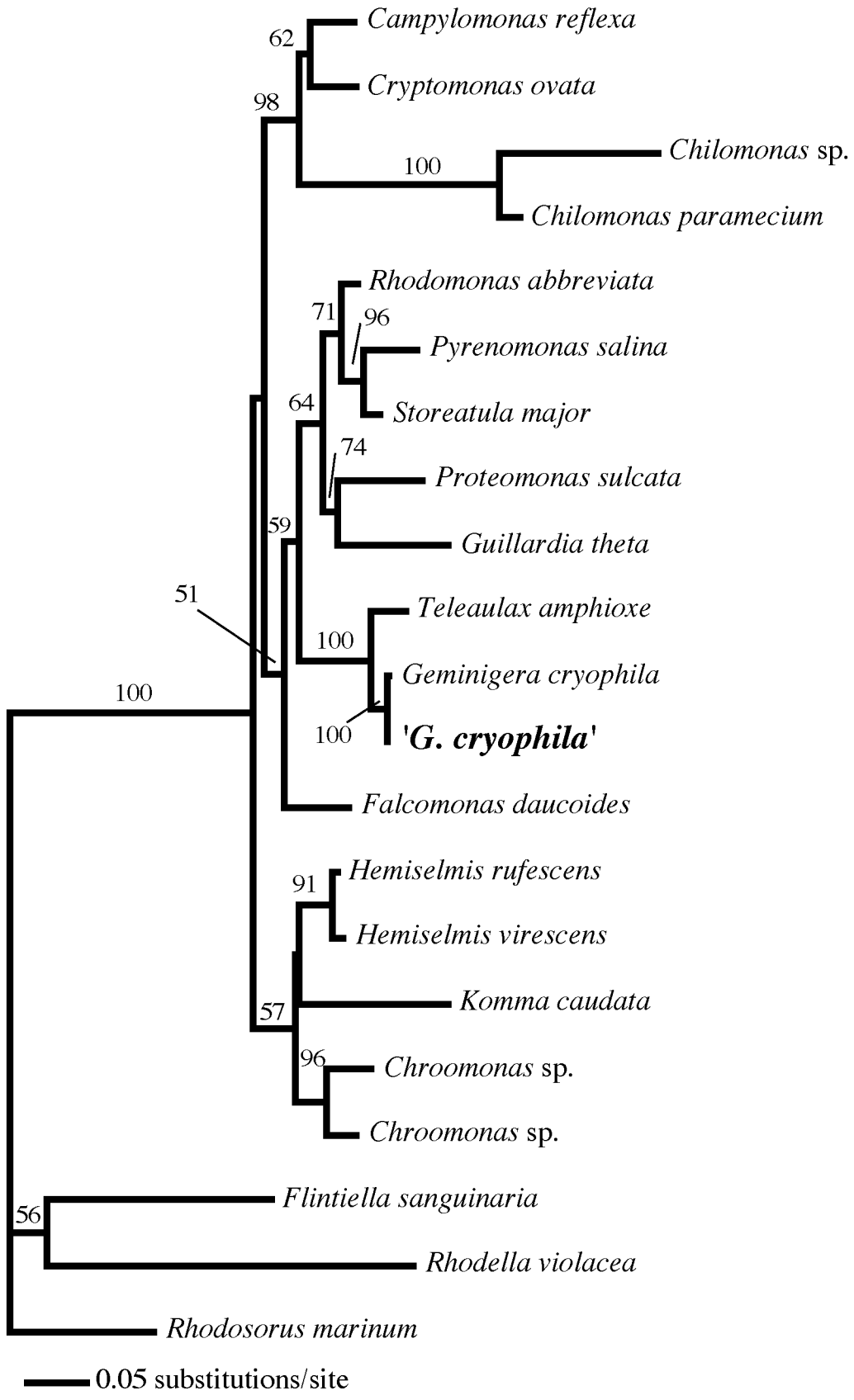
Campylomonas reflexa
62
Cryptomonas ovata
98
Chilomonas sp.
100
Chilomonas paramecium
Rhodomonas abbreviata
71
96
Pyrenomonas salina
64
Storeatula major
74
Proteomonas sulcata
59
Guillardia theta
51
Teleaulax amphioxe
100
Geminigera cryophila
100
100
'G. cryophila'
Falcomonas daucoides
Hemiselmis rufescens
91
Hemiselmis virescens
Komma caudata
57
96
Chroomonas sp.
Chroomonas sp.
Flintiella sanguinaria
56
Rhodella violacea
Rhodosorus marinum
0.05 substitutions/site

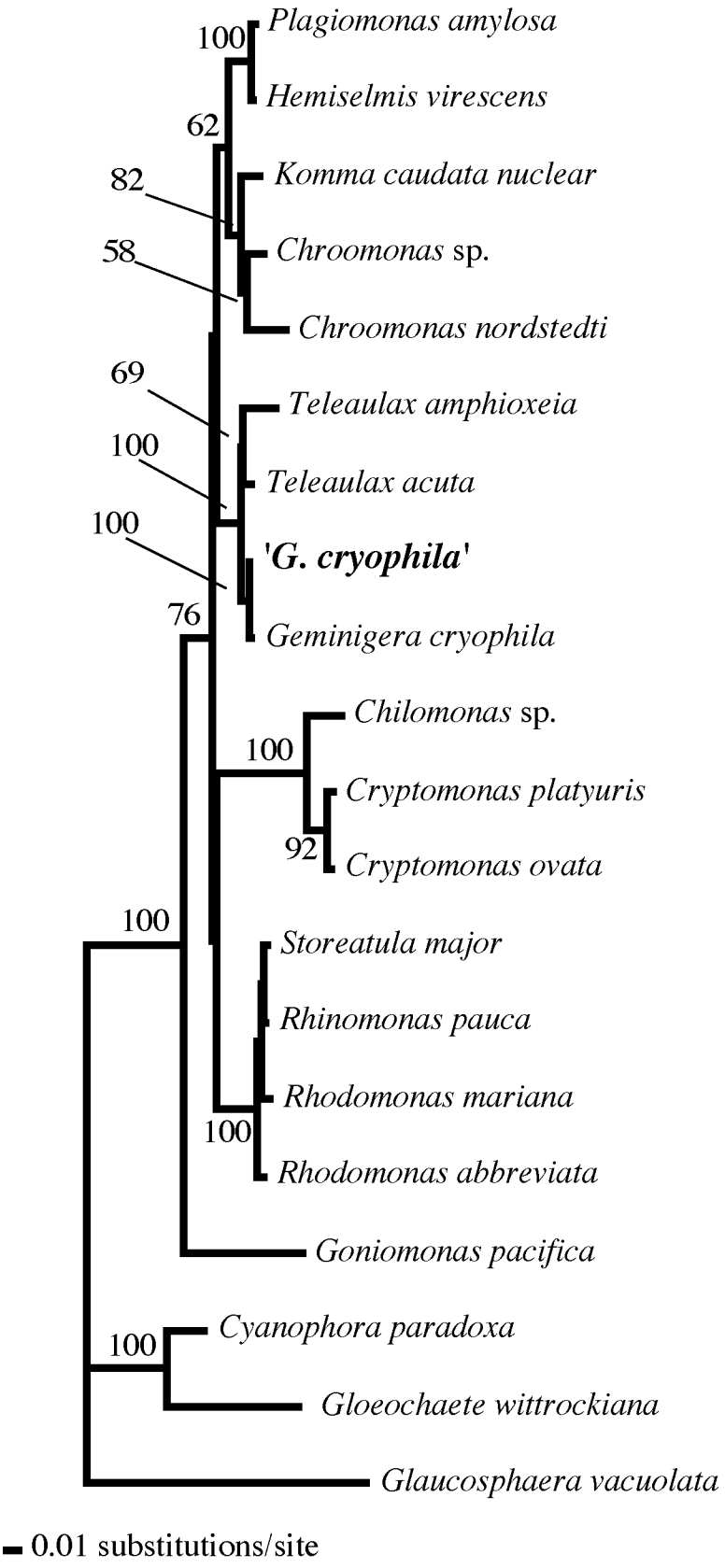
Plagiomonas amylosa
100
Hemiselmis virescens
62
Komma caudata nuclear
82
Chroomonas sp.
58
Chroomonas nordstedti
69
Teleaulax amphioxeia
100
Teleaulax acuta
100
'G. cryophila'
76
Geminigera cryophila
Chilomonas sp.
100
Cryptomonas platyuris
92
Cryptomonas ovata
100
Storeatula major
Rhinomonas pauca
Rhodomonas mariana
100
Rhodomonas abbreviata
Goniomonas pacifica
Cyanophora paradoxa
100
Gloeochaete wittrockiana
Glaucosphaera vacuolata
0.01 substitutions/site

Figure 3.2. Cell abundance and nucleomorph (Nm) genomes cell^{-1} (NGC) (~ plastid number cell^{-1}) over time for a growing *Myrionecta rubra* culture. NGC estimated using quantitative (q) PCR with an assay designed for the *Geminigera cryophila* nucleomorph SSU rRNA gene.

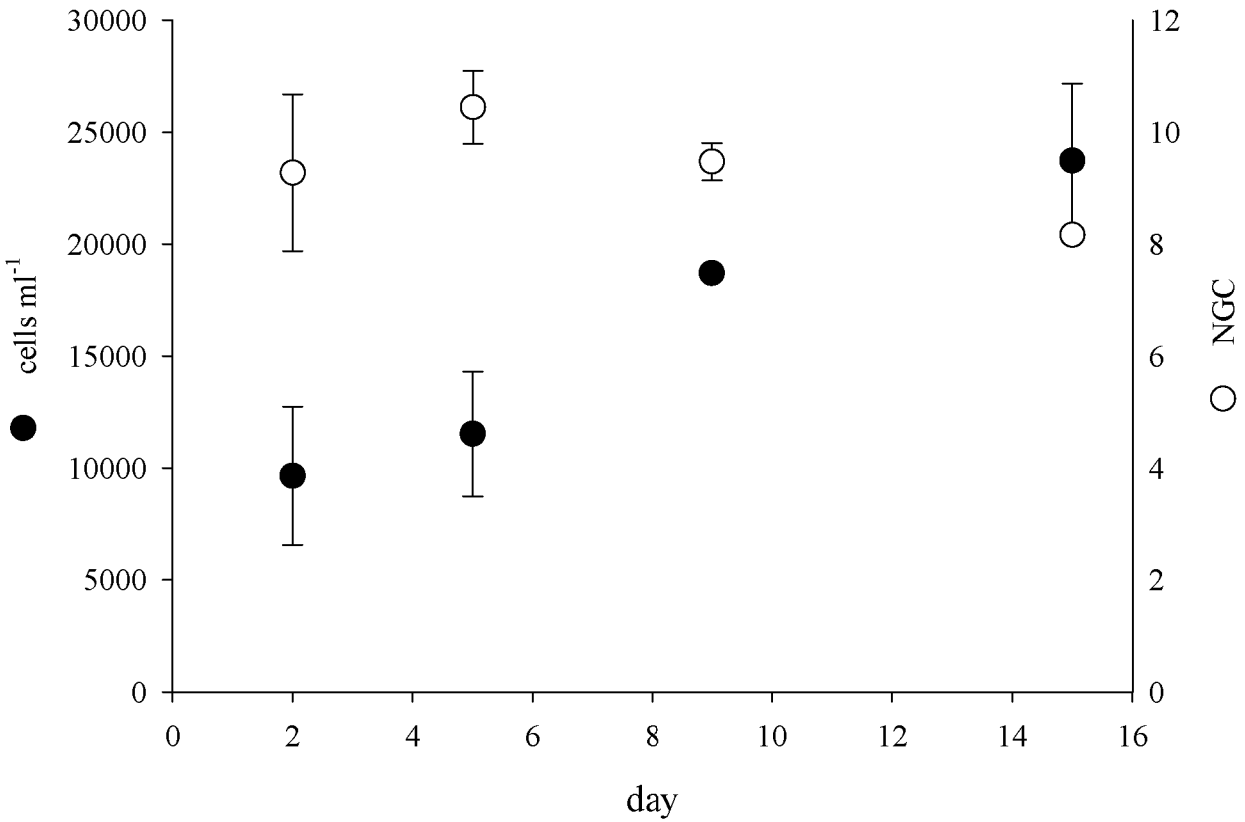
30000
25000
20000
15000
10000
5000
0
cells ml-1
12
10
8
6
4
2
0
NGC
0
2
4
6
8
10
12
14
16
day

Figure 3.3. TEM sections of *Myrionecta rubra* showing the chloroplast-mitochondria complex (CMC) harboring cryptophyte organelles. ER: endoplasmic reticulum, L: lipid droplet, M: cryptophyte mitochondria, NM: nucleomorph, P: pyrenoid; long arrow: periplastidal double membrane, short arrow: CMC outer membrane.

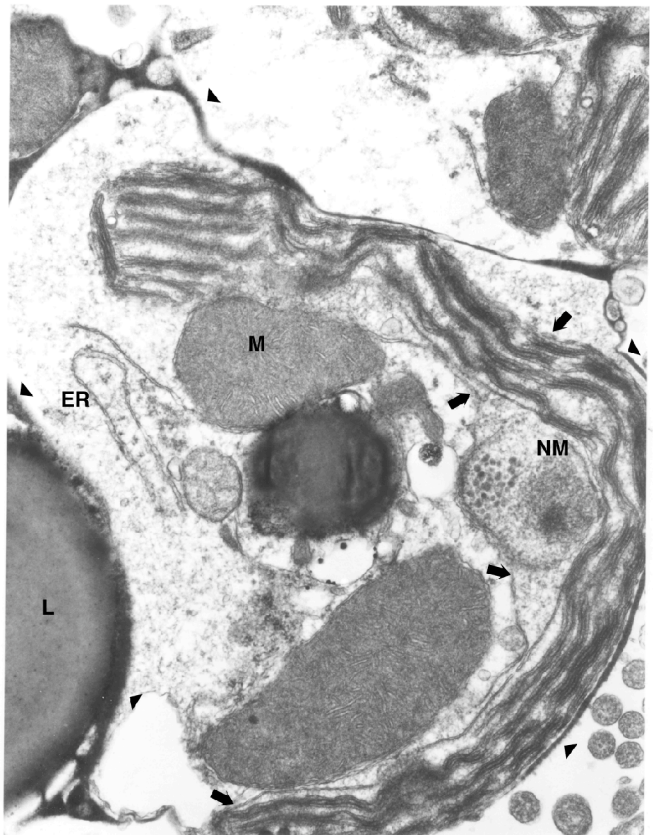
M
ER
NM
L

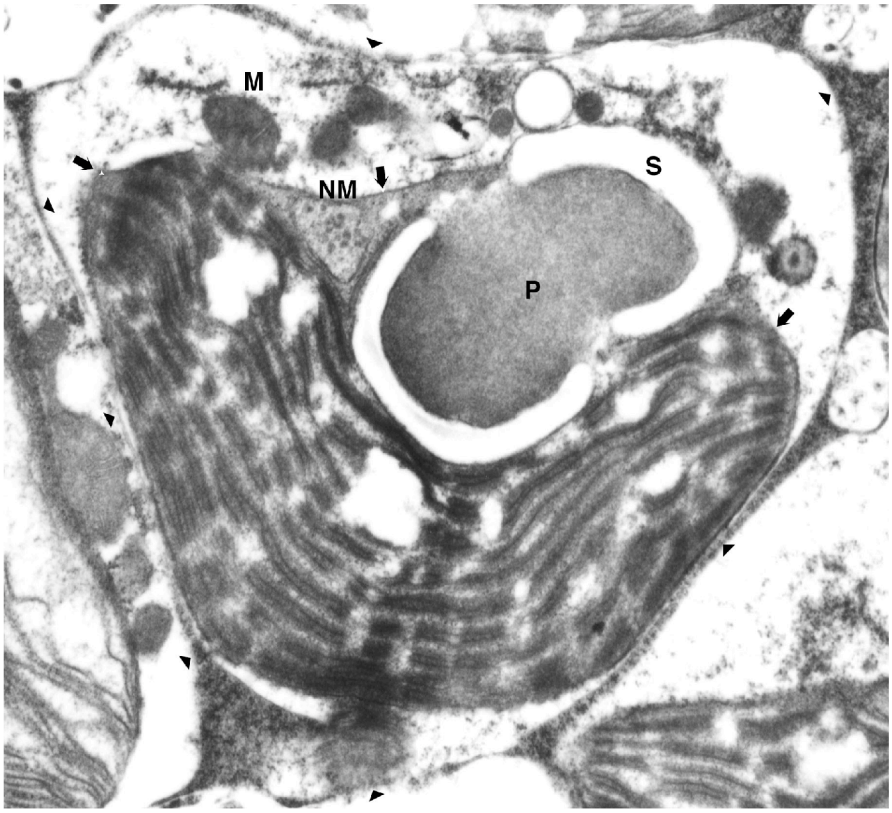
M
NM
S
P

Figure 3.4. UV and visible chlorophyll-specific spectral absorption for (A) *Geminigera cryophila* and (B) *Myrionecta rubra*. Inset is visible spectrum only. All spectrums are means (n=2).

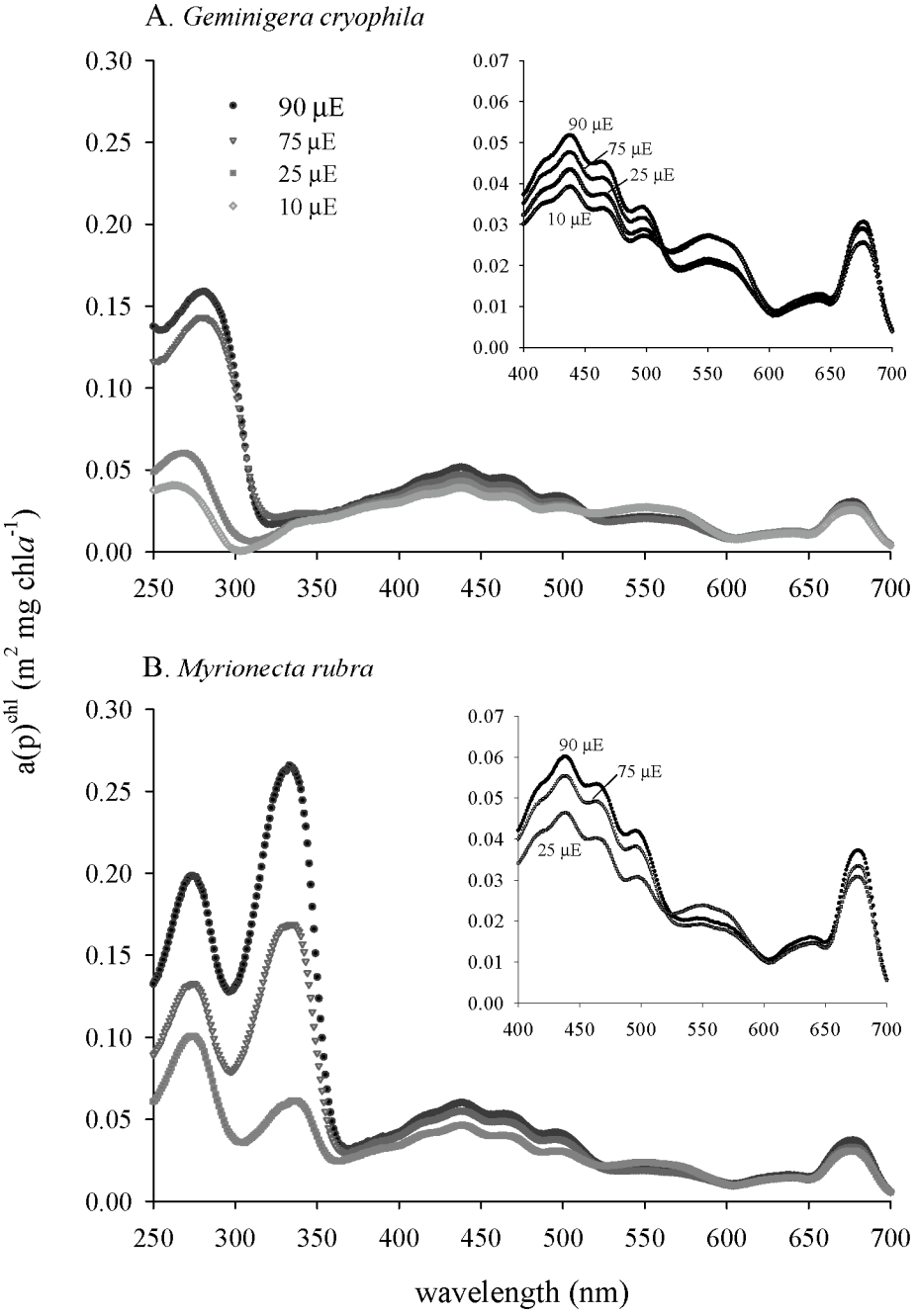
A. Geminigera cryophila
90 µE
75 µE
25 µE
10 µE
B. Myrionecta rubra
a(p)chl (m2 mg chla-1)
wavelength (nm)

Figure 3.5. Analysis of partitioning of photosynthetically fixed C into major biochemical fractions using the serial extraction technique for (A) *Geminigera cryophila* and *Myrionecta rubra* acclimated to low light (25 μmol photons m^{-2} s^{-1}) and (B) *M. rubra* acclimated to LL and high light (HL: 75 and 90 μmol photons m^{-2} s^{-1}). Ttest: *p<0.05, **P<0.01

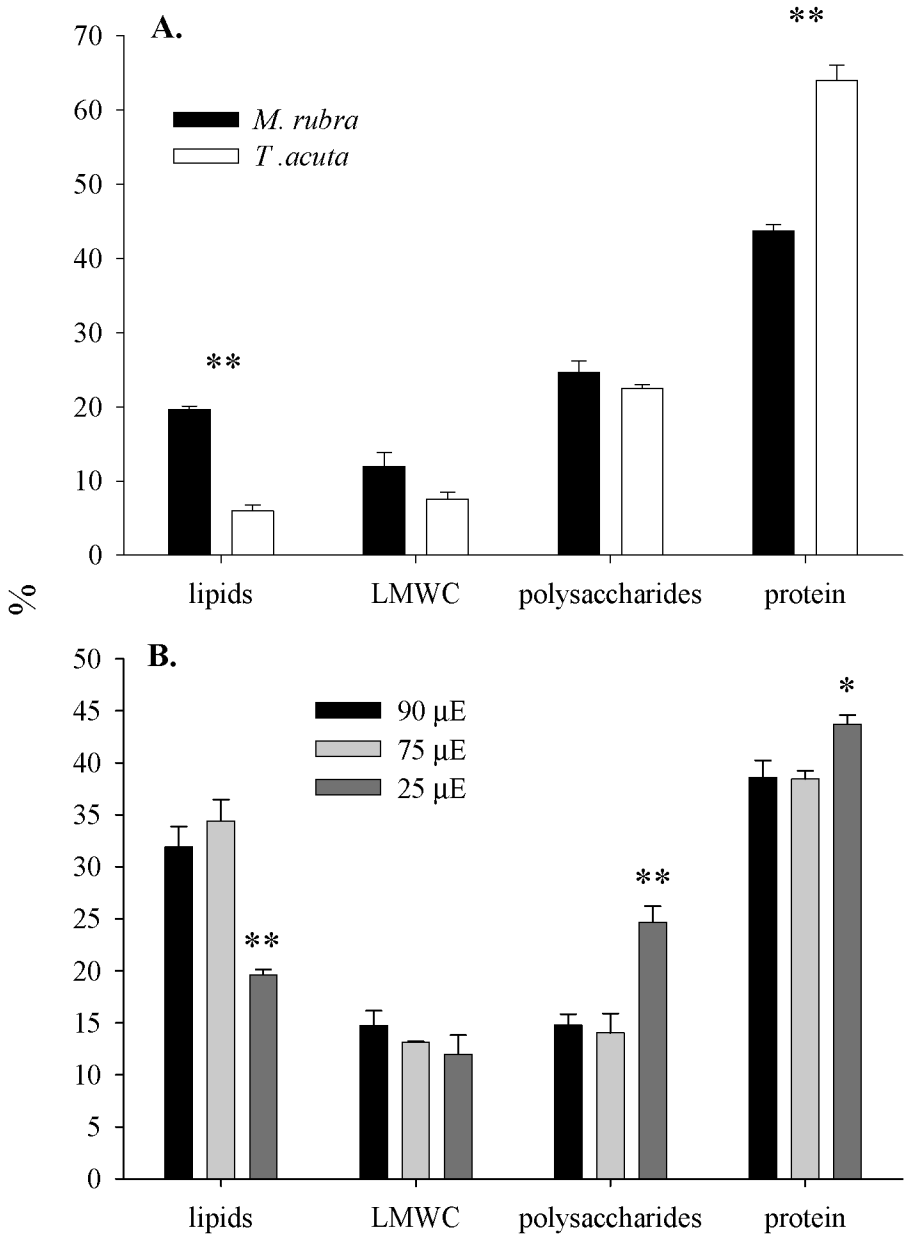
A.
M. rubra
T .acuta
%
70
60
50
40
30
20
10
0
**
**
lipids
LMWC
polysaccharides
protein
B.
90 µE
75 µE
25 µE
50
45
40
35
30
25
20
15
10
5
0
**
**
*
lipids
LMWC
polysaccharides
protein

CHAPTER 4: Retention of Functional Prey Nuclei by the Ciliate *Myrionecta rubra*

Abstract

Herein I present evidence that the phototrophic marine ciliate, *Myrionecta rubra*, sequesters functional nuclei from its cryptomonad prey, *Geminigera cryophila*. *M. rubra* also sequesters prey chloroplasts, mitochondria, and cytoplasm, enclosing them in numerous membrane-bound complexes (CMCs). *M. rubra* cells were labeled with a fluorescent SSU rRNA probe, and the probe hybridized to RNA in the nucleoli of prey nuclei (PN), in addition to pockets of cytoplasm and CMCs in the ciliate. PN were retained for 30+days without net population loss, during which time they were diluted from 0.8 to 0.1 cell^{-1} by cytokinesis. Over the next 20d they disappeared from the population, and cell and plastid division rates declined by ~50%. Expression of PN LHCC10 and GAPDH genes in *M. rubra* varied 32 and 21 fold, respectively, relative to minimum expression and normalized to *M. rubra* β-tubulin expression ($E^{\Delta\Delta\text{-CT}}$). Expression of LHCC10 and GAPDH reached a maximum between 10-20d after t=0, at ~2 and 14 fold, respectively, of expression levels in *G. cryophila* (E^{prey}). After 20d, expression of these genes quickly declined and remained significantly lower ($p<0.0001$). Expression of the plastid gene *psbA* was least variable ($E^{\Delta\Delta\text{-CT}}$: 3.4 fold) and E^{prey} reached levels 12-fold that of *G. cryophila*, while expression patterns of the nucleomorph (Nm) gene *cbbX* was similar to that of nuclear genes ($E^{\Delta\Delta\text{-CT}}$: 20 fold range) and E^{prey} reached 10 fold briefly at day 5. After 5-6 weeks of starvation, plastid division rates became out of synch with cytokinesis, causing a decline in measured Nm genomes cell^{-1}. After 84 days of starvation, cell and plastid division was either negative or 0, quantum efficiency (Fv/Fm) of photosynthesis declined ($p<0.05$), PN were almost absent in the population

(<0.05 cell^{-1}), and expression had declined significantly for all genes. This is the first report of an organism enslaving a foreign nucleus and apparently benefiting from expression of encoded genes.

Introduction

The retention of chloroplast (= plastid) and mitochondria organelles from prey occurs in numerous protists, including ciliates (Blackbourn et al. 1973), dinoflagellates (Fields and Rhodes 1991), and foraminifera (e.g. Grzymski et al. 2002), as well as is some metazoans, such as the sea slug, *Elysia chlorotica* (Trench 1979). Organelle retention differs from symbiosis in that only portions of a prey cell are "enslaved" during the process of ingestion. Plastid retention in ciliates has long been appreciated to be widespread in marine environments (Blackbourn et al. 1973, Stoecker et al. 1987). In protists, there appear to be several modes of organelle sequestration: 1) many plastids are isolated free in the host cell's cytoplasm and not surrounded by a vacuole (e.g. oligotrich ciliates; Blackbourn et al. 1973, Laval-Peuto et al. 1986), 2) a single plastid is retained in a vacuole without digestion (e.g. *Pfiesteria piscicida*; Lewitus et al. 1999), 3) single plastids (sometimes with prey cytoplasm) and mitochondria of prey are separately surrounded by host vacuole membranes (e.g. *Perispira ovum*; Johnson et al. 1995), and 4) a plastid, mitochondrion, and prey cytoplasm are sequestered together and surrounded by a host membrane as one (*Gymnodinium acidotum*; Fields & Rhodes 1991) or numerous units (*Myrionecta rubra*, Taylor et al. 1969). In most ciliates, sequestered plastids are passed on during cell division to daughter cells, but are incapable of division and must be

replenished through feeding (e.g. Laval-Peuto et al. 1986). In choreotrich ciliates the life of a sequestered plastid may vary from hours to days (Stoecker and Silver 1990). The inability of most protists to maintain sequestered organelles long-term is likely due to the absence of an associated prey nucleus and the numerous genes involved in the regulation, division, and function of an organelle.

Myrionecta rubra is a photosynthetic ciliate commonly encountered in estuarine and neritic pelagic environments, and known for forming sporadic non-toxic red tides (Taylor et al. 1971, Lindholm 1985). The chloroplast-mitochondria complexes (CMCs) of *M. rubra* are well documented in wild populations (Taylor et al. 1969, 1971, Hibberd 1977, Oakley and Taylor 1978), and have recently been confirmed for a cultured strain of *M. rubra* (Johnson et al. in prep). Cryptophyte nuclei can also be observed in both wild (Hibberd 1977) and cultured (Gustafson et al. 2000) *M. rubra*, and may persist for weeks after feeding (Johnson et al. 2005). While other photosynthetic ciliates possess plastids and mitochondria (Johnson et al. 1995), the formation of CMCs and retention of prey nuclei are unique. Furthermore, *M. rubra* is capable of pigment synthesis (Gustafson et al. 2000, Johnson & Stoecker 2005) and plastid division (Johnson et al. in prep), which have never been shown in another plastid-retaining organism. Herein I demonstrate that *M. rubra* retains functional prey nuclei from *G. cryophila*, and they remain transcriptionally active for weeks, apparently contributing to the ability of the ciliate to function as a phototroph.

Methods

Experimental conditions and measuring cellular attributes

Myrionecta rubra (CCMP 2563) and *Geminigera cryophila* (CCMP 2564) cultures were maintained at 4°C in 32 PSU media with F/2 (-Si) nutrients in a 24h L regime at 100 (experiment 1) or 45 (experiment 2) μmol photons m^{-2} s^{-1}. All experiments were conducted using batch culture techniques with duplicate or triplicate 1L glass flasks.

Experiment 1: Documenting the fate of prey nuclei with FISH. At t=0 *M. rubra* (924 ± 227 cells ml^{-1}) were fed *G. cryophila* at 4100 ± 1113 cells $ml^{-1}$and samples were taken at t = 0, 10, 30, 60, 180, and 360 minutes in order to measure grazing kinetics using fluorescence in situ hybridization (see FISH section below for fixation protocol). The experiment was allowed to continue for 45 days, with transfer to new media on day 19.

Experiment 2: Measuring expression of prey genes in M. rubra. At the beginning of the experiment, *G. cryophila* were added to *M. rubra* culture duplicates at a 4:1 ratio. *M. rubra* cultures were sampled over time in the absence of *G. cryophila* prey, as described elsewhere (Johnson & Stoecker 2005). At the end of each ~2 week growth period, *M. rubra* cells were given fresh F/2 culture media in order to establish food-starved but nutrient replete cell populations. Division rates for cells and plastids were estimated during the exponential portion of the growth phase using μ (div d^{-1}) = $(\log_2(n_1/n_0))/t_1\text{-}t_0$, where n_0 and n_1 are cell concentrations at the beginning and start of the exponential growth phase, respectively. At all time points cells were fixed using 2% glutaraldehyde and stained with the nucleic acid stain, 4,6-diamidino-2-phenylindole

(DAPI). Cells and prey nuclei were enumerated at 1000x using a Nikon Eclipse compound microscope, equipped with a fluorescence light source, and filter sets EF-4 B-2A (exciter filter 450-490 nm, dichromatic bean splitter (DM) 500nm, barrier filter (BA) 515 nm) and UV 2E/C (exciter filter 340-380 nm, DM 400 nm, BA 435-485 nm). Chlorophyll was extracted by filtering culture aliquots onto a GF/C filter and extracting overnight in 90% acetone at –20°C. Chlorophyll concentrations were determined using a Turner Designs model 10-AU fluorometer.

FISH

A fluorescence *in situ* hybridization (FISH) oligonucleotide probe, TANU2, labeled with fluoroscein isothiocyante (FITC) (see Table 1 for sequence) for the *G. cryophila* SSU rRNA gene was designed by eye from DNA alignments using MacClade 4.05 (Maddison and Maddison 1991). FISH probes for *M. rubra* SSU rRNA gene (MYR2), labeled with 5-N-N'-diethyl-tetramethylindodicarbocyanine (Cy5) (Johnson et al. 2004), positive control (uniC-FITC), and negative (anti-sense) control (uniR-FITC) probes were also used (Miller and Scholin 1998). All probes were ordered from Qiagen, and tested using Primer Express 1.0 (Applied Biosystems) for possible complications due to secondary structure. Cells were preserved with 4% paraformaldehyde with 5X SET (0.75 M NaCl, 5mM EDTA, 0.1M Tris-HCl, pH 7.8), 12-24 hr prior to hybridization. Preserved cells were gently filtered onto a 2.0 μm nucleopore filter, using a 5 μm backing filter, and washed twice with hybridization buffer (final concentration: 5x SET, 1% IGEPAL-CA630, 31.25 μg/ml polyadenylic acid). Cells were resuspended in 0.5 ml of

hybridization buffer and 5 ng/ml of probe was added. All hybridizations were conducted at 45ºC (determined empirically) in a water bath, for 1-2 h. After hybridization, cells were filtered onto a new membrane and washed several times with 45ºC 5x SET. Cells were then resuspended in 45ºC 5X SET and incubated for 2-3 minutes, after which the cells were filtered and resuspended in 1 ml fresh 5X SET buffer and stored at 4ºC in the dark until used for microscopy (<3h). The TANU2 probe was tested first against *G. cryophila* for positive labeling, and then against other algal cultures to evaluate probe specificity (data not shown).

The number of *G. cryophila* nuclei in *M. rubra* over time was accomplished by counting at least 100 cells labeled with the TANU2 probe at each time point, using a compound Nikon Eclipse microscope (described above). For obtaining a micrograph of dual labeled cells, we used a Zeiss LSM 510 confocal system attached to a Zeiss inverted microscope, fitted with a C-Apochromat 63x/1.2 W lens. Single scan or Z-stack imaging analysis was preformed through several representative cells for capturing images. Images were captured using the multi-channel option at three wavelength settings: 1) blue light (for FITC) excitation (ex) 488nm, 2) far red (for Cy5) ex 633nm, and 3) green (for phycoerythrin in chloroplasts) ex 543nm. Emission filters for each channel were as follows: blue: band pass 505-560nm, far-red: long pass (LP) 650nm, and green: LP 560nm.

TEM

Cells were fixed with 4% paraformaldehyde, 2% gluteraldehyde, 0.05 M cacodylic acid, and 0.1 M sucrose for 2h at 4°C, spun (4000 rpm 10 min), washed with 0.05 M cacodylic acid and 0.1 M sucrose buffer, and washed again with 0.05 cacodylic buffer. Cells were then postfixed with 1% osmium for 3 h. Dehydration was in ethanol and embedding in Spurr's resin. Embedded cells were thin sectioned, placed on a copper grid, and stained with uranyl acetate and lead for TEM viewing on a JEOL 1200-EX.

DNA isolation, gene amplification, and sequencing for creation of gene expression assays

Cultures of *M. rubra* were centrifuged in 50 ml centrifuge tubes at 4ºC and 4000 g for 10 min. The Plant DNA Extraction Kit (Qiagen) was used and the manufacturers protocol was followed. PCR was conducted using 1x PCR buffer (TaqPro, Denville), 0.2 μM nucleotides, 0.25mg/ml bovine serum albumin (BSA), 3 mM $MgCl_2$, 0.4 μM primers, and 0.6 u Taq DNA polymerase, and were combined with 10-20 ng of genomic DNA from cultures in a volume of 25 ml. Glyceraldehyde-3-phosphate dehydrogenase (GAPDH) was isolated from *G. cryophila* and beta-tubulin (β-tub) from *M. rubra* using universal primers (Fast et al. 2001, Saldarriaga et al. 2003, respectively). Other genes were isolated with primers designed by eye from gene alignments in MacClade 4.05 (Maddison and Maddison 1991), for a "regulatory gene for ribulose-1,5-bisphosphate carboxylase/oxygenase" (*cbbX*) (F: TTGCATTATCACCTCTAGCAATAAGTTC, R: ATGTCGGTCATACTGCTCCTAAA), the photosystem II D1 protein (*psbA*) (F: WGACAACCGTTTATAYATCGGWTG, R: TTAGCACGGTTAAGGATUTCAGC), and a light-harvesting complex protein (LHCC10) (F:

AGGCTGAGRTCAAGCACGGMCGYATYKSYATG, R: TCAAGAACGGCCGCCTYGCYATGMTCGCC). PCR conditions were as follows: an initial 3 min 95ºC melting step, 40 cycles of 30 sec at 95ºC (melting), 30s at 55ºC (hybridization), and 70s at 72ºC (elongation), followed by a final 10m 72ºC elongation step. Products were then cloned using an Invitrogen TOPO TA cloning kit, following manufacturers instructions. Colonies were then isolated and gene products were reamplified with PCR using the same gene-specific primers. Cloned PCR products were sequenced directly in both directions using the above gene-specific primers and the BigDye terminator kit (Perkin Elmer). All sequencing was conducted using an ABI 377. Gene-specific primers were then designed for all genes (not shown), in order to re-isolate, clone and obtain better sequence reads of all genes. The resulting gene products were then used for designing quantitative RT-PCR assays (Operon) by eye in MacClade (Table 1).

RNA isolation and DNase treatment

RNA was isolated using the RNeasy Plant Mini Kit (Qiagen). Cells were centrifuged at 4000 rpm for 10 min at 4°C in 50 ml conical tubes, after which the media was decanted and pellets were immediately placed on dry ice. Cell pellets were then allowed to thaw on wet ice, after which 450 µl of RLT buffer was immediately added and cells were vortexed vigorously into a suspension. The cell suspension was then transferred to a microtube and the manufacturers instructions for plants and fungi were closely followed, using the optional column DNase 1 treatment for 15 min at room temperature at step 6

(see RNeasy Mini handbook). After extraction, RNA was again treated with DNA-free DNase (Ambion) at 37°C for 15min, after which time 1μl of DNase was again added, and the incubation was repeated. DNase was then deactivated as described per manufacturers instructions (Ambion).

RT-qPCR

Creation of cDNA with reverse transcriptase (RT) was conducted as the first cycle in quantitative (q) PCR reactions for 30 min at 48°C, using the Superscript III one-step RT-PCR system with platinum taq DNA polymerase (Invitrogen). RT-qPCR reactions were combined using 12.5 μl 2x reaction mix, 0.2 μM of each primer, 0.3 μM of probe, 1 μl of the SS III RT/plat mix, 2 μl of sample RNA, and the remaining volume RNase-free water, totaling 25 μl. All primers and probes used in qPCR assays are in table 1. RT-qPCR was conducted using a Smart Cycler (Cepheid) with 25 μl reaction tubes (Cepheid). Following the RT step, qPCR reaction cycles were as follows: 95°C for 2 min, then 50 cycles of 95°C for 15s and 59°C for 30s, for all assays except *cbbX*, which was 57°C. All annealing temperatures were determined empirically for each assay. Determination of threshold cycle numbers (C_T) for sample reactions was determined using default settings as defined by Cepheid. Negative controls were included with identical preparation, but without a RT step. qPCR-only negative controls generally had positive results, but were 13 (GAPDH) to 24 (β-tub) C_T greater than RT-qPCR results, which translates to about a 3-6 log difference in template concentration.

Expression normalization

Gene expression was normalized using two methods. The first method normalized expression of *G. cryophila* genes in *M. rubra* to equivalent expression levels of *G. cryophila*-only cultures, based on linear relationships between RT-qPCR detection cycle number (y) and cell number (x). Linear regressions for prey expression normalization were established for each gene, using a dilution series of *G. cryophila* RNA extracted from cultures during exponential growth. Linear regressions for each gene revealed the following relationships: *cbbX*: y = -1.9079Ln(x) + 42.538, GAPDH: y = -2.3604Ln(x) + 53.427, LHCC10: y = -1.5523Ln(x) + 34.472, *psbA*: y = -2.1615Ln(x) + 39.187. Normalization of expression in *M. rubra* cultures was then accomplished by solving for x based on observed detection cycle numbers, yielding equivalent *G. cryophila* cell numbers, which were then divided by *M. rubra* cell concentrations. The second method was the $2^{-\Delta\Delta C}{}_T$ method (e.g. Livak and Schmittgen 2001), which depends on the relative expression of a gene of interest to that of a housekeeping reference gene. Here I used expression of the *M. rubra* β-tubulin gene as a reference, and the following equation $2^{-\Delta\Delta CT}$, where $-\Delta\Delta C_T = (C_{T,Target} - C_{T,\beta\text{-tub}})_{time\ x} - (C_{T,Target} - C_{T,\beta\text{-tub}})_{time\ y}$. C_T is the cycle threshold number where the amount of amplified target reaches a steady state (determined by Smart Cycler software), time x is any sampling point, while time y is the 1x expression of the target gene normalized to β-tub. In the $\Delta\Delta^{-CT}$ method, expression is generally normalized to levels at t = 0 or prior to application of a treatment. Here I instead use the mean expression during period 5 (days 74-99) for time y, as this was the period of minimal gene expression during the experiment, and was representational of

highly fasted cells. The $2^{-\Delta\Delta CT}$ method assumes that 1) amplification efficiencies of the target and reference are approximately equal and 2) a doubling of target results in a one cycle decrease in measured C_T. To address these assumptions, slopes for ΔC_T during a log change in template (ΔC_T^{Log}) and ΔC_T for doubling of target (ΔC_T^{2}) were calculated for LHCC10, GAPDH, β-tub, *psbA*, and *cbbX*, yielding mean ΔC_T^{Log} of 3.96, 4.0, 4.2, 4.3, and 4.22, respectively, and ΔC_T^{2} of 0.79, 0.77, 0.83, 0.90, and 0.84. No assays were statistically different.

qPCR

Primers and probes for conducting (q) PCR were designed by eye in MacClade and ordered from Operon (Alameda, CA). Primers and probes were added at a final concentration of 0.2 and 0.3 mM, respectively. Taq polymerase was used at final concentration of 0.1 U ml^{-1} (TaqPro, Denville); $MgCl_2$ at a final concentration of 4 mM (Life Technologies, Rockville, MD); a deoxynucleoside triphosphate (dNTP) mixture with each dNTP at a final concentration of 0.2 mM; PCR buffer was at a final concentration of 1x (Denville). For the *G. cryophila* assay, the forward primer (FP) TMTA_Nm-F (CCGAGGCTCTTTGGTTAGACT), reverse primer (RP) TMTA_Nm-R (GCCATGCGATTCGGTTAGT), and probe (P) TMTA_Nm-P (6-FAM-TCGCCATTCATCACCTGATGGAAG-TAMRA) were used, while for the *M. rubra* assay, FP MR-F (ACGTCCGTAGTCTGTAC), RP MR-R (ATGATCCTAAGACGAGAAACTTA), and P MR-P (FAM-GAATGCGGTAGTTTCTGCAGTCACTC-BHQ1) were used. All real-time PCR was

conducted in a Smart Cycler (Cepheid, Sunnyvale, CA), using 25 ml reaction tubes. A standard curve for the nucleomorph (Nm) SSU rRNA gene was created using a dilution series of cells from the '*G. cryophila*' culture. The resulting cycle numbers were then plotted against cell cumber and an equation was obtained using a best-fit linear regression ($y = -1.3854\text{Ln}(x) + 36.316$; $r^2 = 0.987$). Nm ssu rRNA gene content was then normalized to that of *M. rubra* nuclear ssu rRNA gene content, determined using the same approach ($y = -1.5863\text{Ln}(x) + 28.576$; $r^2 = 0.999$), and expressed as a ratio of equivalent cell numbers (solving for x, as above) that should be roughly equivalent to Nm genomes $cell^{-1}$ (NGC). Assuming one Nm genome $plastid^{-1}$, this number therefore approximates plastid number $cell^{-1}$.

Variable fluorescence measurements

A pulse amplitude modulated (PAM) fluorometer (Walz PAM-101 fluorometer) was used with a high sensitivity detector. 10-20 ml of culture was place in a glass test tube, and the tube was illuminated using irradiance from a 150-W xenon lamp and filtered with Schott long-pass filters. Steady-state *in vivo* chl fluorescence (F_s) of cells was measured during illumination with actinic irradiance. At 1-min intervals a saturating pulse (400-ms duration) was applied to obtain a maximum yield (F'_m). The relative efficiency of excitation energy capture by photosystem II was calculated as $(F'_m-F_s)/F'_m$.

Results

Experiment I: using TEM and FISH to document nuclear retention

Using general nucleic acid stains, such as DAPI, small nuclei are readily observed to accumulate in *M. rubra* cells within minutes after the culture is fed (Gustafson et al. 2000). Newly ingested nuclei stain brightly and appear as they do in *G. cryophila* cells. When present, the *G. cryophila* nucleus in *M. rubra* is surrounded by a single membrane, closely associated with what appear to be 2 ciliate endoplasmic reticulum (ER) membranes (Figure 1). In order to verify that these nuclei were indeed from *G. cryophila* and to determine their fate, I developed a fluorescence *in situ* hybridization (FISH) oligonucleotide probe for the *G. cryophila* SSU rRNA nuclear gene (TANU2). Using confocal laser microscopy, it was evident that the probe bound to RNA in both the cytoplasm of *M. rubra* and the nucleolus of retained *G. cryophila* nuclei, indicating that SSU rRNA transcripts from these nuclei are expressed and not contained within a digestive vacuole (Figure 2B,D). A FISH probe for the *M. rubra* nuclear ssu rRNA gene (MYR2) was used in conjunction with TANU2, and together they illustrate the mosaic nature of sequestered and endogenous cytoplasm in *M. rubra* (Figure 2D). Both probes can clearly be seen to label rRNA in the nucleolus of their respective target nuclei and not to DNA of the nuclei (appearing as black). The TANU2 probe can also be seen to label cytoplasm in the chloroplast-mitochondrial complexes (CMCs).

The TANU2 probe was then applied to *M. rubra* cells from a feeding experiment, to confirm the identity of retained *G. cryophila* nuclei over time. At the beginning of this

experiment *M. rubra* cells had been starved for 1 month, and had 0.08 prey nuclei cell^{-1}. Introduction of *G. cryophila* (4.5:1 with *M. rubra*) resulted in an accumulation of prey nuclei in *M. rubra* cells, with a 5-fold increase observed after 1 h (Figure 3A). These newly ingested *G. cryophila* nuclei were small and identical in size to those in *G. cryophila* cells. Maximum ingestion rates during this time reached 0.72 ± 0.04 *G. cryophila M. rubra*$^{-1}$ h^{-1}. Maximum numbers of sequestered prey nuclei cell^{-1} were observed at day 10, with 1.62 ± 0.29 *G. cryophila* nuclei *M. rubra* cell^{-1} (Figure 3B). Over time these nuclei increased in size within *M. rubra*, for unknown reasons (Figure 3B). After 45 days 20.8 ± 4.2 % of *M. rubra* cells possessed prey nuclei, and of these 80 ± 6.8 % were unusually large (Figure 3B).

Experiment II: expression of *G. cryophila* genes in *M. rubra*

Growth and cellular observations

M. rubra cultures were fed (GC:MR = 4) 1 week prior to the beginning this experiment to assure the absence of free-living prey. *G. cryophila* prey remained below detection limit of transect cell counts at 400x magnification for the entire experiment, indicating cell concentrations were less than 40 cells ml^{-1} and yielding *M. rubra*: *G. cryophila* ratios that were minimally within the range of 78-650 (mean = 300). Growth rates of *M. rubra* were greatest after feeding with *G. cryophila* prey and remained the same through period-2 or day 35 (Figure 4A, B). Growth declined by half during periods 3 and 4, before becoming negative in period 5 (Figure 4A, B). Nucleomorph genomes cell^{-1} (NGC), an

approximation of plastid number cell^{-1}, was measured using qPCR assays for the plastid-associated nucleomorph ssu rRNA gene of *G. cryophila* and the nuclear ssu rRNA gene of *M. rubra*. NGC in *M. rubra* averaged around 9 for the first 35 days, and by day 90 declined to 4 (Figure 4C). Decline in NGC can be attributed to differences in plastid and cell division rates (Figure 4A), which were identical through period 2, after which average plastid division rate became 56 and 61 % of average cell division rate in periods 3 and 4, respectively. Prey nuclei were present at 0.85 cell^{-1} at t=0 of the experiment, declining to 0.015 cell^{-1} in period 5 or day 99 (Figure 5A). Calculations of total nuclei in the *M. rubra* population, accounting for dilution with new media additions, revealed no gain in nuclei from t = 0, suggesting that no net nuclei division took place (Figure 5B). Accounting for dilution, the total nuclei number in the population did not change in the first 30 days, suggesting that the limit for retaining functional prey nuclei (considering the initial week delay after feeding) may be near 35-40 days. In the following 10 days, a 6 fold decrease in nuclei were observed, after which concentrations of nuclei remained constant at 20 fold less then t = 0 levels. Photosynthetic quantum efficiency remained steady over most of the experiment with a sudden and significant (p = 0.0013) decline at the end of period 4 or day 73 (Figure 6).

Gene expression

Expression of select prey genes encoded by the nucleus (Nu) (LHCC10, GAPDH), nucleomorph (Nm) (cbbX), and plastid (P) (psbA) of *G. cryophila* were measured in *M. rubra* using RT-qPCR. Gene expression was normalized to 1) end point expression levels

of each gene relative to expression of a ciliate gene, β-tubulin (β-tub), using the $\Delta\Delta^{-CT}$ method (e.g. Livak and Schmittgen 2001; referred to here as $E^{\Delta\Delta-CT}$), and to 2) relative expression of equivalent *G. cryophila* cells (E^{prey}) using linear relationships between C_T and prey cell number. Both normalization methods revealed all gene expression peaked during the first 20 days after t = 0. Prey Nu genes exhibited 15-30 fold greater $E^{\Delta\Delta-CT}$ in the first 20 days after t = 0 (Figure 7A,C). While $E^{\Delta\Delta-CT}$ on days 18 and 22 for LHCC10 were significantly higher than all other days (ANOVA, $p<0.0001$), expression averaged over the entire first period (days 0-18) was not greater than other periods (Table 2). In contrast, GAPDH $E^{\Delta\Delta-CT}$ in period-1 was higher than all other periods (Table 2). E^{prey} of LHCC10 in *M. rubra* was equivalent to at least 1 PN cell^{-1} in period 1, while GAPDH was at or above this level through period 4 (Figure 7B,D). GAPDH E^{prey} reached 14 *G. cryophila* · *M. rubra*$^{-1}$ in period 1, indicating intense over-expression of the gene (Figure 7D). Overall, mean E^{prey} of GAPDH was 3.7 fold that of LHCC10, with maximum expression nearly 7 fold greater (Figures 7B,D).

Expression of *psbA* $E^{\Delta\Delta-CT}$ did not differ during the first 3 periods, while the final 2 periods were lower than period 1(Table 2). $E^{\Delta\Delta-CT}$ of *psbA* had the least amount of variability (i.e. lowest coefficient of variation, CV) for all measured genes (Table 2). Over the experiment *psbA* had the lowest average cycle threshold detection limit (C_T) for any assay (data not shown), probably indicating the greatest pool of transcripts. While $E^{\Delta\Delta-CT}$ for *psbA* reached a maximum of 7 fold of minimal levels, most of the variability was less than 4 fold (Figure 7E). E^{prey} of *psbA* also had lowest CV for all genes (Table 2), with period means remaining at least 2 fold that of *G. cryophila* throughout the experiment. Maximum E^{prey} of *psbA* reached 12 *G. cryophila* · *M. rubra*$^{-1}$ (Figure 7F),

with the highest overall mean (4.94) during the experiment (Table 2). Comparison of mean *psbA* E^{prey} and NGC (~ plastid number $cell^{-1}$) during the experiment (7.69) suggests that expression of *psbA* is greater in *G. cryophila* then in starved *M. rubra* over time. The Nm encoded *cbbX* gene had maximum $E^{\Delta\Delta\text{-}CT}$ during the first period (Table 2), after which expression did not differ, remaining ~ 4 fold lower than maximum levels in the period 1 (Figure 7G). E^{prey} of *cbbX* was also greatest in period 1 (Table 2), reaching a maximum of 10 *G. cryophila* · *M. rubra*$^{-1}$, thereafter declining and remaining at steady low levels (Figure 7H).

Discussion

Organelle retention

My results, using a FISH probe for the SSU rRNA gene of *G. cryophila*, confirm earlier observations of Gustafson et al. (2000) who showed accumulation of DAPI stained PN in *M. rubra* cytoplasm within hours after feeding (Figure 3A). Sequestered PN in *M. rubra* are temporary fixtures in the cell, lasting about 35 days and through multiple cell divisions (Figure 5B), before disappearing through egestion or digestion. This period of nuclear retention (i.e. no net population loss of PN; Figure 5B) coincides with highest observed growth and plastid division rates (Figure 4A), as well as photosynthetic rates (Johnson & Stoecker 2005). *G. cryophila* nuclei do not regularly divide in *M. rubra*, and for unknown reasons grow in volume over time.

In contrast, sequestered plastids appear to be very stable in *M. rubra* and undergo division for >8 weeks (Figure 4A). After feeding, chl cell^{-1} in *M. rubra* increases dramatically as cells begin synthesizing pigments (Gustafson et al. 2000, Johnson & Stoecker 2005). In this experiment when *M. rubra* was starved, nucleomorph genomes cell^{-1} (NGC) (~ plastid number cell^{-1}) remained constant until period 3, after which plastid loss occurred as rates of plastid division fell out of balance with cytokinesis (Figure 4A). In natural populations, and in culture, *M. rubra* is almost never observed to be in a non-pigmented state (Johnson pers. obs.), and my results suggest that *M. rubra* stops dividing as they lose the ability to divide plastids. Mitochondria division was not measured here, however it is assumed to occur in synchrony with plastid division, as CMCs are always observed with both organelles (Johnson pers. obs) and have been observed in synchronous division in cells from natural assemblages (Oakley and Taylor 1978). Choreotrich ciliates have chloroplast turnover rates that range between hours to a week (Stoecker and Silver 1990), while the dinoflagellates *Pfiesteria piscicida* and *Gyrodinium gracilentum* may be able to use sequestered chloroplasts for about a week (Lewitus et al. 1999, Skovgaard 1998). The sea slug, *Elysia chlorotica*, has long been known to sequester "endosymbiotic" chloroplasts from macroalgae, and can survive for 9 months in the laboratory without food (West 1979). While comparisons between physiological performance of a complex metazoan and single celled protist are difficult to make, there are some similarities in observations of sequestered plastid performance (discussed below).

Expression of prey nuclear (PN) genes

Prey nuclei in *M. rubra* are transcriptionally active, as evidenced by both positive FISH labeling of rRNA transcripts in the nucleoli, cytoplasm, and chloroplast-mitochondrial complexes (CMCs) of *M. rubra* (Figure 2), and 15-30 fold greater expression of PN genes relative to starved and nearly PN-devoid cells (Figures 7A-D). Both PN *GAPDH* and *LHCC10* genes are plastid-targeted, owing their origin to a plastid-to-nucleus (Liaud et al. 1997) and a nucleus-to-nucleus (Deane et al. 2000) endosymbiotic transfer, respectively. Enhanced expression for *LHCC10* and *GAPDH* was a transient phenomenon, occurring during the first 20-30 days of retention/starvation. Differences in expression patterns between the two normalization methods occurred because one ($E^{\Delta\Delta\text{-CT}}$) is normalized to endogenous *M. rubra* (β-tub) expression and scales fold change to minimal expression observed (per gene), while the other (E^{prey}) is normalized to equivalent *G. cryophila* prey expression established with a standard. Both PN genes were over-expressed in *M. rubra* when normalized as E^{prey} (Figure 7B,D). However, when expression was normalized instead to number of prey nuclei present in those cells (E^{NU}), it revealed severe over-expression (not shown). E^{NU} indicated that *LHCC10* and *GAPDH* (period means) were over-expressed by 5-32 and 13-125 fold, respectively. For both Nu genes, E^{NU} were lower (*LHCC10*: 4.7 and 6.7; *GAPDH*: 16.2 and 12.6) during the first 2 periods (ANOVA, $p<0.05$), then increased dramatically and did not vary for the remaining 3. While the E^{prey} method was normalized using relationships between C_T and *G. cryophila* cell numbers from exponential growth phase, transcription is a highly dynamic process with variability in induction mechanisms

occurring on time scales of minutes. It is possible that an actual maximum of *G. cryophila* gene expression was not realized in creating these standards, and thus E^{prey} overestimates potential prey-relative expression. Alternatively, the low and relatively constant C_T values, yielding high E^{NU} after period 2, may reflect low background expression. If true, this could suggest that the efficiency of RNA extraction or cDNA formation was lower in making the *G. cryophila* standards. While the E^{prey} data may or may not be quantitative, they nevertheless illustrate that transcription of PN genes occurred within *M. rubra*.

The $2^{-\Delta\Delta\text{-}CT}$ expression method has been shown to be useful, assuming 100% reaction efficiency and identical slopes for each gene compared. While it is unlikely that these assumptions are always upheld, I did find that slopes for each assay were equal (see methods). Both PN genes reached maximum $E^{\Delta\Delta\text{-}CT}$ in period one, with dramatic decline thereafter. This decline could be partially explained by PN becoming diluted in the population as *M. rubra* divided, and thus expression of ciliate β-tub increased relative to PN genes. However, E^{prey} data indicate that absolute PN expression decreased by 14 and 11 fold for LHCC10 and GAPDH, respectively, when comparing maximum (period 1) expression to the period-5 average. Thus declines for LHCC10 and GAPDH appear to be a result of declines in PN transcription.

The translation of nuclear-encoded, plastid-targeted transcripts is thought to occur in the cytosol of cryptophytes, before proteins with signal and transit peptides cross four membranes to enter the plastid (Liaud et al. 1997, Deane et al. 2000). If indeed PN transcripts in *M. rubra* are translated and target organelles within CMCs, their transport is made even more complex with additional membranes surrounding CMCs and perhaps

separating them from prey nuclei (e.g. Taylor et al. 1971, Hibberd 1977, Oakley and Taylor 1978). Hibberd (1977) found some connectivity of membranes between cryptophyte nuclei and CMCs in *M. rubra*, as well as between hemispheres of the cell. My FISH results confirm earlier observations using TEM (e.g. Taylor et al. 1969, 1971, Hibberd 1977, Oakley and Taylor 1978) that *M. rubra* contains membrane-delineated pockets of "symbiont" cytoplasm in addition to what is found in the CMCs, which can be differentiated using TEM by differences in ribosome density and mitochondria type. Hibberd's (1977) observations of nuclear-CMC connections were not confirmed by Oakley and Taylor (1978), who portrayed a much more compartmentalized picture of "symbiont" organelles. However, this may not be surprising considering the challenge of locating the small connections of membranes observed by Hibberd (1977). If such connections do exist, then it would provide a plausible mechanism for PN transcript targeting to sequestered CMCs, and perhaps plastid-regulated (e.g. Gray et al. 2002) PN expression in *M. rubra*.

Expression of plastid and nucleomorph genes

Although the red lineage of plastids possess a larger genome size than the green lineage, there is no evidence that this leads to increased autonomy of plastid function or regulation (Martin and Herrmann 1997, Maier et al. 2000). Similarly, while the Nm encodes hundreds of genetic housekeeping and several plastid genes, it requires import of Nu-encoded genes to carry out DNA replication and periplastidal protein synthesis (Douglas et al. 2001), thus adding little to plastid autonomy. One plastid-targeted gene in

the Nm is the RuBisCo regulatory protein *cbbX*. The Nm *cbbX*, however, is not linked to RuBisCo genes (*rbcS* & *rbcL*) and has uncertain plastid function, while a second (duplicated) *cbbX* gene (rbc-linked) is encoded in the plastid genome (Maier et al. 2000). Expression patterns of the Nm *cbbX* gene in *M. rubra* resembled those of the Nu-encoded genes with maximum expression occurring in the first period and precipitously declining thereafter (Figures 7G,H). This suggests that transcription of cbbX was quickly effected by loss of PN. Maximum *cbbX* E^{prey} during period-1 was 10-fold *G. cryophila*, which was similar to plastid $cell^{-1}$ content during this time (Figures 4c, 7h).

Expression of the P-encoded *psbA* gene revealed the least variability for both normalization methods (Figures 7E,F), varying only 3 and 6 fold between maximum expression and the period-5 mean, for E^{prey} and $E^{\Delta\Delta\text{-}CT}$, respectively. *PsbA* also had the highest E^{prey} at the end of 99 days, in addition to having the highest overall experiment-wide mean, suggesting that expression of this gene was perhaps the least effected by PN presence. Similar results have been shown with the plastid retaining sea slug, *E. chlorotica*, where transcripts of *psbA* were constant for 3 months before gradually declining over the next 5 months (Mujer et al. 1996). Proteins (synthesized *de vovo*) from *psbA* (D1) were also found at high levels in *E. chlorotica* after 2-4 months, remaining at lower but constant levels after 6 months (Mujer et al. 1996). Translation initiation of psbA in chlorophytes requires expression of Nu-encoded poly(A)-binding protein, RB47 (Yohn et al. 1998). For plastid transcription and translation machinery to continue to function in sequestered plastids, proteins such as RB47 must have low turnover rates. Conversely, the D1 protein is a pivotal protein in photosystem II of chloroplasts, and is well known to have high turnover when exposed to high irradiance (Mattoo et al. 1984),

with transcription induced by oxidation of plastoquinone (Pfannschmidt et al. 1999). Longevity of sequestered plastids in *M. rubra* and other plastid-retaining organisms may be highly dependent on exposure to light, due to light sensitive proteins such as D1. Johnson and Stoecker (2005) have previously found that *M. rubra* exposed to high light stop growing before cultures in lower irradiance.

A model for organelle retention in *M. rubra*

M. rubra cells used in this experiment (at t = 0) were by no means satiated with *G. cryophila* prey (0.85 PN cell^{-1}) when compared to the maximum in experiment-1 (1.62 PN cell^{-1}), thus gene expression presented here should not be considered maximum. Here I used relatively low amounts of *G. cryophila* to feed *M. rubra* to be sure that prey would be removed sufficiently, so as to not have an appreciably effect on gene expression measurements. The data presented here for retention time of transcriptionally active PN (20-30 d), support earlier findings where after 2 weeks of starvation significant declines are observed in cell growth, pigment synthesis, and gross growth efficiency (Johnson & Stoecker 2005). Previous findings of photosynthesis persisting long after substantial growth declines were also supported here, with Fv/Fm remaining constant until day 70 (Figure 6). The delayed decline in photosynthetic capacity, out of synch with loss in PN gene expression, may reflect the robustness of certain nuclear-encoded plastid-targeted proteins. Alternatively, ER-associated immature nuclear proteins could persist for some time within cytoplasm of CMCs. In the sea slug *E. chlorotica*, a putative nuclear-encoded plastid-targeted light-harvesting complex protein (LHCP) was apparently maintained for

9 months without detectable transcription (Green et al. 2000). *E. chlorotica* and other plastid retaining organisms, have never been shown to divide their plastids. This, taken with the observation that *M. rubra* loses plastid division (Figure 4A) and pigment synthesis (Johnson & Stoecker 2005) capacity after loss of PN, suggests that regulatory proteins for plastid division and pigment synthesis are less abundant and/or less stable then certain Nu encoded plastid-targeted genes (e.g. the LHC family). In nature it is unlikely that *M. rubra* would be starved from cryptophyte prey for durations used here, as cryptophytes are abundant in nearly all coastal marine ecosystems (e.g. Novarino 2003). If expression of prey genes can occur at high levels for >20 days, this would imply that feeding, for an organism with a division cycle of <2 days, is perhaps only important to acquire PN, as PN do not divide in *M. rubra*. In cultured *M. rubra*, cells offered more cryptophyte food have higher growth rates (Yih et al. 2004), yet C from cryptophyte prey contributes negligibly to growth (Yih et al. 2004, Johnson et al. 2005). Thus because CMCs in *M. rubra* can undergo division, it is probable that feeding is most important for anucleate daughter cells to obtain PN for regulating and dividing CMCs.

Nuclear retention: an evolutionary perspective

While no organism has ever been described to sequester functional nuclei of another, other protists have been observed with foreign nuclei in their cells. In the plastid retaining dinoflagellate *Gymnodinium acidotum*, a prey nucleus is sometimes observed in the cell after ingesting cryptophytes (Schnepf et al. 1989, Fields and Rhodes 1991). It is unclear if prey nuclei in *G. acidotum* are actually retained or digested, and plastids in the

dinoflagellate have been reported to last only about 12 days (Fields & Rhodes 1991). The notion of a nucleus remaining functional in foreign cytoplasm is not entirely new. Red algal adelphoparasites deliver a nucleus into their host cell cytoplasm, where it undergoes DNA synthesis and karyokinesis within the host's cytoplasm (Goff and Coleman 1995). Several adelphoparasites also infect their host with plastids, derived from another host, and mitochondria belonging to the parasite (Goff and Coleman 1995). Thus while organelles are not genetically autonomous entities, they are more promiscuous then generally regarded.

Present day observations of organelle retention, symbiosis, and parasitism offer dynamic pictures of interspecies organelle and genomic interactions, and help to understand the chimeric evolutionary history of eukaryotic cells. According to the serial endosymbiosis theory (SET), the logical evolutionary endpoint of harboring a photosynthetic endosymbiont is the establishment of the plastid organelle (Margulis 1970). Conversely, kleptoplastidy is inherently unstable, in an evolutionary sense, due to the absence of myriad photosynthetic genes encoded in an algal nucleus and inability to replicate plastids. In the case of *M. rubra* the line between symbiont and kleptochloroplast is blurred, as chloroplasts can be divided for many weeks after feeding (Figure 4A, see also Johnson & Stoecker 2005, Johnson et al. in prep). I believe that no current functional classification satisfactorily describes the trophic strategy of *M. rubra*. While the relationship is clearly not symbiotic, numerous features starkly contrast *M. rubra* with most other kleptoplastidic organisms. These include the retention of functional prey nuclei, formation of an efficient and replicable compartment to house

prey organelles (i.e. CMCs), and the apparent independence from heterotrophy (Johnson et al. 2005).

For a phototrophic survival strategy, the stability of which depends on stealing the genome of its prey, nuclear retention has proven remarkably successful, as evidenced by the widespread distribution of *M. rubra* and its conspicuous role in forming red tides (Taylor et al. 1971, Lindholm 1985). It is unclear if organelle retention, *sensu* nuclear retention, is an evolutionary step towards permanent establishment of a genetically integrated plastid, or rather an evolutionary endpoint. The former would ultimately require horizontal gene transfer (HGT), which has occurred between eukaryotic genomes during secondary and tertiary plastid acquisitions (Delwiche 1999). Recently, conceptual models for HGT from predator-prey interactions (i.e. the "gene ratchet" hypothesis, Doolittle 1998) have also been proposed (e.g. Schubbert et al. 1997, Noto and Endoh 2004). While I have no evidence for such, nuclear retention as described here, occurring at high frequency with transcription of prey genes from a specific prey species, could also conceivable provide conditions for HGT. Schnepf and Seichgäber (1984) proposed that plastids or "symbionts" surrounded by a single membrane (e.g. *Peridinium balticum*, euglenoids) could have arisen through organelle retention via myzocytotic feeding. While clearly the SET theory is the only acceptable theory for the primary endosymbiotic acquisition of plastids or mitochondria (e.g. Gray 1992), organelle retention, *sensu* nuclear retention, provides an alternative evolutionary mechanism for acquisition of secondary and tertiary plastids.

References

Blackbourn DJ, Taylor FJR, Blackbourn J (1973) Foreign organelle retention by ciliates. J Protozool 20: 286-288

Deane JA, Fraunholz M, Su V, Maier U-G, Martin W, Durnford DG, McFadden GI (2000) Evidence for nucleomorph to host nucleus gene transfer: light-harvesting complex proteins from cryptomonads and chlorarachniophytes. Protist 151: 239-252

Delwiche CF (1999) Tracing the thread of plastid diversity through the tapestry of life. Am Nat 154: S164-S177

Doolittle WF (1998) You are what you eat: a gene ratchet could account for bacterial genes in eukaryotic nuclear genomes. Trends Genet 14: 307-311

Douglas S, Zauner S, Fraunholz M, Beaton M, Penny S, Deng L-T, Wu X, Reith M, Cavalier-Smith T, Maier U-G (2001) The highly reduced genome of an enslaved algal nucleus. Nature 410: 1091-1096

Falkowski PG, Raven JA (1997) Aquatic photosynthesis. Malden: Blackwell

Farmer MA, Roberts KR (1990) Organelle loss in the endosymbiont of *Gymnodinium acidotum* (Dinophyceae) Protoplasma 153: 178-185

Fast N, Kissinger JC, Roos DS, Keeling PJ (2001) Nuclear-encoded, plastid-targeted genes suggest a single common origin for apicomplexan and dinoflagellate plastids. Mol Biol Evol 18: 418-426

Fields SD, Rhodes RG (1991) Ingestion and retention of *Chroomonas* spp. (Cryptophyceae) by *Gymnodinium acidotum* (Dinophyceae). J Phycol 27: 525-529

Goff LJ Coleman AW (1995) Fate of parasite and host organelle DNA during cellular transformation of red algae by their parasites. Plant Cell 7: 1899-1911

Gray MW (1992) The endosymbiont hypothesis revisited. Int Rev Cytol 141: 233-357

Gray JC, Sullivan JA, Wang J-H, Jerome CA, MacLean D (2002) Coordination of plastid and nuclear gene expression. Phil Trans R Soc Lond B 358: 135-145

Green BJ, Li WY, Manhart JR, Fox TC, Summer EJ, Kennedy RA, Pierce SK, Rumpho ME (2000) Mollusc-algal chloroplast endosymbiosis. Photosynthesis, thylakoid protein maintenance, and chloroplast gene expression continue for many months in the absence of the algal nucleus. Plant Physiol 124: 331-342

Gustafson DE, Stoecker DK, Johnson MD, Van Heukelem WF, Sneider K (2000) Cryptophyte algae are robbed of their organelles by the marine ciliate *Mesodinium rubrum*. Nature 405: 1049-1052

Grzymski J, Schofield OM, Falkowski PG, Bernhard JM (2002) The function of plastids in the deep-sea benthic foraminifer, *Nonionella stella*. Limnol Oceanogr 47: 1569-1580

Hibberd, DJ (1977) Observations on the ultrastructure of the cryptomonad endosymbiont of the red water ciliate *Mesodinium rubrum*. J Mar Biol Assoc UK 57:
45-61

Jankowski AW (1976) Revision of the classification of the cyrtophorids. In Markevich AP, Yu I (eds) Materials of the II All-union Conference of Protozoology, Part I, general protozoology, Naukova Dumka, pp 167-168

Johnson PW, Donaghay PL, Small EB, McN. Sieburth J (1995) Ultrastructure and ecology of *Perispira ovum* (Ciliophora: Litostomatea): an anaerobic, planktonic ciliate

that sequesters chloroplasts, mitochondria, and paramylon of *Euglena proxima* in a micro-oxic habitat. J Euk Microbiol 42: 323-335

Johnson MD, Tengs T, Oldach DW, Delwiche CF, Stoecker DK (2004) Highly divergent SSU rRNA genes found in the marine ciliates *Myrionecta rubra* and *Mesodinium pulex*. Protist 155: 347-359

Johnson MD, Stoecker DK (2005) The role of feeding in growth and the photophysiology of *Myrionecta rubra*. Aquat Microb Ecol 39: 303-312

Laval-Peuto M, Salvano P, Gayol P, Greuet C (1986) Mixotrophy in marine planktonic ciliates: ultrastructural study of *Tontonia appendiculariformis* (Ciliophora, Oligotrichina) Mar Microb Food Webs 1: 81-104

Lewitus AJ, Glasgow HB, Burkholder JM (1999) Kleptoplastidy in the toxic dinoflagellate *Pfiesteria piscicida* (Dinophyceae). J Phycol 35: 303-312

Liaud M-F, Brandt U, Scherzinger M, Cerff R (1997) Evolutionary origin of cryptomonad microalgae: two novel chloroplast/cytosol-specific GAPDH genes as potential markers of ancestral endosymbiont and host cell components. J Mol Evol 44: S28-S37

Lindholm T (1985) *Mesodinium rubrum*- a unique photosynthetic ciliate. Adv Aquat Microbiol 3: 1-48

Maddison WP, Maddison DR (1992) MacClade- analysis of phylogeny and character evolution. Sinauer, Sunderland, MA

Maier U-G, Fraunholz M, Zauner S, Penny S, Douglas S (2000) A nucleomorph-encoded CbbX and the phylogeny of RuBisCo regulators. Mol Biol Evol 17: 576-583

Margulis L (1970) Origin of eukaryotic cells. New Haven: Yale University Press

Mattoo AK, Hoffman-Falk H, Marder JB, Edelman M (1984) Regulation of protein metabolism: coupling of photosynthetic electron transport to in vivo degradation of the rapidly metabolized 32-KD protein of the chloroplast membranes. PNAS 81: 1380-1384

Miller PE, Scholin CA (1998) Identification and enumeration of cultured and wild *Pseudo-nitzschia* (Bacillariophyceae) using species-specific LSU rRNA-targeted fluorescent probes and filter-based whole cell hybridization. J Phycol 34: 371-382

Muher CV, Andrews DL, Manhart JR, Pierce SK, Rumpho ME (1996) Chloroplast genes are expressed during intracellular symbiotic association of *Vaucheria litorea* plastids with the sea slug *Elysia chlorotica*. PNAS 93: 12333-12338

Noto T, Endoh H (2004) A "chimera" theory on the origin of dicyemid mesozoans: evolution driven by frequent lateral gene transfer from host to parasite. Biosystems 73: 73-83

Novarino G (2003) A companion to the identification of cryptomonad flagellates (Cryptophyceae = Cryptomonadea). Hydrobiol 502: 225-270

Oakley BR and Taylor FJR (1978) Evidence for a new type of endosymbiotic organization in a population of the ciliate *Mesodinium rubrum* from British Columbia. BioSystems 10: 361-369

Pfannschmidt T, Nilsson A, Allen JF (1999) Photosynthetic control of chloroplast gene expression. Nature 397: 625-628

Ryther JH (1967) Occurrence of red water off Peru. Nature 214: 1318-1319

Saldarriaga JF, McEwan ML, Fast NM, Taylor FJR, Keeling PJ 2003. Multiple protein phylogenies show that *Oxyrrhis marina* and *Perkinsus marinus* are early branches of the dinoflagellate lineage. Int J Syst Evol Microbiol 53: 355-365

Schnepf E, Deichgräber G (1984) “Myzocytosis”, a kind of endocytosis with implications of compartmentalization in endosymbiosis. Naturwissenschaften 71, S. 218

Schnepf E, Winter S, Mollenhauer D (1989) *Gymnodinium aeruginosum* (Dinophyta): a blue-green dinoflagellate with a vestigial, anucleate, cryptophycean endosymbiont. Pl Syst. Evol. 164: 75-91

Schubbert R, Renz D, Schmitz B, Doerfler W (1997) Foreign (M13) DNA ingested by mice reaches peripheral leukocytes, spleen, and liver via the intestinal wall mucosa and can be covalently linked to mouse DNA. PNAS 94: 961-966

Skovgaard A (1998) Role of chloroplast retention in a marine dinoflagellate. Aqu Microb Ecol 15: 293-301

Stoecker DK, Michaels AE, Davis LH (1987) Large proportion of marine planktonic ciliates found to contain functional chloroplasts. Nature 326: 790-792

Stoecker DK, Silver MW (1990) Replacement and aging of chloroplasts in *Stombidium capitatum* (Ciliophora: Oligotrichida). Mar Biol 107: 491-502

Taylor FJR, Balckbourn, DJ, Blackbourn, J (1969) Ultrastructure of the chloroplasts and associated structures within the marine ciliate *Mesodinium rubrum* (Lohmann). Nature 224: 819-821

Taylor FJR, Blackbourn DJ, Blackbourn J (1971) The red-water ciliate *Mesodinium rubrum* and its “incomplete symbionts”: a review including new ultrastructural observations. J Fish Res Bd Canada 28: 391-407

Trench RK (1979) The cell-biology of plant-animal symbiosis. A Rev. Plant Physiol 30: 485-453

Yih W, Kim HS, Jeong HJ, Myung G, Kim YG (2004) Ingestion of cryptophyte cells by the marine photosynthetic ciliate *Mesodinium rubrum*. Aquat Microb Ecol 36: 165-170

Yohn CB, Cohen A, Rosch C, Kuchka MR, Mayfield SP (1998) Translation of the chloroplast psbA mRNA requires the nuclear-encoded poly(A)-binding protein, RB47. J Cell Biol 142: 435-442

Table 1. Novel primers and probes used for FISH and RT-qPCR for *Geminigera cryophila* and *Myrionecta rubra*

Probe	Gene	Sequence	Target	Genome
		FISH Probe		
TANU2	ssu rRNA	FL-CTAAGAAGTAGCCGCCAATCAT	*G. cryophila*	nuclear
		RT-qPCR taqman assays		
LHCC_F1	LHCC10	CACTGGAGCCGTTGTCCA	*G. cryophila*	nuclear
LHCC_R1	LHCC10	GTCAATGGAACCGTTCGCAAG	*G. cryophila*	nuclear
LHCC_P	LHCC10	FAM-TCCACGACGCCGCCATCAAGTCG-BHQ	*G. cryophila*	nuclear
TA-GAP_F	GAPDH	TCAATCAAGGGCAAGCTGACA	*G. cryophila*	nuclear
TA-GAP_R	GAPDH	GCTTCACCTCAGCGCAGAT	*G. cryophila*	nuclear
TA-GAP_P	GAPDH	FAM-ACGTGTCCGTTGTTGACCTTACCTGCAGAA-BHQ	*G. cryophila*	nuclear
PsbA_TM2F	psbA	AACAACTCTCGTGCTCTTCA	*G. cryophila*	plastid
PsbA_TM2R	psbA	TTGGCTATCAACAACCGATTG	*G. cryophila*	plastid
PsbA_TM2P	psbA	FAM-CTGGTTCACAGCTCTAGGTGTAATGACA-BHQ	*G. cryophila*	plastid

Cbbx_TM-F	cbbX	CAATTGACAACAATTCATCTGCT	*G. cryophila*	nucleomorph
Cbbx_TM-R	cbbX	TCTTAGCAGGATATAAAGACAG	*G. cryophila*	nucleomorph
Cbbx_TM-P	cbbX	FAM-TTCCTATTCTCGATGACATTCCAGGAAT-BHQ	*G. cryophila*	nucleomorph
MR-BT-F	β-tub	CTGACAGAATCATGGAGACATT	*M. rubra*	nuclear
MR-BT-R	β-tub	TGACCATGACTTCGTCTGAGTT	*M. rubra*	nuclear
MR-BT-P	β-tub	TET-TCAGACACCGTCGTCGAGCCATACAAT-BHQ	*M. rubra*	nuclear

FL = fluoroscein isothiocyante, FAM = 5-Carboxyfluorescein, BHQ = black hole quencher, TET = 4,7,2',7'-tetrachloro-6-carboxyfluorescein

Table 2. Effects of starvation on expression of *Geminigera cryophila* genes in *Myrionecta rubra* over time determined using ANOVA for β-tubulin normalized ($E^{\Delta\Delta\text{-}CT}$) and prey-relative ($E^{prey}$) expression.

Comparisons for period means (days in parentheses) using Tukey's studentized range test (HSD)									
gene	mean$^{(0\text{-}99)}$	MSE	F (d.f)	*p*	1$^{(0\text{-}18)}$	2$^{(19\text{-}35)}$	3$^{(36\text{-}53)}$	4$^{(53\text{-}73)}$	5$^{(74\text{-}99)}$
β-tubulin normalized expression ($E^{\Delta\Delta\text{-}CT}$)									
LHCC10	4.75	170	2.97 (4, 41)	0.0303	**8.48 (9.76)**	9.95 (13.5)	2.20 (1.10)	0.88 (0.44)	0.97 (0.54)
GAPDH	4.07	122	13.9 (4, 40)	0.0001	**9.25 (4.93)**	2.81 (2.37)*	3.62 (2.17)*	1.01 (0.84)*	0.77 (0.47)*
psbA	2.1	10.26	5.73 (4, 37)	0.0011	**3.49 (2.01)**	2.07 (0.98)	3.36 (1.36)	0.99 (0.69)*	1.02 (0.65)*
cbbX	3.49	84.4	9.17 (4, 41)	0.0001	**7.88 (5.52)**	1.74 (1.53)*	3.24 (1.45)*	1.46 (0.76)*	1.03 (0.62)*
prey-relative expression (E^{prey})									
LHCC	0.99	5.75	13.4 (4, 41)	0.0001	**2.20 (1.2)**	0.72 (0.50)*	0.80 (0.13)*	0.50 (0.17)*	0.25 (0.16)*
GAPDH	3.69	80.9	9.99 (4, 40)	0.0001	**7.93 (5.16)**	1.55 (1.02)*	3.67 (1.34)*	1.97 (1.41)*	1.25 (0.49)*
psbA	4.94	41.67	5.62 (4, 37)	0.0011	**7.43 (4.42)**	2.13 (1.48)*	5.89 (1.49)	4.22 (2.10)	3.53 (1.78)
cbbX	1.64	20.3	117 (4, 41)	0.0012	**3.78 (3.55)**	0.42 (0.35)*	1.52 (0.95)	0.94 (0.52)*	0.51 (0.35)*

*signifies a significantly different mean from period-1 ($p<0.05$),

Figure 4.1. TEM section of *Myrionecta rubra* showing the *Geminigera cryophila* nucleus and a chloroplast-mitochondria complex (CMC), harboring *G. cryophila* organelles. CER: ciliate endoplasmic reticulum, PN: prey nucleus, n: nucleolus.

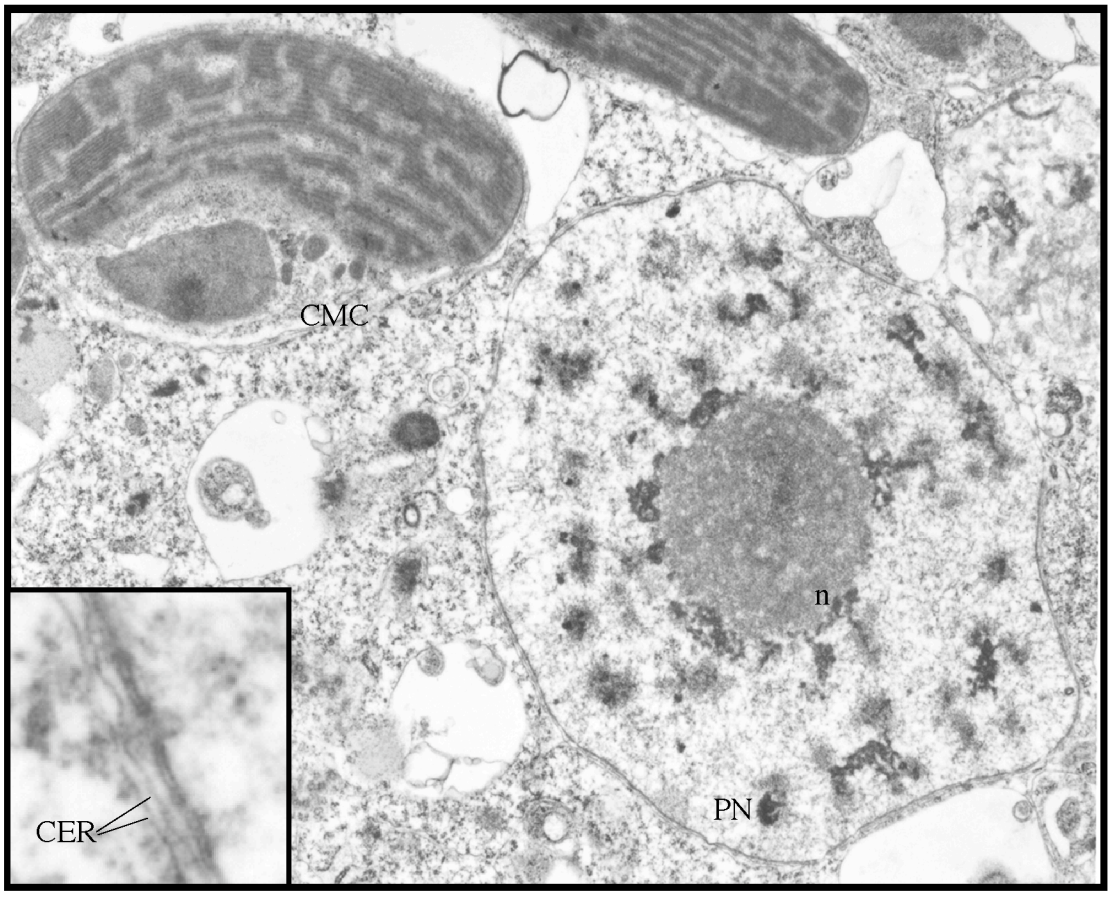
CMC
n
PN
CER

Figure 4.2. Confocal laser scanning micrograph of a typical dual SSU rRNA probe hybridization to *Myrionecta rubra,* with a FITC-labeled probe for the *Geminigera cryophila* SSU rRNA gene and a Cy-5 labeled probed for the *M. rubra* SSU gene. (A) red channel (em 543nm) showing plastid autofluorescence; (B) green channel (ex 488) showing TANU2 probe (FITC) hybridization; (C) far-red channel (ex 633) showing Myr2 probe (Cy5) hybridization; (D) images from A-C layered. CMC = chloroplast-mitochondrial complex; Cmac = ciliate macronucleus; PN = prey nucleus.

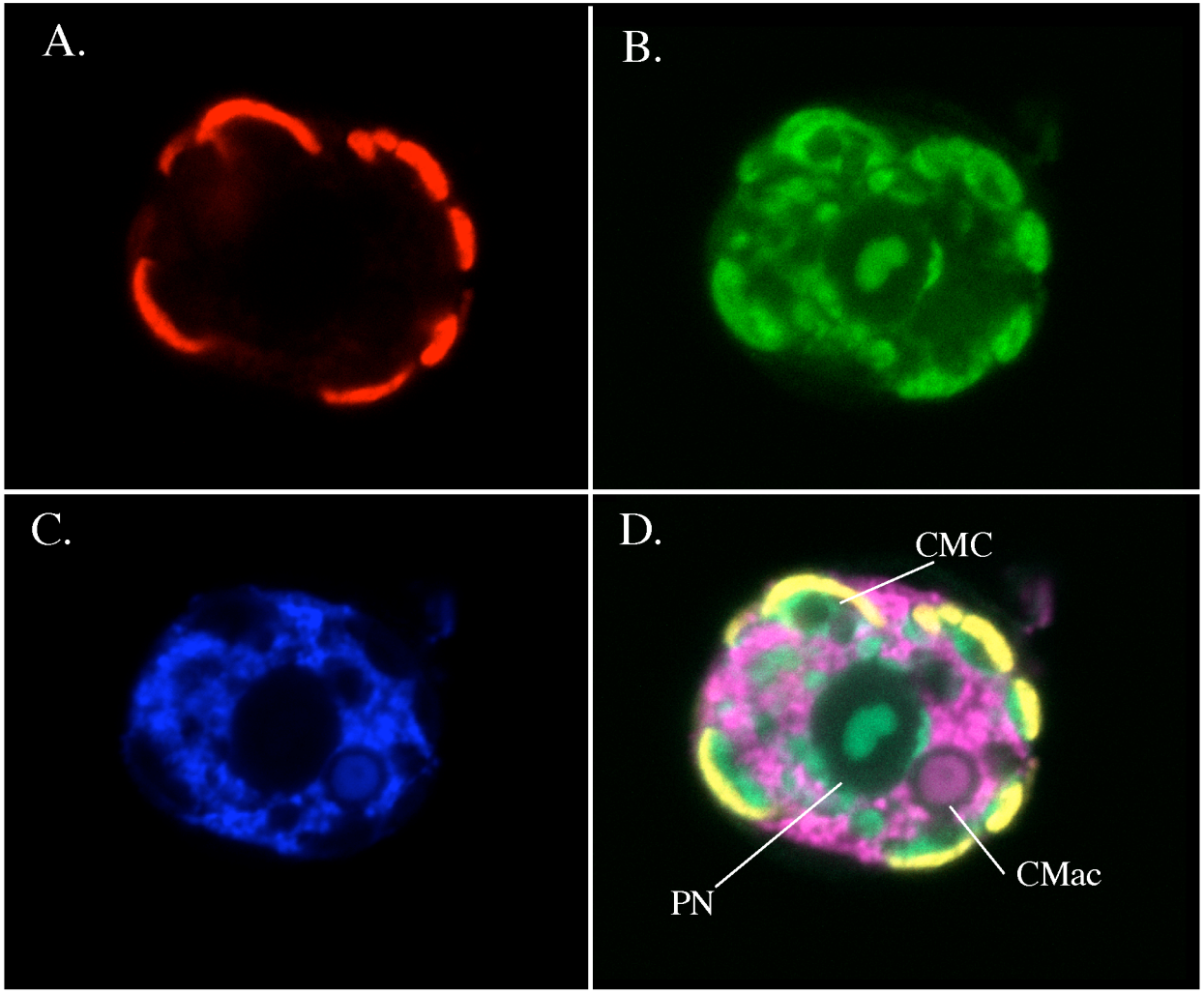
A.
B.
C.
D.
CMC
PN
CMac

Figure 4.3. Grazing dynamics for experiment-1 documented by labeling *Myrionecta rubra* with a fluorescence *in situ* hybridization probe (TANU2) for the *Geminigera cryophila* SSU rRNA gene; (A) short-term (hours) increase in prey nuclei (PN) per *M. rubra* cell as a result of ingestion of *G. cryophila* and (B) changes in total PN per *M. rubra* cell (open circles) and the proportion of unusually large PN (LPN; closed triangles) over time (mean ± standard deviation).

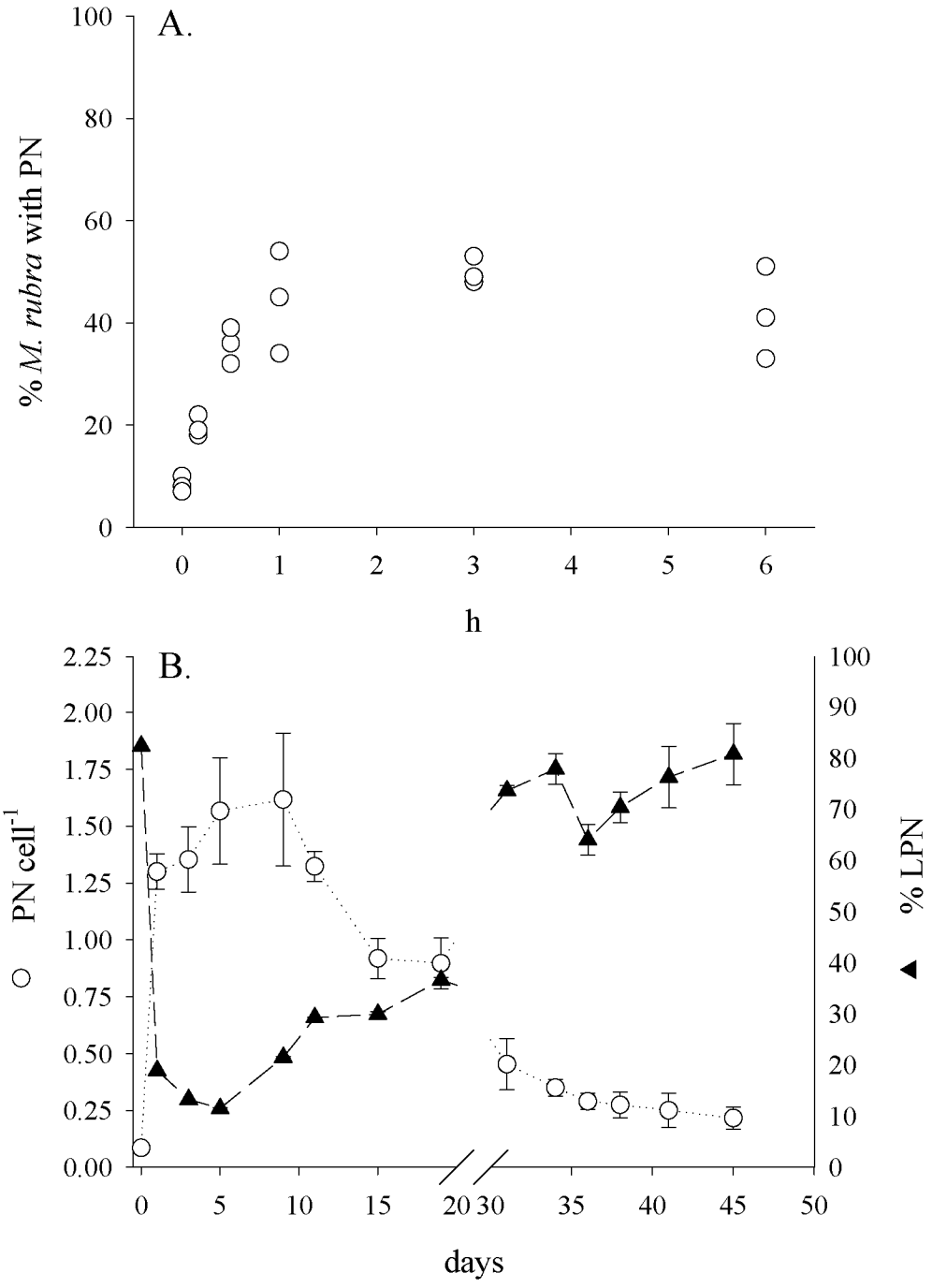
A.
% M. rubra with PN
h
B.
PN cell-1
% LPN
days

Figure 4.4. (A) Maximum cell and plastid division rates (d^{-1}) for *Myrionecta rubra* by growth period (with days in parentheses), *$p<0.05$, bars are mean ± standard deviation (n = 2); (B) Abundance of *M. rubra* over the course of the experiment; (C) Nucleomorph genomes $cell^{-1}$ (NGC) (~ plastid number $cell^{-1}$) over time for a growing *Myrionecta rubra* culture, estimated using quantitative (q) PCR with an assay designed for the *Geminigera cryophila* nucleomorph SSU rRNA gene.

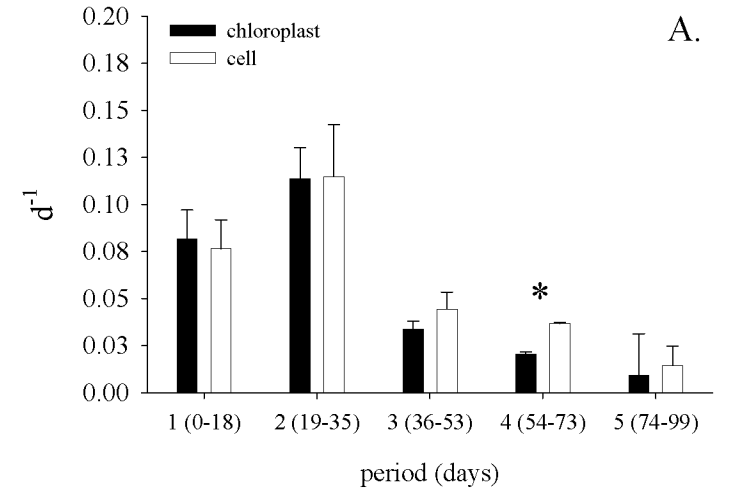
A.
chloroplast
cell
0.20
0.18
0.15
0.13
0.10
0.08
0.05
0.03
0.00
d-1
*
1 (0-18)
2 (19-35)
3 (36-53)
4 (54-73)
5 (74-99)
period (days)

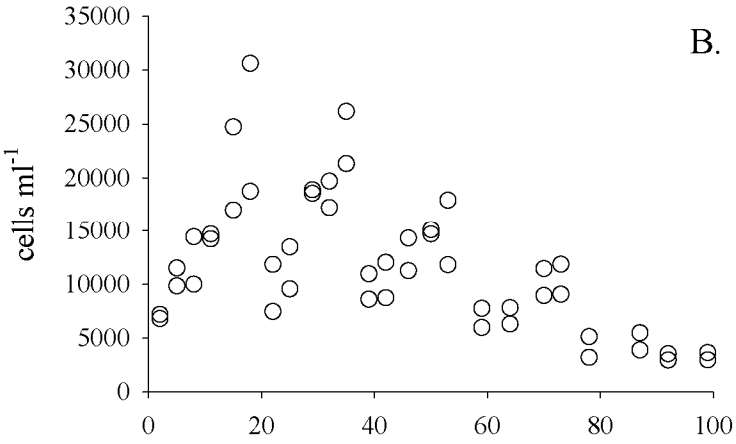
B.
35000
30000
25000
20000
15000
10000
5000
0
cells ml-1
0
20
40
60
80
100

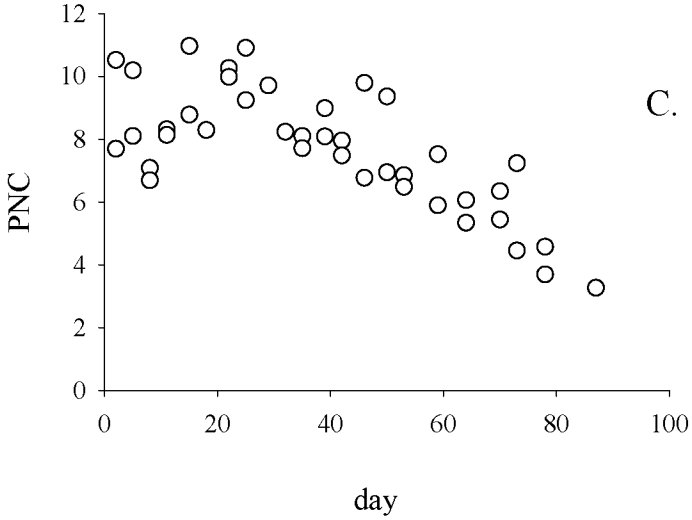
C.
12
10
8
6
4
2
0
PNC
0
20
40
60
80
100
day

Figure 4.5. (A) *Geminigera cryophila* nuclei per *Myrionecta rubra* cell over course of entire experiment (mean ± standard deviation) and (B) total *G. cryophila* nuclei ml^{-1} during experiment, showing actual numbers and concentrations corrected for dilution between periods with new media.

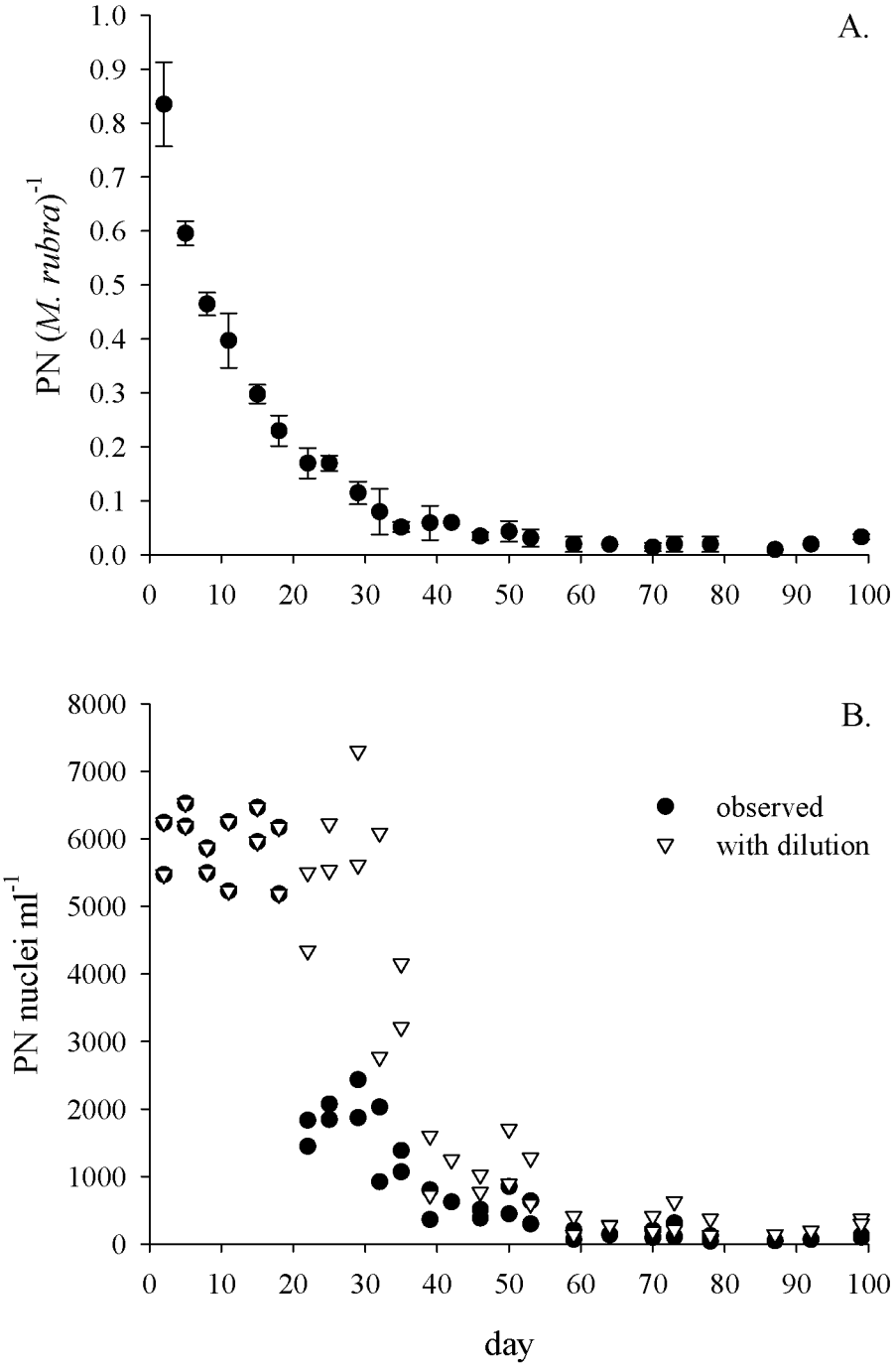
A.
PN (M. rubra)-1
1.0
0.9
0.8
0.7
0.6
0.5
0.4
0.3
0.2
0.1
0.0
0
10
20
30
40
50
60
70
80
90
100
B.
PN nuclei ml-1
8000
7000
6000
5000
4000
3000
2000
1000
0
observed
with dilution
day

Figure 4.6. The quantum yield of photosynthesis (Fv/Fm) for photosynthesis in *Myrionecta rubra* over entire experiment (n =2). Mean ± standard deviation.

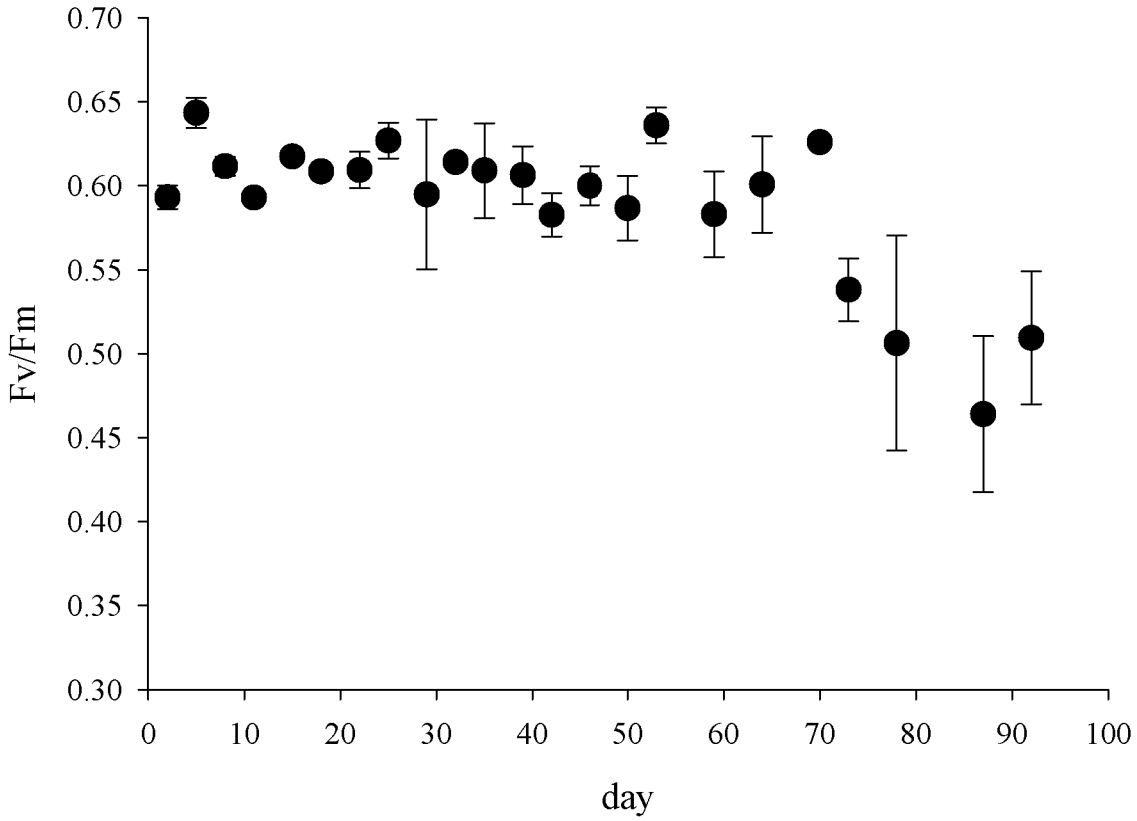
0.70
0.65
0.60
0.55
0.50
0.45
0.40
0.35
0.30
Fv/Fm
0
10
20
30
40
50
60
70
80
90
100
day

Figure 4.7. Gene expression of *Geminigera cryophila* genes in *Myrionecta rubra* over time, as measured by RT-qPCR taqman assays for a the nuclear encoded (A&B) light-harvesting chloroplast complex (LHCC10) and (C&D) glyceraldehydes-3-phosphate dehydrogenase (GAPDH) genes, the plastid-encoded (E&F) D1 protein gene for photosystem II (psbA), and the nucleomorph-encoded (G&H) putative RuBisCo regulatory protein (cbbX). Expression is normalized to either (left column) *M. rurba* β-tubulin gene expression and in relation to minimal experimental expression (i.e. period 5) using the $2^{\Delta\Delta\text{-}C}{}_T$ method, or (right column) relative to a exponentially growing *G. cryophila* RNA standards for each gene (relationships determined by linear regression). Reference line across graphs in left column (at 1 on y-axis), represents zero change from the period-5 average, where below this expression is lower.

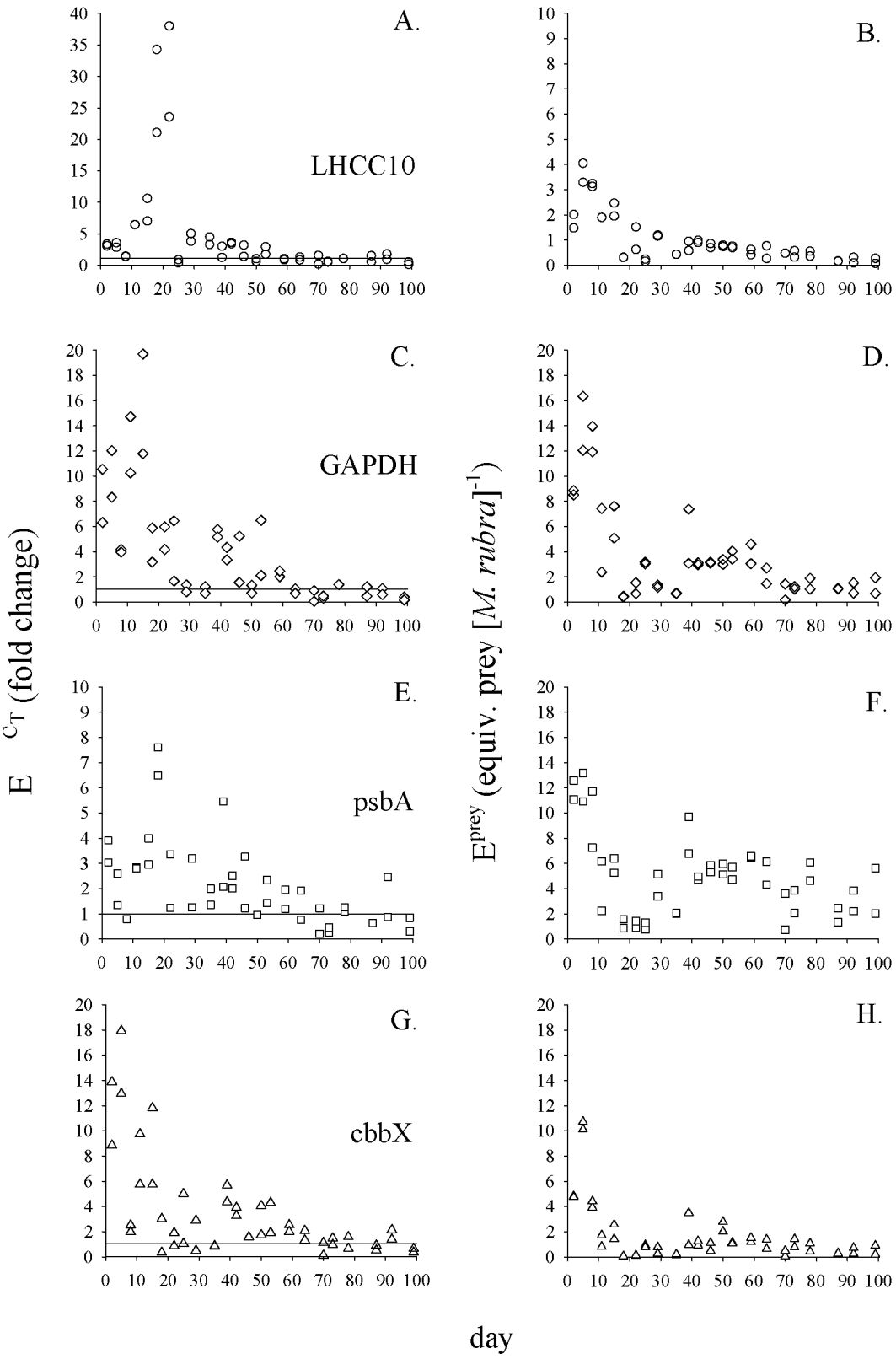
A.
LHCC10
B.
C.
GAPDH
D.
E.
psbA
F.
G.
cbbX
H.
E CT (fold change)
E^prey (equiv. prey [M. rubra]^-1)
day

Conclusions

Research on protistian ecology and functional biology during the last 30 years has shown that if protists are relatively simple in their metabolic diversity compared to prokaryotes, they are remarkably flexible and diverse in their predation strategies and feeding mechanisms. The discovery of widespread mixotrophy in microbial food webs (MFWs) has challenged our conceptual paradigms of trophic C flow within and out of microbial assemblages, and our perception of protist autecology (Sanders 1991, Jones 1994, Stoecker 1998). Mixotrophy blurs our perception of "plant" and "animal" trophic concepts in MFWs, with phagotrophic "algae" (i.e. plants that eat) and plastidic "protozoa" (i.e. animals with chloroplasts). These processes illustrate both the evolutionary roots of heterotrophy in all eukaryotes, and the remarkable ability of protists to adapt to and retain multiple trophic strategies. The rise, and partial loss, of several plastid lineages in dinoflagellates alone (e.g. Saldarriaga et al. 2001) underscores the evolutionary adaptability of genomes to assimilate (and lose) massive amounts of genetic information from symbionts or prey. Symbiosis and parasitism are commonplace in many protist groups, particularly with bacteria, most of which have poorly understood functions within their hosts (e.g. Lee et al. 1985). Thus, the intracellular environment of many protists can be dynamic and flexible, particularly for those able to engulf prey and efficiently form and recycle inner vacuolar membranes.

The retention of functional plastids (= chloroplasts) from algal prey is common amongst pelagic choreotrich ciliates (e.g. Stoecker et al. 1987). Plastid retention is practiced by ciliates (Blackbourn et al. 1973), dinoflagellates (Fields and Rhodes 1991), and foraminifera (Grzymski et al. 2002) amongst protists, and occurs in a few metazoans,

such as the sea slug *Elysia chlorotica* (Trench 1978). Most plastid retaining (or kleptoplastidic) organisms gain advantage from photosynthesis in the form of a labile C source for covering respiratory costs and increasing growth efficiency (e.g. Putt 1988, Skovgaard 1998). Strictly kleptoplastidic protists are not able to grow phototrophically, as they depend on ingestion and heterotrophic digestion of prey to satisfy most nutritional requirements (Stoecker 1998). However, some oligotrich ciliates may not be able to survive without light (Stoecker et al. 1988). Kleptoplastidy may be a mechanism to survive brief periods of low prey abundance (Stoecker 1998) and, in some ciliates, has been hypothesized to have a role in forming cyst structures (Dolan and Pérez 2000). Generally plastid retention time is relatively short, from hours to 2 weeks in oligotrich ciliates (e.g. Stoecker and Silver 1987) and from 2 to 12 days in dinoflagellates (Field and Rhodes 1991, Skovgaard 1998). For many kleptoplastidic protists, however, little is known about their physiology and most are not routinely or easily cultured. Plastid retention is clearly a transient fate for stolen plastids in most protists, as evidenced by absence of plastid division, loss of plastids when starved (Skovgaard 1998), observations of food vacuoles housing apparently old plastids (Laval-Peuto et al. 1986), and plastids from multiple prey species coexisting and replacing one another (Stoecker and Silver 1990).

The presence of cryptophyte organelles in *Myrionecta* rubra has long been debated as to whether it represents a permanent or temporary association (Taylor et al. 1969, 1971, Hibberd 1977, Oakley and Taylor 1978). The formation of chloroplast-mitochondrial complexes (CMCs) (Taylor et al. 1969, 1971) surrounded by a host membrane and enclosing cryptophyte cytoplasm (with ER), resembles symbiotic

compartments seen in some protists with permanent associations (e.g. *Kryptoperidinium foliaecum* Chesnick et al. 1996). The plastid-retaining and bloom-forming freshwater dinoflagellate *Gymnodinium acidotum* also appears to share some structural similarities in housing prey organelles to *M. rubra*. Like *M. rubra*, *G. acidotum* appears to retain chloroplasts, mitochondria, and cytoplasm together, separated from endogenous cytoplasm by a single membrane (Schnepf et al. 1989). The relationship, however, appears to be less stable in *G. acidotum*, as colorless cells can readily be observed, and plastid survival time has been estimated to be only about 12 days (Fields and Rhodes 1991). While TEM sections have documented multiple cryptophyte nuclei in *G. acidotum* (Farmer and Robert 1990), these are likely from ingestion of prey, rather than nuclear division, and no data are available documenting their duration in the dinoflagellate. Observations by Gustafson et al. (2000) provided the first evidence that *M. rubra* feeds on cryptophytes and apparently "robs" them of organelles. This research demonstrated that feeding enhances growth and photosynthesis and appears to stimulate chlorophyll production (Gustafson et al. 2000). My dissertation research was undertaken in an effort to better understand *M. rubra*, as it had never been cultured before its isolation from McMurdo Sound, Antarctica (by DE Gustafson and DK Stoecker). Specifically, I was interested in how organelle-retention operates in *M. rubra* and the physiological, evolutionary, and ecological implications of this process. It is important to note that the strain used in my research may differ physiologically from other strains isolated since the onset of my work in several locations around the world, and furthermore, that *M. rubra* may well be a species complex. It is possible that other strains/species may feed more, on other prey, and may have different organelle retention mechanisms or "strategies".

Highly divergent SSU rRNA genes in *M. rubra*: a cloudy evolutionary perspective

While numerous studies have described the ultrastructure and ecology of *M. rubra*, less attention has been paid to its taxonomic status. The only ciliates known to share major synapomorphies with *Myrionecta* belong to the genus *Mesodinium*. Many ecologists have retained an older taxonomic designation for *M. rubra*, *Mesodinium rubrum,* due to the absence of information describing the life history of *M. rubra* and inconsistencies in the reports of tentacle structures. Jankowski (1976) created the genus *Myrionecta* and distinguished it from *Mesodinium* by having dikineteds along the pre-equatorial cilia belt, a wider anterior hemisphere of the cell, bifurcated tentacles, and several other major differences in cellular structures. These differences are consistent with observations of cultured and field populations of *Myrionecta* and *Mesodinium* from several well-described populations (e.g. Taylor et al. 1971, Hibberd 1977, Lindholm 1985). The Antarctic *M. rubra* culture used in my dissertation research shares morphological traits that are consistent with those described by others (Taylor et al. 1969, 1971, Jankowski 1976) (Appendix1). Several plesiomorphic traits have been described for *Myrionecta* that make its current taxonomic placement within the Litostomatia ambiguous. These include tentacles composed of 14 microtubules (Lindholm and Mörk 1987), the absence of alveoli, greatly reduced ciliature restricted to two girdles in the cells center, and two macronuclei with a single micronucleus (Taylor et al. 1969, 1971).

Lynn (1991) commented on the highly divergent nature of somatic kinetids in the Mesodinidae compared to the rest of the litostomes.

Analysis of SSU rRNA genes from *M. rubra* and *M. pulex* may have provided little in the way of useful phylogenetic information. SSU genes from both ciliates had unusually high substitution rates and deletions compared to most eukaryotes, resulting in unusually short (<1600 bp) sequences that were difficult to align and nearly impossible to analyze with out long branch attraction (LBA) artifacts. LBA has been used to explain when fast evolving and seemingly unrelated taxa are drawn to one another in a tree (Philippe and Laurent 1998). Highly divergent SSU rRNA genes, resulting in phylogenetic misplacement of taxa, have been found in several other alveolates, including the apicomplexan *Plasmodium* (Goggin & Barker 1993). In general rRNA phylogenies for ciliates are congruent with traditional classifications, and form deep branches that reveal most of the 5 major morphologically defined ciliate classes (Tourancheau et al. 1998). In *M. rubra* and *M. pulex*, it is possible that these SSU sequences may be expressed pseudogenes, and that more conserved SSU genes could yet be discovered (however, they are highly expressed in *M. rubra* cells, evident by FISH; chapter 1). Preliminary analyses of protein coding genes from *M. rubra* are much more ciliate-like (Johnson unpub. data) and may help to resolve their phylogenetic placement.

While rDNA genes of ciliates generally seem to have typical eukaryotic substitution rates (e.g. Van de Peer and Wachter 1997), ciliate protein encoding genes have much faster rates of sequence divergence, such as the elongation factor 1α (EF-1α) (Moreira et al. 1999), actin (Villalobo et al. 2001), and histone (H4) (Berhard and Schlegel 1998, Katz et al 2004) genes. In other phylogenetic clades, long branches have

been explained by asexuality and population bottlenecks enhancing rDNA substitution rates, relaxed selection on rDNA primary and/or secondary structure, or positive selection for sequence change (e.g. Stiller and Hall 1999). These forces of evolutionary change have been evoked to explain observed accelerated rates of divergence in symbiotic and parasitic organisms (Stiller and Hall 1999).

If the SSU rRNA gene data have any fidelity for the evolutionary placement of *Myrionecta* and *Mesodinium*, then it is possible that the clades are an early branch of the ciliates and do not belong within the Litostomes (e.g. Lynn and Small 2002). If so, then perhaps ancestral taxa (i.e. with few extant closely related relatives) are subject to higher rates of sequence divergence in certain genes, as appears to be the case with *Oxyrrhis marina* (Saldarriaga et al. 2003). Alternatively, it is temping to speculate that by sequestering the nuclear and organelle associated (plastid, nucleomorph, mitochondrial) genomes from its cryptophyte prey, *M. rubra* may be subject to unusual selective forces, enhancing molecular substitution rates. Regardless, it is likely that protein phylogenies will find a better phylogenetic placement for the Mesodiniidae within the ciliates.

Divergent SSU rRNA sequences and protistian diversity

The propensity for which divergent (i.e. high substitution rates) gene sequences are prone to LBA artifacts (Philippe and Laurent 1998) creates formidable challenges for the phylogenetic analysis of divergent and unknown environmental genes. Recent studies that amplify and sequence rDNA from ocean samples have revealed a great deal of uncharacterized genetic diversity (Lopez-Garcia et al. 2001, van der Staay et al. 2001,

Dawson and Pace 2002). These studies have been valuable in order to identify regions of the eukaryotic phylogenetic tree that possess the greatest amount of uncharacterized diversity in these habitats. However, some genes that are believed to represent new genetic diversity may actually be divergent sequences from already recognized taxa. I found numerous sequences within Genbank representing novel eukaryotic diversity, which are closely affiliated or nearly identical to the *Myrionecta* and *Mesodinium* sequences. These environmental sequences have been generated from several diverse habitats, including deep Antarctic water (Lopez-Garcia et al. 2001), the Bay of Fundy (Savin et al. 2004), and microaerobic water samples from Cape Cod, MASS, USA, (Stoeck and Epstein 2003). *Myrionecta* and *Mesodinium* are believed to have a cosmopolitan oceanic, estuarine, and, in some cases for *Mesodinium*, fresh water distribution (Taylor et al. 1971, Foissner et al. 1999). In all of the above studies, clones matching the *Myrionecta* sequence are described as having uncertain phylogenetic ascription and are weakly affiliated with various amoeboid organisms (Lopez-Garcia et al. 2001, Stoeck and Epstein 2003, Savin et al. 2004). These results underscore the need for more sequence analysis of known pelagic protists, particularly those that are difficult to culture, and perhaps the use of cell sorters for isolating cell populations for both molecular and microscopy analysis.

Physiological and molecular observations of the functional biology of *Myrionecta rubra*

Earlier observations of the effects of feeding by *M. rubra* on the cryptophyte *Geminigera cryophila* revealed enhanced growth and photosynthesis rates, as well as the ability to synthesis pigments (Gustafson et al. 2000). Further experiments, representing the bulk of my dissertation research, involved determining the precise relationship of feeding to growth and photophysiology over time, and the potential role of *G. cryophila* nuclei that were shown to accumulate in *M. rubra* shortly after feeding (Gustafson et al. 2000). As a first step towards these ends, the culture (which at this time more closely resembled an *M. rubra* dominated community) was re-isolated to remove *M. rubra* from at least several contaminating co-inhabitants, including a diatom, oligotrich ciliate, choanoflagellate, and a heterotrophic dinoflagellate. Early measurements of pigments and photosynthetic uptake of C^{14} were carried out using "single cell" techniques, thus removing potentially contaminating signals. In the earliest experiments for my dissertation it was surprising to find some "unfed" treatments did not differ in growth or pigment levels to "fed" treatments (not shown). It quickly became apparent that loss of phototrophic growth occurred slowly over time, and thus experiments were designed to measure this rate.

Subsequent feeding-starvation experiments involved pulse feeding with sub-saturating *G. cryophila* prey concentrations and following bulk-measured physiological parameters over ~3 months (chapters 2 & 4). Virtually all other experiments conducted on plastidic ciliates or kleptoplastidic dinoflagellates have been conducted over 1-2 weeks. The duration of experiments herein with *M. rubra* may seem excessive, but proved necessary to fully document the total collapse of growth in at least one treatment (high-light). One important factor to consider, which surely lowered the rate of change in

physiological processes for *M. rubra*, is temperature, as this work was conducted with an Antarctic strain grown at 0-5 °C (see chapter 2 for discussion of Q10). After the first of such experiments focusing on changes in photophysiology, it became apparent that *M. rubra* could function phototrophically, without significant losses of growth for 4 weeks, after which growth declined and continued at low levels for 8+ weeks in low light (LL) and 4 weeks in high light (HL) (chapter 2, Johnson & Stoecker 2005). Photosynthesis continued for both treatments through the end of the experiment with only minor decline in P_{max}^{cell} and α^{cell} rates, especially for HL treatments. Pigment synthesis and plastid division capabilities also decline after 4 weeks of starvation and continued to decline thereafter at rates higher than that for growth (chapters 2, 4).

When recently fed, *M. rubra* is capable of using *G. cryophila* plastids about as effectively as in the cryptophyte, evidenced by nearly identical P_{max}^{chl} rates, although photosynthetic efficiency is lower (α^{chl}), especially in LL (chapter 3). Photosynthetic measurements normalized to cell rates for *M. rubra* roughly scale to the amount of chl *a* $cell^{-1}$ and thus (presumably) plastids $cell^{-1}$ (Chapter 3). However, photosynthetic rates normalized per cell C are lower in *M. rubra* (61-67%), as are chl *a*:C (θ) ratios (50-66%), both of which scale well with comparisons of growth between the cultures (64-68% of *G. cryophila*) (Chapter 3).

Research to further investigate the role of prey nuclei in *M. rubra* used a nearly identical experimental design as in Chapter 2, except *M. rubra* was fed for only 1 growth period, rather than for 2 consecutive periods. This study verified the presence of prey nuclei in *M. rubra* with fluorescence *in situ* hybridization (FISH). Previously prey nuclei had been measured using DAPI staining (Gustafson et al. 2000, Johnson & Stoecker

2005). Using FISH revealed that *G. cryophila* SSU rRNA was expressed in *M. rubra*, as the nucleolus, cytoplasm, and CMCs were all positively labeled (Chapter 4). Furthermore, expression of two nuclear-encoded *G. cryophila* genes (*LHCC10*, GAPDH) was measured over time, revealing that retained prey nuclei (PN) are transcriptionally active for 20-30 days (Chapter 4). While enhanced photosynthesis (P_{max}^{cell}; chapter 2) and plastid quantum efficiency (Fv/Fm; chapter 4) continue long after PN are lost, growth and chl synthesis/plastid-division decline more quickly (Chapters 2 & 4). Excess fixed C during declines in growth rate is probably stored, as *M. rubra* uses a proportionately large fraction of photosynthate to make lipids, and lipid droplets are visible in HL grown cells when sectioned for TEM (pers. obs.).

The persistence of functional plastids with declines in phototrophic growth, suggests that the ability of *M. rubra* to survive phototrophically is likely tied to the presence of PN. While most kleptoplastidic protists have an upper retention time of ~14 days for plastids, the survival of plastids in *M. rubra* can occur for >8 weeks (chapter 2, 4). This is likely due in part to the efficient packaging mechanism for the CMCs. Endoplasmic reticulum (ER) is visible in cytoplasm of CMCs (Taylor et al. 1971, Chapter 3), suggesting that *de novo* protein synthesis takes place, although this has not been measured directly. One factor that may help increase the longevity of plastids in *M. rubra* is the production of mycosporine-like aminoacids (MAAs), which are produced by *M. rubra* depending on light exposure, while absent in *G. cryophila* (chapter 3). MMAs are known to absorb UV radiation and are thought to be protective mechanisms against UV damage to nucleic acids and protein (Neale et al. 1998).

Together these data portray a model of efficient phototrophic growth for *M. rubra* populations that are able to feed within a 2 week window to acquire nuclei, after which growth remains positive for some time, but at ever decreasing rates with starvation. In nature, it is likely that *M. rubra* can easily satisfy these needs, perhaps on a daily basis, as cryptophytes are widespread and abundant in nature (Novarino 1993). Natural populations of *M. rubra* in Chesapeake Bay (USA) have been shown to ingest fluorescently labeled cryptophytes at rates exceeding 1 prey cell *M. rubra*$^{-1}$ h^{-1}, while clearance rates can exceed 300 nl *M. rurba*$^{-1}$ h^{-1} (Johnson, unpub. data.), suggesting that *M. rubra* can be a significant factor in regulating cryptophyte abundance. Collectively, these data imply that *M. rubra* blooms should be preceded either by blooms or high abundance of cryptophytes. This pattern has never been documented, probably due to the episodic timing of such blooms. Feeding prior to bloom events would allow *M. rubra* to grow phototrophically and regulate sequestered plastids, as cells would possess nuclei. Persistence of *M. rubra* in deep layers may be due to starved, and prey-nuclear-free, cells seeking refuge from photooxidative stress, in addition to cryptophyte prey.

Evolutionary considerations

While many ciliates are kleptoplastidic or harbor algal symbionts, none are thought to have permanently integrated chloroplasts. However, as part of the alveolates, ciliates may possess a photosynthetic ancestry (Fast et al. 2001). Alveolates include the dinoflagellates, half of which are photosynthetic with several plastid origins (e.g. Delwiche 1999), and the obligate intracellular parasites, apicomplexans, some of which

possess a vestigial non-photosynthetic plastid (Köhler et al. 1997). Despite this, no unequivocal photosynthetic genes or vestigial plastid (i.e. leucoplast) have been found in the ciliates (with completion of the *Paramecium* genome). It is now believed that most dinoflagellates, with the exception of early branching lineages, arose from a peridinin plastid containing ancestry and, in the absence of this plastid in extant species, have either lost the plastid or replaced it with another (Saldarriaga et al. 2001). However, among the heterotrophic dinoflagellates no traces of photosynthetic genes have yet been found. Thus while many ciliates and dinoflagellates are kleptoplastidic, it remains unclear if they are somehow able to use plastids based or remnant genes from a photosynthetic ancestry. Success of plastid sequestration may, rather, be based on how well the plastid is extracted and repackaged by the predator/host and spared from digestive processes.

Thus far all molecular evidence suggest that cryptophyte plastids in *M. rubra* are obtained via feeding. Cultured *M. rubra* have identical plastids to their prey, the number of which scales with cell pigment quotas (Chapter 3). Furthermore, *M. rubra* in Chesapeake Bay have been found to possess plastids that are identical to free-living cryptophytes (unpub. data), implying that they are actively sequestered, as genes in "permanent" plastids would be expected to have diverged. While the evolutionary implications of plastids in *Myrionecta rubra* are debatable, the ciliate is unequivocally a functional phototroph, and differs greatly from other kleptoplastidic protists. The obligate presence of cryptophyte organelles organized into discrete chloroplast-mitochondrial complexes (CMCs), the ability to divide and maintain CMCs, an apparent independence from heterotrophy, and the sequestration of prey nuclei, clearly differentiate *M. rubra* from other kleptoplastidic protists. The ability to divide CMCs is an important distinction

from other kleptoplastidic organisms, despite also sharing the origin of their plastids from prey. Most cryptophyte plastids in *M. rubra*, at least in Chesapeake Bay, appear to be of the *Geminigera/Teleaulax* clade (Johnson unpub data). However, "blue" phycocyanin containing plastids are also sometimes observed in *M. rubra* (Hargraves 1991), in estuarine, reed, and marsh environments and often near hypoxic layers (Lindholm pers. comm.). It is unclear as to how CMC interaction with prey nuclei function when different prey plastid and mitochondrial types coexist in a single cell, or even if certain estuarine *M. rubra* are perhaps a separate species. The coastal and oceanic varieties of bloom-forming *M. rubra* are typified by relatively large cell size, high rates of phototrophic growth, ability to use inorganic N, and are known to periodically form massive red tides (e.g. Packard et al. 1978). The latter three points clearly distinguishes the ecophysiology of *M. rubra* from kleptoplastidic protists, as reported blooms of plastidic oligotrichs (e.g. Dale and Dahl 1987) are rare and probably due to concentrating advective mechanisms.

Perhaps the most important distinction is the retention of functional prey nuclei, which apparently allow *M. rubra* to operate as a phototroph and thereby gain more advantages of stealing a plastid than other kleptoplastidic protists (chapter 4). Nuclear retention is a unique process and has never before been documented, to the best of my knowledge. Perhaps some similarities may be drawn with the lifecycle of rhodophyte adelphoparasites, which transfer nuclei to their hosts during infection (Goff & Coleman 1995). Interestingly, these parasites also pass on stolen plastids to their host as well (Goff & Coleman 1995). In nuclear retention, the prey nucleus is sequestered into predator/host cytoplasm and surrounded by ER membranes. These surrounding membranes may also include prey cytoplasm and mitochondria (Oakley and Taylor 1978). Some membrane

connectivity may occur between the nucleus and CMCs in *M. rubra* (e.g. Hibberd 1977), however this has not been conclusively established. The nuclei are apparently not replicated, and are transcriptionally active for at least 20 days, disappearing after ~30 days (Chapter 4). The retention of functional PN and coordinated division of CMCs in *M. rubra* create an intracellular environment reminiscent of those observed in some cells with permanent associations (e.g. *K. foliacium*; Chesnick et al. 1996). In *M. rubra,* a functionally phototrophic metabolism appears to be, more or less, constantly reestablished by nuclear retention. Over time, exposure to prey genes could conceivably result in horizontal gene transfer, through mechanisms proposed by Doolittle (1998). Thus, it is reasonable to speculate that organelle-retention, *sensu* nuclear retention, could result in the permanent acquisition of plastids, as proposed by the serial endosymbiosis theory. Because nuclear retention appears to be a key character separating *M. rubra* from other organelle sequestering protists, perhaps it should be used to label the trophic strategy of the ciliate (karyokleptic or karyokleftis: from Greek karydi: nut or kernel; kleftis: meaning thief).

Appendix 1: Morphological observations

Preliminary observations of ciliature structures and numbers were determined for a Antarctic *M. rubra* culture using protargol staining (PS), live observation (LO), and transmission electron microscopy (TEM). The number of cirri along the equatorial kinety belt (EKB) was counted using PS, and found to vary between 44-56 (m ± sd: 52 ± 4; n = 13). According to Lindholm (1985) cirri number is highly variable, between 30-112 depending upon cell size. *M. rubra* was found to possess rows of dikineteds along the EKB as described previously (Taylor et al. 1969, 1971), however these were only discernable in the culture using TEM. According to Krainer and Foissner (1990), the pre-equatorial kinety belt (PKB) is arranged in square-packed basal bodies. The feeding tentacles were only visible by LO, and when present, varied in number between 8-12 (n = 8), and were always forked. Vacuolated cytoplasm is sometimes apparent in portions of *M. rubra* cells using PS, while the related ciliate *Mesodinium pulex* always possesses a single vacuole at the apical posterior end.

Interphase cells always possessed a single micronucleus and two macronuclei, usually found in the anterior portion of the cell. The number and arrangement of nuclei in *M. rubra* appear to be most similar to the karyorelictid ciliate *Geleia nigriceps* (Kahl) (Raikov 1992), which also has two macronuclei and a single micronucleus. Like *M. rubra*, *G. nigriceps* has a large sphere within the macronucleus with high concentrations of RNA, little DNA in the macronucleus, similar orientation and grouping of micro and macronuclei, and condensed chromatin within the micronucleus (Raikov 1992). A cryptophyte prey nucleus is sometime present (depending on feeding history), as a single large nucleus in the lower anterior half of the cell. Cell size, shape, and volume are highly

variable in *M. rubra*. In one experiment cell volume was found to range between 600-21500 mm^3 (mean = 3773 μm^3), and appears to be dependent upon feeding history, light levels, and growth rate (Johnson & Stoecker 2005). Cell division for cultured *M. rubra* appears consistent with previous observations for the species (Lindholm 1985), and with that described for *M. acarus* (Tamar 1987), with division of the cell by traverse (homothetogenic) binary fission.

Bibliography

Adolf JE, Stoecker DK, Harding Jr LW (2003) Autotrophic growth and photoacclimation in *Karlodinium micrum* (Dinophyceae) and *Storeatula major* (Cryptophyceae). J Phycol 39: 1101-1108

Altschul SF, Gish W, Miller W, Myers EW, Lipman DJ (1990) Basic local alignment search tool. J Mol Biol 215: 403-410

Bernhard D, Schlegel M (1998) Evolution of histone H4 and H3 genes I different ciliate lineages. L Mol Evol 46: 344-354

Berry J, Bjorkman O (1980) Photosynthetic response and adaptation to temperature in higher plants. Annul Rev Plant Physiol 31: 491-543

Azam, F, T Fenchel, JG Field, JS Gray, LA Meyer-Reil, F Thingstad. 1983. The ecological role of water-column microbes in the sea. Mar. Ecol. Prog. Ser. 10: 257-263

Blackbourn, DJ, FJR Taylor, and J Blackbourn. 1973. Foreign organelle retention by ciliates. J. Protozool. 20: 286-288

Caron, DA and JC Goldman. 1990. Protozoa nutrient regeneration. In GM Capriulo (Ed). Ecology of marine protozoa. Oxford Univ. Press Inc. NY, NY

Caron DA, Goldman JC, Fenchel T (1990) Protozoan respiration and metabolism. In: Capriulo GM (ed) Ecology of marine protozoa. Oxford Univ Press, New York

Caron, DA and NR Swanberg. 1990. The ecology of planktonic sarcodines. Rev. Aquat. Sci. 3: 147-180.

Caron, DA. 2000. Symbiosis and mixotrophy among pelagic microorganisms. In DL Kirchman (Ed.), Microbial Ecology of the Oceans, Wiley-Liss, Inc., p 495-523

Chesnick JM, Morden CW, Schmieg AM (1996) Identity of the endosymbiont of *Peridinium foliaecum* (Pyrrophyta): analysis of the rbcLS operon. J Phycol 32: 850-857

Cota GF, Smith WO Jr, Mitchell BG (1994) Photosynthesis of *Phaeocystis* in the Greenland Sea. Limnol Oceanogr 39: 948-953

Crawford, DW. 1989. *Mesodinium rubrum*: the phytoplankter that wasn't. Mar. Ecol. Prog. Ser. 58: 161-174

Crawford DW, Purdie DA (1992) Evidence for avoidance of flushing from an estuary by a planktonic, phototrophic ciliate. Mar Ecol Prog Ser 79: 259-265

Crawford DW, Purdie DA, Lockwood APM, Weissman P (1997) Recurrent red-tides in the Southampton Water Estuary by the phototrophic ciliate *Mesodinium rubrum*. Estuar Coast Shelf Sci 45: 799-812

Dale T, Dahl E (1987) Mass occurrence of planktonic oligotrichous ciliates in a bay in southern Norway. J Plank Res 9:871-879

Darwin, C. 1839. Journal of researches into the geology and natural history of the various countries visited by H.M.S. Beagle. 1st Ed. London

Dawson SC, Pace NR (2002) Novel kingdom-level eukaryotic diversity in anoxic environments. PNAS 99: 8324-8329

Deane, JA, M Fraunholz, V Su, UG Maier, W Martin, DG Dunford, and GI McFadden. 2000. Evidence for nucleomorph to host nucleus gene transfer: light-harvesting complex proteins from cryptomonads and chlorarachniophytes. Protist. 151: 239-252

Delwiche, CF. 1999. Tracing the thread of plastid diversity through the tapestry of life. Am. Nat. 154: S164-S177

Dolan JR, Coats DW (1991) A study of feeding in predacious ciliates using prey ciliates

labeled with fluorescent microspheres. J Plank Res 13: 609-627

Dolan, J. 1992. Mixotrophy in Ciliates: A review of *Chlorella* symbiosis and chloroplast retention. Mar. Microb. Food Webs. 6: 115-132

Dolan JR, Marrasé C (1995) Planktonic ciliate distribution relative to a deep chlorophyll maximum: Catalan Sea, NM Mediterranean, June 1993. Deep-Sea Res I 42: 1985-1987

Dolan, JR, F Vidussi, and H Claustre. 1999. Planktonic ciliates in the Mediterranean Sea: longitudinal trends. Deep-Sea Res. I. 46: 2025-2039

Dolan, JR and MT Pérez. 2000. Costs, benefits and characteristics of mixotrophy in marine oligotrichs. Fresh. Biol. 45: 227-238

Doolittle WF (1998) You are what you eat: a gene ratchet could account for bacterial genes in eukaryotic nuclear genomes. Trends Genet 14: 307-311

Douglas, SE, CA Murphy, DF Spence, and MW Gray. 1991. Cryptomonad algae are evolutionary chimaeras of two phylogenetically distinct unicellular eukaryotes. Nature. 350: 148-151

Douglas S, Zauner S, Fraunholz M, Beaton M, Penny S, Deng L-T, Wu X, Reith M, Cavalier-Smith T, Maier U-G (2001) The highly reduced genome of an enslaved algal nucleus. Nature 410: 1091-1096

Dugdale, RC and JJ Goering. 1967. Uptake of new and regenerated forms of nitrogen in primary productivity. Limnol. Oceanogr. 12: 196-206

Falkowski PG, Raven JA (1997) Aquatic photosynthesis. Malden: Blackwell, pp

Farmer MA, Roberts KR (1990) Organelle loss in the endosymbiont of *Gymnodinium acidotum* (Dinophyceae) Protoplasma 153: 178-185

Fast, NM, JC Kissinger, DS Roos, and PJ Keeling. 2001. Nuclear-encoded, plastid-targeted genes suggest a single common origin for apicomplexan and dinoflagellate plastids. Mol. Biol. Evol. 18: 418-426

Fields SD, Rhodes RG (1991) Ingestion and retention of *Chroomonas* spp. (Cryptophyceae) by *Gymnodinium acidotum* (Dinophyceae). J Phycol 27: 525-529

Fenchel T (1968) On "red water" in the Isefjord (inner Danish waters) caused by the ciliate *Mesodinium rubrum*. Ophelia 5: 245-253

Fields, SD, and RG Rhodes. 1991. Ingestion and retention of *Chroomonas* spp. (Cryptophyceae) by *Gymnodinium acidotum* (Dinophyceae). J. Phycol. 27: 525-529

Foissner W, Berger H, Schaumburg J (1999) Identification of limnetic planktonic ciliates. Informationsberichte des Bayer. Landesamtes für Wasserwirtschaft, Heft 3/99, 793pp

Fraunholz M, E Mörschel, UG Maier. 1998. Prokaryotic cell division protein FtsZ is encoded by eukaryotic endosymbiont's nuclear equivalent in cryptomonad algae. Mol. Gen. Genet. 260: 207-211

Gibson, JAE, Swalding KM, Pitman TM, Burton HR (1997) Overwintering populations of *Mesodinium rubrum* (Ciliophora: Haptorida) in lakes of the Vestfold Hills, East Antarctica. Polar Biol 17: 175-179.

Glibert, PM, C Garside, JA Fuhrman, and MR Roman. 1991. Time-dependent coupling of inorganic and organic nitrogen uptake and regeneration in the plume of the Chesapeake Bay estuary and its regulation by large heterotrophs. Limnol. Oceanogr. 36: 895-909

Goff LJ Coleman AW (1995) Fate of parasite and host organelle DNA during cellular transformation of red algae by their parasites. Plant Cell 7: 1899-1911

Goggin CL, Barker SC (1993) Phylogenetic position of the genus *Perkinsus* (Protista, Apicomplexa) based on small subunit ribosomal RNA. Mol Biochem Parasitol 60: 65–70

Gray MW (1992) The endosymbiont hypothesis revisited. Int Rev Cytol 141: 233-357

Gray JC, Sullivan JA, Wang J-H, Jerome CA, MacLean D (2002) Coordination of plastid and nuclear gene expression. Phil Trans R Soc Lond B 358: 135-145

Green, BJ, WY Li, JR Manhart, TC, Fox, EJ Summer, RA Kennedy, SK Pierce, and ME Rumpho. 2000. Mollusc-algal chloroplast endosymbiosis. Photosynthesis, thylakoid protein maintenance, and chloroplast gene expression continue for many months in the absence of the algal nucleus. Plant Phys. 124: 331-342

Guillard RRL (1975) Culture of phytoplankton for feeding marine invertebrates. In Smith WL, Chanley MH (eds) Culture of marine invertebrate animals. Plenum Publishing Corp, New York, pp 29-60

Gustafson Jr., DE, DK Stoecker, MD Johnson, WF Van Heukelem, and K Sneider. 2000. Cryptophyte algae are robbed of their organelles by the marine ciliate *Mesodinium rubrum*. Nature, 405: 1049-1051

Grzymski J, Schofield OM, Falkowski PG, Bernhard JM (2002) The function of plastids in the deep-sea benthic foraminifer, *Nonionella stella*. Limnol Oceanogr 47: 1569-1580

Hargraves P (1991) Narrow River phytoplankton. Maritimes 35: 6-8

Hayes GC, Purdie DA, Williams JA (1989) The distribution of ichthyoplankton in Southampton Water in response to low oxygen levels produced by a *Mesodinium rubrum* bloom. 1989. J Fish Biol 34: 811-813

Herzig R, Falkowski PG (1989) Nitrogen limitation in *Isochrysis galbana* (Haptophyceae). I. Photosynthetic energy conversion and growth efficiencies. J Phycol 25: 462-471

Hibberd, DJ (1977) Observations on the ultrastructure of the cryptomonad endosymbiont of the red water ciliate *Mesodinium rubrum*. J Mar Biol Assoc UK 57: 45-61

Heinbokel, JF. 1978. Studies on the functional role of tintinnids in the southern California Bight. I. Grazing and growth rates in laboratory cultures. Mar. Biol. 47: 177-189

Hibberd, DJ. 1977. Observations on the ultrastructure of the cryptomonad endosymbiont of the red water ciliate *Mesodinium rubrum*. J. Mar. Biol. Ass. U.K. 57: 45-61

Horiguchi, T, and RN Pienaar. 1992. *Amphidinium latum* Lebour (Dinophyceae), a sand-dwelling dinoflagellate feeding on cryptomonads. Jpn J Phycol. 40: 353-363

Horstman DA (1981) Reported red-water outbreaks and their effects on fauna of the west and south coasts of South Africa, 1959-1980. Fish Bull S Afr 15: 71-88

Jakobsen, HH, PJ Hansen, and J Larsen. 2000. Growth and grazing responses of two chloroplast-retaining dinoflagellates: effect of irradiance and prey species. Mar. Ecol. Prog. Ser. 201: 121-128

Jankowski AW (1976) Revision of the classification of the cyrtophorids. In Markevich AP, Yu I (eds) Materials of the II All-union Conference of Protozoology, Part I, general protozoology, Naukova Dumka, pp 167-168

Jassby, AD and T Platt. 1976. Mathematical formulation of the relationship between photosynthesis and light for phytoplankton. Limnol. Oceanogr. 21: 540-547

Jeffrey SW, MacTavish HS, Dunlap WC, Vesk M, Groenewoud K (1999) Occurrence of UVA- and UVB-absorbing compounds in 152 species (206 strains) of marine microalgae. Mar Ecol Prog Ser 189: 35-51

Jiménez R, Intriago P (1987) Observations on blooms of *Mesodinium rubrum* in the upwelling area off Ecuador. Oceanol Acta Special issue No 6: 145-154

Johnson PW, Donaghay PL, Small EB, Sieburth JMcN (1995) Ultrastructure and ecology of *Perispira ovum* (Ciliophora: Litostomatea): an anaerobic, planktonic ciliate that sequesters the chloroplasts, mitochondria and paramylon of *Euglena proxima* in a micro-ocix habitat. J Euk Microbiol 42: 323-335

Johnson, MD, DE Gustafson, and DK Stoecker. 2001. The physiology of *Mesodinium rubrum*. Amer. Soc. Limnol. Oceanogr. Meeting, Albuquerque, NM

Johnson MD, Tengs T, Oldach DW, Delwiche CF, Stoecker DK (2004) Highly divergent SSU rRNA genes found in the marine ciliates *Myrionecta rubra* and *Mesodinium pulex*. Protist 155: 347-359

Johnson MD, Stoecker DK (2005) The role of feeding in growth and the photophysiology of *Myrionecta rubra*. Aquat Microb Ecol 39: 303-312

Jones, RI. 1994. Mixotrophy in planktonic protists as a spectrum of nutritional strategies. Mar. Microb. Food Webs. 8: 87-96

Jonsson, PR. 1987. Photosynthetic assimilation of inorganic carbon in marine oligotrich ciliates (Ciliophora, Oligotrichina). Mar. Microb. Food Webs. 2: 55-68

Kana TM, Glibert PM (1987) Effect of irradiances up to 2000 μE m^{-2} s^{-1} on marine *Synechococcus* WH7803: I. Growth, pigmentation, and cell composition. Deep Sea Res 34: 479-495

Katz LA, Bornstein JG, Lasek-Nesselquist E, Muse SV (2004) Dramatic diversity of ciliate histone H4 genes revealed by comparisons of patterns of substitutions and paralog divergences among eukaryotes. Mol Biol Evol 21: 555-562

Kirst GO, Wiencke C (1995) Ecophysiology of polar algae. J Phycol 31: 181-199

Kishino M, Takahashi M, Okami N, Ichimura S (1985) Estimation of the spectral absorption coefficients of phytoplankton in the sea. Bull Mar Sci 37: 634-642

Köhler S, Delwiche CF, Denny PW, Tilney LG, Webster P, Wilson RJM, Palmer JD, Roos DS (1997) A plastid of probable green algal origin in apicomplexan parasites. Science 275: 1485-1489

Krainer KH, Foissner W (1990) Revision of the genus *Askenasia* Blochmann, 1895, with proposal of two new species, and description of *Rhabdoaskenasia minima* N G, N Sp (Ciliophora, Cyclotrichida). J Euk Microb 37: 414-427

Landry, MR, and RP Hassett. 1982. Estimating the grazing impact of marine microzooplankton. Mar. Biol. 67: 283-288

Larsen, J. 1988. An unusual ultrastructural study of *Amphidinium poecilochroum* (Dinophyceae), a phagotrophic dinoflagellate feeding on small cryptophytes. Phycologica. 27: 366-377

Laval-Peuto, M, P Salvano, P Gayol, and G Greuet. 1986. Mixotrophy in marine planktonic ciliates: ultrastructural study of *Tontonia appendiculariformis* (Ciliophora, Oligotrichina). Mar. Microb. Food Webs. 1: 81-104

Laval-Peuto, M and M Febvre. 1986. On plastid symbiosis in *Tontonia appendiculariformis* (Ciliophora, Oligotrichina). BioSystems. 19: 137-157

Laybourn-Parry J, Bell EM, Roberts EC (2000) Protozoan growth rates in Antarctic Lakes. Pol Biol 23: 445-451

Leander BS, Kuvardina ON, Aleshin VV, Mylnikov AP, Keeling PJ (2003) Molecular phylogeny and surphase morphology of *Copodella edax* (Alveolata): Insights into the phagotrophic ancestral of apicomplexans. J Euk Microbiol 50: 334-340

Lee JJ, Soldo AT, Reisser W, Lee MJ, Jeon KW, Görtz H-D (1985) The extent of algal and bacterial endosymbiosis in protozoa. J Protozool 32: 391-403

Lee SY (2001) Unalignable sequences and molecular evolution. TRENDS Ecol Evol 16: 681-687

Lewis, MR and JC Smith. 1983. A small volume, short incubation time method for measurement of photosynthesis as a function of incident irradiation. Mar. Ecol. Prog. Ser. 13: 99-102

Lewitus, AJ, HG Glasgow, and LM Burkholder. 1999. Kleptoplastidy in the toxic dinoflagellate *Pfiesteria piscicida* (Dinophyceae). J. Phycol. 35: 303-312

Li, A, DK Stoecker, DW Coats, and EJ Adam. 1996. Ingestion of fluorescently labeled and phycoerythrin-containing prey by mixotrophic dinoflagellates. Aquat. Microb. Ecol. 10: 139-147

Liaud M-F, Brandt U, Scherzinger M, Cerff R (1997) Evolutionary origin of cryptomonad microalgae: two novel chloroplast/cytosol-specific GAPDH genes as potential markers of ancestral endosymbiont and host cell components. J Mol Evol 44: S28-S3

Lindholm T (1978) Autumnal mass development of the “red water” ciliate *Mesodinium rubrum* in the Åland archipelago. Mem Soc Fauna Flora Fennica 54: 1-5

Lindholm, T. 1985. *Mesodinium rubrum*- a unique photosynthetic ciliate. Adv. Aquat. Microb. 3: 1-48

Lindholm, T, P. Lindroos, and AC Mörk. 1988. Ultrastructure of the photosynthetic ciliate *Mesodinium rubrum*. BioSystems. 21: 141-149

Lindholm T, Lindroos P, Mörk AC (1990) Depth maxima of *Mesodinium rubrum* (Lohmann) Hamburger and Buddenbrock- Examples from a stratified Baltic Sea inlet. Sarsia 75: 53-64

López-Garcia P, Rodríguez-Valera F, Pedrós-Alió C, Moreira D (2001) Unexpected diversity of small eukaryotes in deep-sea Antarctic plankton. Nature 409: 371-656

Lynn DH (1991) The implications of recent descriptions of kinetid structure to the systematics of the ciliated protists. Protoplasma 164: 123-142

Lynn DH, Small EB (2000) Phylum Ciliophora. In Lee JJ, Leedale GF, Bradbury P, (eds) An illustrated guide to the protozoa. Society of Protozoologists, Lawrence, pp 477-478

MacIntyre HL, Kana TM, Anning T, Geider R (2002) Photoacclimation of photosynthesis irradiance response curves and photosynthetic pigments in microalgae and cynaobacteria. J Phycol 38: 17-38

Maddison WP, Maddison DR (1992) MacClade- analysis of phylogeny and character evolution. Sinauer, Sunderland, MA

Maier, UG, S Douglas, and T Cavalier-Smith. 2000. The nucleomorph genomes of cryptophytes and chlorarachniophytes. Protist. 151: 103-109

Margulis L (1970) Origin of eukaryotic cells. New Haven: Yale University Press

Medlin L, Elwood HJ, Stickel S, Sogin ML (1988) The characterization of enzymatically amplified eukaryotic 16S-like rRNA-coding regions. Gene 71: 491-499

Marshall W, Laybourn-Parry J (2002) The balance between photosynthesis and grazing in Antarctic mixotrophic cryptophytes during summer. Fresh Biol 47: 2060-2070

Mattoo AK, Hoffman-Falk H, Marder JB, Edelman M (1984) Regulation of protein metabolism: coupling of photosynthetic electron transport to in vivo degradation of the rapidly metabolized 32-KD protein of the chloroplast membranes. PNAS 81: 1380-1384

Menden-Deuer S, Lessard EJ (2000) Carbon to volume relationships for dinoflagellates, diatoms, and other protist plankton. Limnol Oceanogr 45: 569-579

Miller PE, Scholin CA (1998) Identification and enumeration of cultured and wild *Pseudo-nitzschia* (Bacillariophyceae) using species-specific LSU rRNA-targeted fluorescent probes and filter-based whole cell hybridization. J Phycol 34: 371-382

Montagnes, DJS and DH Lynn. 1989. The annual cycle of *Mesodinium rubrum* in the waters surrounding the Isles of Shoals, Gulf of Maine. J. Plank. Res. 11: 193-201

Moreira D, Guyader HL, Philippe H (1999) Unusually high evolutionary rate of the elongation factor 1a genes from the Ciliophora and its impact on the phylogeny of eukaryotes. Mol Biol Evol 16: 234-245

Moreira D and López-Garcia P (2002) The molecular ecology of microbial eukaryotes unveils a hidden world. TRENDS Microbiol 10: 31-38

Morris, I, HE Glover, and CS Yentsch. 1974. Products of photosynthesis by marine phytoplankton: the effect of environmental factors on the relative rates of protein synthesis. Mar. Biol. 27: 1-9

Morris I (1981) Photosynthesis products, physiological state, and phytoplankton growth. In: Platt T (Ed) Physiological basis of phytoplankton ecology. Can Bull Fish Aquat Sci 210: 83-102

Mujer, CV, DL Andrews, JR Manhart, SK Pierce, and ME Rumpho. 1996. Chloroplast genes are expressed during intracellular symbiotic association of *Vaucheria litorea* plastids with the sea slug *Elysia chlorotica*. Proc. Nat. Acad. Sci. 93: 12333-12338

Neale PJ, Banaszak AT, Jarriel CR (1998) Ultraviolet sunscreens in *Gymnodinium saunguineum* (Dinophyceae): mycosporine-like amino acids protect against inhibition of photosynthesis. J Phycol 34: 928-938

Noto T, Endoh H (2004) A "chimera" theory on the origin of dicyemid mesozoans: evolution driven by frequent lateral gene transfer from host to parasite. Biosystems 73: 73-83

Novarino G (2003) A companion to the identification of cryptomonad flagellates (Cryptophyceae = Cryptomonadea). Hydrobiol 502: 225-270

Oakley, BR and FJR Taylor. 1978. Evidence for a new type of endosymbiotic organization in a population of the ciliate *Mesodinium rubrum* from British Columbia. BioSystems. 10: 361-369

Oldach DW, Delwiche CF, Jakobsen KS, Tengs T, Brown, EG, Kempton JW, Schaefer EF, Bowers HA, Glasgow Jr HB, Burkholder JM, Steidinger KA, Rublee PA (2000) Heterodouplex mobility assay-guided sequence discovery: elucidation of the small subunit (18s) rDNA sequences of *Pfiesteria piscicida* and related dinoflagellates from complex algal cultures and environmental sample DNA pools. PNAS 97: 4303-4308

Packard, TT, D Blasco, and RT Barber. 1978. *Mesodinium rubrum* in the Baja California upwelling system. In Boje, R and M Tomczak (eds). Upwelling systems. p. 73-89. Springer-Verlag, Berlin

Palmisano AC, Smith GA, White DC, Nichols PD, Lizotte MP, Cota G, Sullivan CW (1987) Changes in photosynthetic metabolism in sea-ice microalgae during a spring bloom in McMurdo Sound. Antarc J 22: 176-7.

Parsons TR, Maita Y, Lalli CM (1984) A manual of chemical and biological methods for seawater analysis. Pergamon Press, Oxford

Passow U (1991) Vertical migration of *Gonyaulax catenata* and *Mesodinium rubrum*. Mar Biol. 110: 455-463

Petroni G, Rosati G, Vannini C, Modeo L, Dini F, Verni F (2003) *In situ* identification by fluorescently labeled oligonucleotide probes of morphologically similar, closely related ciliate species. Microb Ecol 45: 156-162

Pfannschmidt T, Nilsson A, Allen JF (1999) Photosynthetic control of chloroplast gene expression. Nature 397: 625-628

Philippe H, Laurent J (1998) How good are deep phylogenetic trees? Curr Opin Gen Dev 8: 616-623

Pierce, SK, RW Biron, and ME Rumpho. 1996. Endosymbiotic chloroplasts in mulluscan cells contain proteins synthesized after plastids capture. J. Exp. Biol. 199: 2323-2330

Platt T, Gallegos CL, Harrison WG (1980) Photoinhibition of photosynthesis in natural assemblages of marine phytoplankton. J Mar Res 38: 687-701

Pomeroy LR. 1974. The ocean's food web, a changing paradigm. BioScience, 24: 499-504

Posada D, Crandall KA (1998) MODELTEST: testing the model of DNA substitution. Bioinformatics 14: 817-818

Putt, M and DK Stoecker. 1989. An experimentally determined carbon: volume ratio for marine “oligotrichous” ciliates from estuarine and coastal waters. Limnol. Oceanogr. 34: 1097-1103

Putt, M. 1990. Abundance, chlorophyll content and photosynthetic rates of ciliates in the Nordic Seas during summer. Deep-Sea Res. 37: 1713-1731

Putt, M. 1990. Metabolism of photosynthate in the chloroplast-retaining ciliate *Loboea strobila*. Mar. Ecol. Prog. Ser. 60: 271-282

Raikov IB (1992) Dimorphic nuclei of the karyorelictid ciliate *Gelia nigriceps* Kahl: Fine structure. Eur J Protist 28: 442-450

Raven, JA. 1997. Phagotrophy in phototrophs. Limnol. Oceanogr. 42: 198-205

Robinson DH, Kolber Z, Sullivan CW (1997) Photophysiology and photoacclimation in surface sea ice algae from McMurdo Sound, Antarctica. Mar Ecol Prog Ser 147: 243-256

Rychert K (2004) The size structure of the *Mesodinium rubrum* population in the Gdansk Basin. Oceanologia 46(3): 439-444

Ryther JH (1967) Occurrence of red water off Peru. Nature 214: 1318-1319

Sakshaug E, Slagstad D (1991) Light and productivity of phytoplankton in polar marine ecosystems: a physiological view. In: Sakshaug E, Hopkins CCE, Oritsland NA (Eds) Proceedings of the Pro Mare Symposium on polar marine ecology. Pol Res 10: 69-85

Saldarriaga JF, McEwan ML, Fast NM, Taylor FJR, Keeling PJ (2003). Multiple protein phylogenies show that *Oxyrrhis marina* and *Perkinsus marinus* are early branches of the dinoflagellate lineage. Int J Syst Evol Microbiol 53: 355-365

Sanders RW (1991) Mixotrophic protists in marine and freshwater ecosystems. J Protozool 38: 76-81

Sanders, RW. 1995. Seasonal distributions of the photosynthesizing ciliates *Laboea strobila* and *Myrionecta rubra* (=*Mesodinium rubrum*) in an estuary of the Gulf of Maine. Aquat. Microb. Ecol. 9: 237-242

Satoh H, Watanabe K (1991) A red-water bloom caused by the autotrophic ciliate, *Mesodinium rubrum*, in the austral summer in the fast ice area near Syowa station, Antarctica, with note on their photosynthetic rate. J Tokyo Univer Fish 78: 11-17

Savin MC, Martin JL, LeGresley M, Giewat M, Rooney-Varga J (in press) Planktonic diversity in the Bay of Fundy as measured by morphological and molecular methods. Microb Ecol

Scholin, CA, KR Buck, T Britschgi, G Cangelosi, and EP Chavez. 1996. Identification of *Pseudo-nitzschia australis* (Bacillariophytceae) using rRNA-targeted probes in whole cell and sandwich hybridization formats. Phycologia. 35:190-197

Schnepf E and G Deichgräber. 1984. "Myzocytosis", a kind of endocytosis with implications to compartmentation in endosymbiosis. Naturwiss. 71: 218-219

Schnepf, E, R Meier, and G Drebes. 1988. Stability and deformation of diatom chloroplasts during food uptake of the parasitic dinoflagellate, *Paulsenella* (Dinophyta). Phycologia. 27: 283-290

Schnepf, E, S Winter, and D Mollenhauer. 1989. *Gymnodinium aeruginosum* (Dinophyta): a blue-green dinoflagellate with a vestigial, anucleate, cryptophycean endosymbiont.

Schubbert R, Renz D, Schmitz B, Doerfler W (1997) Foreign (M13) DNA ingested by mice reaches peripheral leukocytes, spleen, and liver via the intestinal wall mucosa and can be covalently linked to mouse DNA. PNAS 94: 961-966

Setälä O, Kivi K (2003) Planktonic ciliates in the Baltic Sea in summer: distribution, species association, and estimated grazing impact. Aquat Microb Ecol 32: 287-297

Sherr, EB, BF Sherr, RD Fallon, SY Newell. 1986. Small, aloricate ciliates as a major component of the marine heterotrophic nanoplankton. Limnol. Oceanogr. 31: 177-183

Sherr, EB and BF Sherr. 1994. Bactivory and herbivory: key roles of phagotrophic protists in pelagic food webs. Microb. Ecol. 28: 223-235

Skovgaard, A. 1998. Role of chloroplast retention in a marine dinoflagellate. Aquat. Microb. Ecol. 15: 293-301

Smith Jr., WO and RT Barber. 1979. A carbon budget for the autotrophic ciliate *Mesodinium rubrum*. J. Phycol. 15: 27-33

Snoeyenbos-West OL, Salcedo T, McManus GB, Katz LA (2002) Insights into the diversity of choreotrich and oligotrich ciliates (Class: Spirotrichea) based on genealogical analyses of multiple loci. Int J Syst Evol Microbiol 52: 1901-1913

Sorokin, YI. 1977. The heterotrophic phase of phytoplankton succession in the Japan Sea. Mar. Biol., 41: 107-117

Sorokin YI, Sorokin PY, Ravagnan G (1999) Analysis of lagoonal ecosystems in the Po River Delta associated with intensive aquaculture. Estuar Coast Shelf Sci 48: 325-341

Stiller JW, Hall BD (1999) Long-branch attraction and the rDNA model of early eukaryotic evolution. Mol Biol Evol 16: 1270-1279

Stoecker, DK, AF Michaels, and LH Davis. 1987. Large proportion of marine planktonic ciliates found to contain functional chloroplasts. Nature. 326: 790-792

Stoecker, DK, MW Silver, AE Michaels, and LH Davis. 1988. Obligate mixotrophy in *Loboea strobila*, a ciliate which retains chloroplasts. Mar. Biol. 99: 415-423

Stoecker, DK, MW Silver, AE Michaels, and LH Davis. 1988/1989. Enslavement of algal chloroplasts by four Strombidium spp. (Ciliophora, Oligotrichida). Mar. Microb. Food Webs. 3: 79-100

Stoecker, DK, A Taniguchi, AE Michaels. 1989. Abundance of autotrophic, mixotrophic and heterotrophic planktonic ciliates in shelf and slope waters. Mar. Ecol. Prog. Ser. 50: 241-254

Stoecker DK and JM Capuzzo. 1990. Predation on protozoa: its importance to zooplankton. J. Plank. Res. 12: 891-908

Stoecker DK and MW Silver. 1990. Replacement of aging chloroplasts in *Strombidium capitatum* (Ciliophora: Oligotrichida). Mar. Biol. 107: 491-502

Stoecker DK, and AE Michaels. 1991. Respiration, photosynthesis and carbon metabolism in planktonic ciliates. Mar. Biol. 108: 441-447

Stoecker, DK. 1991. Mixotrophy in marine planktonic ciliates: physiological and ecological aspects of plastid retention by oligotrichs. In Reid, PC et al. (Eds) Protozoa and their role in marine processes. p 161-179. Springer-Verlag, Berlin

Stoecker, DK, M Putt, LH Davis, and AE Michaels. 1991. Photosynthesis in *Mesodinium rubrum*: species-specific measurements and comparison to community rates. Mar. Ecol. Prog. Ser. 73: 245-252

Stoecker, DK. 1998. Conceptual models of mixotrophy in planktonic protists and some ecological and evolutionary implications. Europ. J. Protistol. 34: 281-290

Stoeck T, Epstein S (2003) Novel eukaryotic lineages inferred from small-subunit rRNA analysis of oxygen-depleted marine environments. Appl Eviron Microbiol 69: 2657-2663

Struder-Kypke MC, Lynn DH (2003) Sequence analysis of the small subunit rRNA gene conform the paraphyly of oligotrich ciliates sensu lato and support the monophyly of the subclass Oligotrichia and Choreotrichia (Ciliophora, Spirotrichea). J Zool 260: 87-97

Swofford DL (1999) PAUP*: Phylogenetic analysis using parsimony. Sinauer, Sunderland, MA

Tamar H (1987) On division in a freshwater *Mesodinium acarus*. Acta Protozool 26: 213-218

Tartarotti B, Baffico G, Temporetti P, Zagarese HE (2004) Mycosporine-like amino acids in planktonic organisms living under different UV exposure conditions in Patagonian lakes. J Plank Res 26: 753-762

Taylor, FJR, DJ Blackbourn, and J Blackbourn. 1969. Ultrastructure of the chloroplasts and associated structures within the marine ciliate *Mesodinium rubrum* (Lohmann). Nature. 224: 819-821

Taylor, FJR, DJ Blackbourn, and J Blackbourn. 1971. The red-water ciliate *Mesodinium rubrum* and its "incomplete symbionts": a review including new ultrastructural observations. J. Fish. Res. Bd. Can. 28: 391-407

Taylor, WD and DRS Lean. 1981. Radiotracer experiments on phosphorous uptake and release by limnetic microzooplankton. Can. J. Fish. Aquatic Sci. 38: 1316-1321

Tengs T, Dahlberg OJ, Shalchian-Tabrizi K, Klaveness D, Rudi K, Delwiche C, Jakobsen KS (2000) Phylogenetic analyses indicate that the 19'Hexanoyloxy-fucoxanthin-containing dinoflagellates have tertiary plastids of haptophyte origin. Mol Biol Evol 17: 718-729

Thompson JD, Gibson TJ, Plewniak F, Jeanmougin F, Higgins DG (1997) The CLUSTAL_X windows interface: flexible strategies for multiple sequence alignment aided by quality analysis tools. Nuc Acids Res 25: 4876-4882

Tourancheau AB, Villalobo E, Tsao N, Torres A, Pearlman PE (1998) Protein-coding genes in ciliates: comparison with rRNA-based phylogenies. Mol Phylo Evol 10: 299-309

Trench RK (1979) The cell-biology of plant-animal symbiosis. A Rev. Plant Physiol 30: 485-453

Van de Peer Y, De Wachter R (1997) Evolutionary relationships among the eukaryotic crown taxa taking into account site-to-site rate variation in 18s rRNA. J Mol Evol 45: 619-630

Verity, P. 1985. Grazing, respiration, excretion, and growth rates of tintinnids. Limnol. Oceanogr. 30: 1268-1282

Villalobo E, Perez-Romero P, Sanchez-Silva R, Torres A (2001) Unusual characteristics of ciliate actins Int Microbiol 4: 167-174

Walsh, JJ. 1981. Shelf-sea ecosystems. In Longhurst, AR (ed.) Analysis of marine ecosystems. Academic Press, NY, p. 159-196

Welschmeyer, NA and CJ Lorenzen. 1984. Carbon-14 labeling of phytoplankton carbon and chlorophyll *a* carbon: determining of specific growth rates. Limnol. Oceanogr. 29: 135-145

Wilkerson, FP and G Grunseich. 1990. Formation of blooms by the ciliate *Mesodinium rubrum*: the significance of nitrogen uptake. J. Plank. Res. 12: 973-989

Wilcox, LW and GJ Wedemayer. 1984. *Gymnodinium acidotum* Nygaard (Pyrrphyta), a dinoflagellates with an endosymbiotic cryptomonad. J. Phycol. 20: 236-242

Witek M (1998) Annual changes of abundance and biomass of planktonic ciliates in the Gdansk Basin, Southern Baltic. Internat Rev Hydrobiol 83: 163-182

Wright A-DG, Dehority BA, Lynn DH 1997. Phylogeny of the rumen ciliates *Entodinium*, *Epidinium* and *Polyplastron* (Litostomatea: Entodiniomorphida) inferred from small subunit ribosomal RNA sequences. J Euk Microbiol 44: 61-67.

Wuyts J, De Rijk P, Van de Peer Y, Pison G, Rousseeuw P, De Wachter R (2000) Comparative analysis of more than 3000 sequences reveals the existence of pseudoknots in area V4 of eukaryotic small subunit ribosomal RNA. Nuc Acid Res 28: 4698-4708.

Yih, W and JH Shim. 1997. The planktonic phototrophic ciliate, *Mesodinium rubrum*, as a useful organism for marine biotechnological applications. J. Mar. Biotech. 5: 82-85

Yih W, Kim HS, Jeong HJ, Myung G, Kim YG (2004) Ingestion of cryptophyte cells by the marine photosynthetic ciliate *Mesodinium rubrum*. Aquat Microb Ecol 36: 165-170

Zauner, S, M. Fraunholz, J Wastl, S Penny, M Beaton, T Cavalier-Smith, UG Maier, and S. Douglas. 2000. Chloroplast protein and centrosomal genes, a tRNA intron, and odd telomeres in an unusually compact eukaryotic genome, the cryptophyte nucleomorph. Proc. Nat. Acad. Sci. 97: 200-205

Yohn CB, Cohen A, Rosch C, Kuchka MR, Mayfield SP (1998) Translation of the chloroplast psbA mRNA requires the nuclear-encoded poly(A)-binding protein, RB47. J Cell Biol 142: 435-442